TECHNISCHE UNIVERSITÄT MÜNCHEN
Lehrstuhl für Echtzeitsysteme und Robotik

An Efficient Method for Testing Autonomous Driving Software against Nondeterministic Influences

Pascal Marcel Minnerup

Vollständiger Abdruck der von der Fakultät für Informatik der Technischen Universität München zur Erlangung des akademischen Grades eines

Doktors der Naturwissenschaften (Dr. rer. nat.)

genehmigten Dissertation.

Vorsitzender:	Prof. Alfons Kemper, Ph.D.
Prüfer der Dissertation:	1. Prof. Dr.-Ing. habil. Alois Knoll
	2. Prof. Dr.-Ing. Ren C. Luo

Die Dissertation wurde am 09.05.2017 bei der Technischen Universität München eingereicht und durch die Fakultät für Informatik am 13.09.2017 angenommen.

Acknowledgements

First of all, I would like to thank Prof. Dr. Alois Knoll for offering the opportunity to work on this fascinating and challenging topic, as well as for his encouragement and support. Many thanks also go to Prof. Dr. Ren C. Luo for his valuable inputs and suggestions. I would also like to thank Prof. Dr. Bernd Radig for his last-minute commitment in my Rigorosum and Prof. Alfons Kemper, Ph.D. for chairing the defense. Moreover, I would like to thank Dr. Markus Rickert for his great support in mentoring my research efforts. Special thanks go to Dominik Bauch, Julian Bernhard, Martin Büchel, Dr. Chao Chen, Klemens Esterle, Patrick Hart, Gereon Hinz, Tobias Kessler, David Lenz and all other colleagues and students who supported me during my time at fortiss. Finally, I would like to thank my wife, my parents, my siblings, my parents-in-law and my friends for proof reading and for the constant support while working on the thesis.

Für Katta

Abstract

Autonomous driving planning and control functions have to ensure reliable execution in all situations for which they can be activated. The reliability is challenged by the large number of scenarios, by nondeterministic behavior of traffic participants and by inaccurate sensors and actuators. All three conditions can be controlled and reproduced in a simulation environment. Additionally, the simulation environment can execute the same planning and control code as the real vehicle and thus include all implemented improvements. However, it remains a challenge to cover combinations of the conditions above efficiently. This thesis presents a new method that directly tests the implementation of the planning system and efficiently provokes undesired behavior. The method maps the states of the tested system to a discrete state space. Similar to model checking, it covers all reachable states in this space. In contrast to traditional model checking, state transitions are performed by dynamically executing the actual implementation of the checked system. Furthermore, each analysis step increases the density of the state space and reduces the discretization error. Reaching different states requires branching the execution of the simulation at intermediate points. For this purpose, the state of the entire software system is stored. This allows restoring and continuing from it with different influences of the nondeterministic parts. Omitting states that are similar to already analyzed states reduces the complexity of the search. This way, the method finds undesired behaviors more efficiently than state of the art methods dealing with nondeterminism by random execution. The approach is shown to be applicable to planning and control software used in the automotive industry. It can be integrated into the automotive pre-development process supporting iterations of tests and software improvements.

Inhaltsangabe

Planungs- und Regelungsfunktionen für das autonome Fahren müssen eine zuverlässige Ausführung in allen Situationen sicherstellen, in denen sie aktiviert werden können. Die Zuverlässigkeit kann beeinträchtigt werden durch die große Zahl unterschiedlicher Szenarien, durch nichtdeterministisches Verhalten von Verkehrsteilnehmern und durch Sensor- und Aktorungenauigkeiten. Alle drei Einflussfaktoren können in einer Simulationsumgebung kontrolliert und reproduziert werden. Außerdem kann die Simulationsumgebung dieselbe Planungs- und Regelungssoftware wie das echte Fahrzeug ausführen und dementsprechend alle implementierten Verbesserungen testen. Allerdings bleibt es eine Herausforderung, auch Kombinationen dieser Einflussfaktoren effizient zu testen. Die vorliegende Arbeit stellt eine neue Methode vor, die die Implementierung des Planungssystems direkt testet und die effizient ungewolltes Verhalten provoziert. Die Methode bildet die Zustände des zu testenden Systems auf einen diskreten Zustandsraum ab. Analog zum Model-Checking deckt sie alle Zustände in diesem abstrakten Zustandsraum ab. Im Gegensatz zu traditionellem Model-Checking werden Zustandsübergänge durch die dynamische Ausführung der Softwareimplementierung des zu testenden Systems umgesetzt. Außerdem wird der diskrete Zustandsraum mit jedem Schritt dichter, so dass Diskretisierungsfehler reduziert werden. Um unterschiedliche Zustände zu erreichen ist es nötig, die Ausführung an Zwischenpunkten verzweigen zu lassen. Zu diesem Zweck wird der Zustand des gesamten Softwaresystems gespeichert. Dadurch kann dieser Zustand geladen werden und die Ausführung mit unterschiedlichem Einfluss der nichtdeterministischen Bestandteile wiederholt werden. Indem Zustände ausgelassen werden, die ähnlich zu bereits analysierten Zuständen sind, wird die Komplexität der Suche reduziert. Auf diese Weise findet die präsentierte Methode ungewolltes Verhalten effizienter als aktuelle Methoden, die auf zufällige Ausführung setzen, um unterschiedliche Verhalten zu produzieren. Es wird gezeigt, dass der Ansatz auf Planungs- und Regelungssoftware in der Automobilindustrie anwendbar ist. Er kann in den Vorentwicklungsprozess integriert werden, um eine iterative Entwicklung aus Tests und Softwareverbesserungen zu unterstützen.

Contents

Chapter 1

Introduction

Autonomous driving is one of the most revolutionary techniques that will be developed in the near future. It is expected to increase road safety, redesign urban areas and push new industry branches. According to the WHO (World Health Organization), there have been 1.25 million traffic deaths in 2013 and 3% of the world's GDP (Gross Domestic Product) [1], [2] has been spent on the consequences of traffic accidents. In the USA (United States of America) alone, $212 billion are lost every year [3]. By using autonomous driving, car manufacturers aim to prevent all "traffic fatalities" [4]. Furthermore, autonomous driving might reduce the need for parking space in urban areas by more than 5.7 billion square meters [3] allowing the redistribution of the space to bicycle lanes, parks or new housing. It also makes areas that are less accessible by current public transport systems more attractive and reduces housing costs in city centers [5]. By improving traffic flow [6], autonomous driving can reduce congestion and thereby improve the accessibility of some areas. Autonomous driving can deliver an increase in safety, efficiency, comfort, social inclusion and accessibility of city centers [7]. The new mobility gained by autonomous driving will push business models like car sharing and peer-to-peer rentals. For example, logistic companies cut down their costs [3]. This way, transporting products that are currently not shipped because of cost and delays might become profitable. Overall, autonomous driving promises large benefits to customers and financial gains to service providers.

Because of these benefits, automotive companies are developing increasingly capable driver assistance systems that will ultimately lead to fully autonomous driving [8]. As the complexity of driver assistance systems increases, so does the necessary effort for testing and evaluation [9]. Each function has to work for a billion hours without severe accidents [10], which makes exhaustive physical vehicle tests for validation economically infeasible. Instead, engineers can test autonomous driving functions in a simulation. Unfortunately, simulated tests do no exhibit the same behavior as physical tests, due to inaccurate models and environmental uncertainty [11]. The inaccuracy includes the behavior of the sensors and actuators that are not performing equally to their ideal models. This difference is called the "reality gap" [12]. Furthermore, traffic

participants have a large set of possible motions, which lead to different interactions with the autonomous vehicle. In the physical world, this leads to faults but in simulation, these faults do not appear. For these reasons, thorough and economically feasible testing requires new test methods [13]. A recent example of a fault occurring only in reality is the Google self-driving car colliding with a bus, even though the sensors did detect the bus and the actuators would have been capable of decelerating the vehicle in time [14]. The issue occurred only in a specific constellation of traffic behavior and ego vehicle motion that the Google engineers did not test in simulation.

1.1 Importance of Systematic Testing

There are several development steps for performing simulated tests in the automotive industry. Early tests are performed as SIL (Software In the Loop)-tests. SIL-tests represent the environment of the tested software as a software simulation. This allows early dynamic testing of the software component [15]. HIL (Hardware In the Loop)-tests add more realism by executing parts of the system on real hardware.

Systematic testing of autonomous vehicles has to cope with several challenges as illustrated in Figure 1.1. It can be performed in simulation or in the physical world. In order to perform these tests in simulation, engineers have to determine the right scenarios to be tested. These scenarios have to include particularly dangerous situations in order to have meaningful test results. However, the dangerous situations cannot be determined in advance. The difficulty of the simulation (top right step in Figure 1.1) is that it has to mirror the possible behaviors of the real world. Otherwise, it would miss many of the weaknesses of the planning and control software. The alternative to simulation are physical tests (bottom left step). Physical tests offer the advantage that the real world is full of testing scenarios and engineers can use the actual vehicle instead of creating models. The disadvantage is that the tests are resource intensive. Testing in simulation helps to prepare physical tests and remove as many defects as possible before testing physically. If either simulation or physical tests uncover a fault, engineers have to resolve that fault. Often, the cause of the fault is not obvious, in particular if the test driver and the development engineer are different persons. In these cases, the development engineers can only access the stored log information and the fault description of the test driver. Using this information, they need to reproduce the fault in a simulation environment. For faults detected in simulation, this step consumes relatively little time while faults detected in physical test-drives are more difficult to reproduce. A fix for a detected fault can affect the autonomous vehicle's behavior in previously tested situations as well (bottom arrow in Figure 1.1). Repeating all previous physical tests is very costly. Therefore, it is again valuable to obtain as much information in simulation as possible.

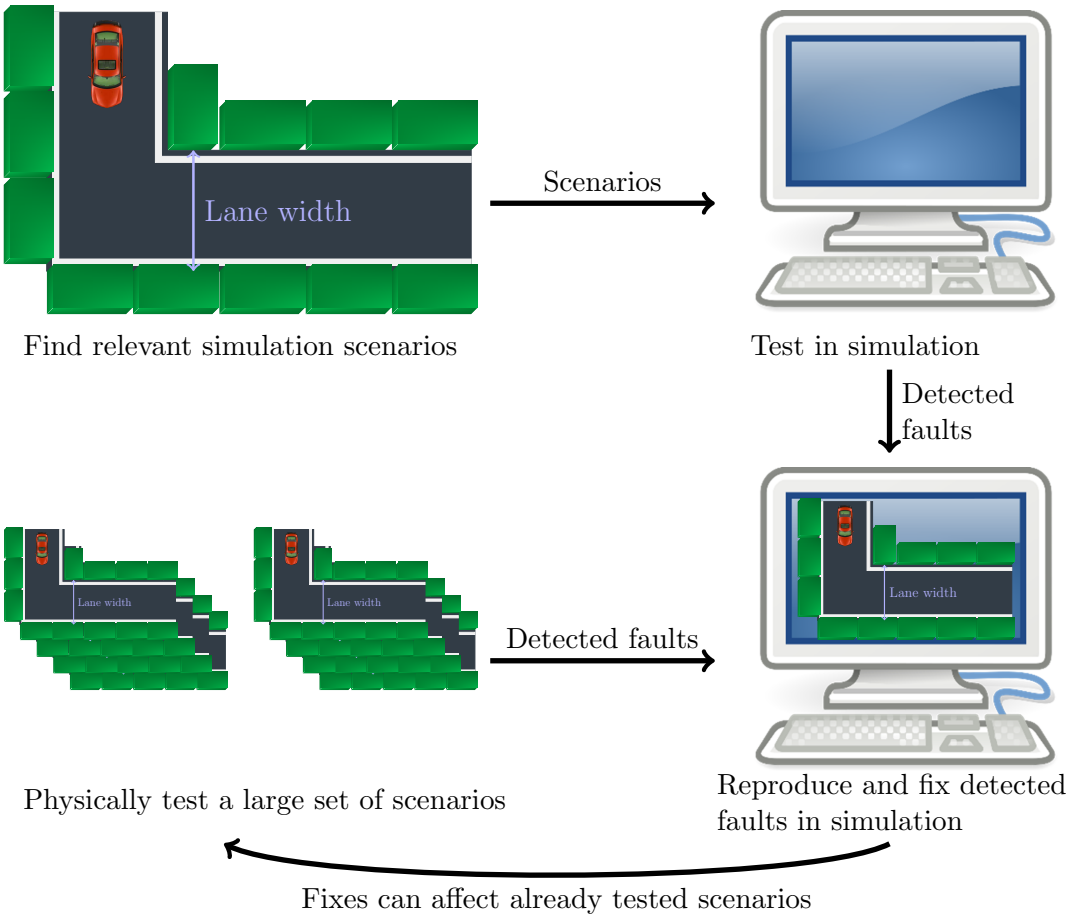

Figure 1.1: Challenges of testing in simulation or the physical world. Testing in simulation requires determining relevant dangerous scenarios to be tested. Testing in the physical world is resource intensive and may have to be repeated if a defect is found.

In summary, testing systematically is important for limiting the costs of assessing autonomous driving systems. Major challenges for testing planning and control systems are:

- The relevant scenarios to be tested in simulation need to be determined.
- Some faults seldom occur in physical test-drives and never in imperfect simulation environments. They require many driven test kilometers.
- Faults need to be reproduced in order to resolve them.
- Fixes of faults can necessitate the repetition of expensive tests.

The approach presented in this thesis addresses these challenges.

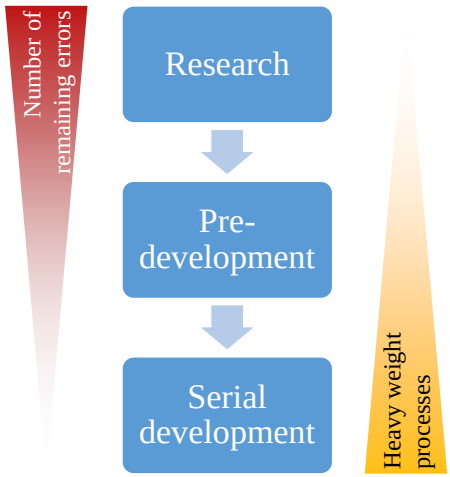

Figure 1.2: Coming closer to the serial production, the software development processes become more heavyweight and tolerate fewer defects remaining in the system.

1.2 Software Development Process

The development of new automotive features starts with researching the technical possibilities and ends with a serial product. Along this path, the development process becomes more heavyweight and tolerates fewer errors remaining in the system as depicted in Figure 1.2. The first two steps are research and pre-development. Both share the goal to determine whether a technical function can be realized. The main difference is that while pre-development focuses "on contemporary vehicle deployment" [16], research can target applications in the more distant future. For this reason, research results need to be less robust. They mainly need to work for a small set of demonstration scenarios, proving the feasibility of the general approach.

Pre-development also targets later application, but work in a larger set of scenarios. The goal of pre-development is to survey the core requirements and evaluate the possible technical realization for serial production [17]. This includes determining the limitations of the developed approach and building demonstrators that are sufficiently robust for conducting user studies. For these purposes, engineers have to test a subset of the physical scenarios mentioned in Section 1.1 in reality and in simulation.

Serial development has to produce systems that are very unlikely to fail even if executed for a much longer time than the total test time. For this part of the development process, engineers need methods that identify seldom-occurring corner cases. Thus, they have to test the autonomous driving system systematically both in the physical world and in simulation.

1.3 Contributions and Structure

This thesis focuses on efficiently testing variations of scenarios that involve inaccurate sensor measurements and actuator responses as well as nondeterministic behavior of traffic participants in a simulation environment. It presents a new concept that combines directly testing the implementation of the planning system with the goal of covering reachable states, which corresponds to model checking. This way, it can support the development of autonomous driving systems.

Chapter 2 summarizes and discusses the state of the art for ensuring the correctness of autonomous driving systems. These methods include design considerations, tests in simulation and tests in the physical world.

Modeling the physical part of an autonomous driving system is discussed in Chapter 3. It models the environment, the vehicle and the inaccuracies such that events in the physical world can be reproduced in simulation. Nondeterminism allows achieving this with incomplete models. The chapter ends with the representation of an undesired behavior that should be found in the simulation system.

Finding these behaviors is the focus of Chapter 4. It first presents a new concept for efficiently searching for these undesired behaviors. Next, it explains methods for optimizing the speed within the presented concepts. The resulting function is applied to scenarios that can be derived as described in Section 4.3. Section 4.4 describes how complex patterns of undesired behaviors can be represented for the algorithm described above. Additionally, the scenarios can contain dynamic traffic participants modeled in Section 4.5.

Chapter 5 describes the framework that integrates the methods described in Chapter 4. It starts with the architecture of the involved software components. Next, the integration of the framework into development processes and the use for debugging purposes are described. Finally, the path towards application in learning systems is presented.

The methods and concepts developed in the main part of the thesis are evaluated in Chapter 6. It compares the *STARVEC (Systematic Testing of Autonomous Road Vehicles against Error Combinations)* approach to several other algorithms in different scenarios.

Chapter 7 discusses how future research projects can continue the work described in this thesis. Finally, the results are summarized in Chapter 8.

Chapter 2

State of the Art for Testing Autonomous Driving Systems

Achieving safe and correct autonomous driving systems is targeted from multiple perspectives. The first approach is to design planning and control functions such that they can cope with all situations. Several such methods are described in Section 2.1. However, the simplifications of these methods applied for gaining efficiency can lead to undesired behavior in some situations. Therefore, some researchers try to prove their planning principle to work in all situations as explained in Section 2.2. This section also explains some weaknesses due to which the proofs do not replace tests. Section 2.3 describes approaches for testing in a simulation environment. For a good coverage, the simulation needs to consider nondeterministic events as explained in Section 2.4. Such events are automatically included in real world tests, which are discussed in Section 2.5. The disadvantage of such tests is a worse cost efficiency. Instead, Section 2.6 explains how to use the real world as a source for test scenarios in simulation.

2.1 Planning and Control Algorithms

The first step for achieving safe autonomous driving is to design the planning and control methods such that they do not cause collisions with obstacles. Figure 2.1 shows some basic approaches for collision avoidance. Figure 2.1(a) depicts the most common approach. A shape around the vehicle (light green rounded rectangles) is checked against collisions with obstacles (dark green box) for any predicted position along the planned path. The shape is the vehicle shape enlarged by some safety margin or, alternatively, the shape of the obstacle is enlarged. The distance may depend on the type of the obstacle [18]. This collision check is used in combination with path or trajectory planning methods like [19]–[23]. An overview of planning methods is presented in [24]. The challenge is to choose a safety margin that allows the planning component

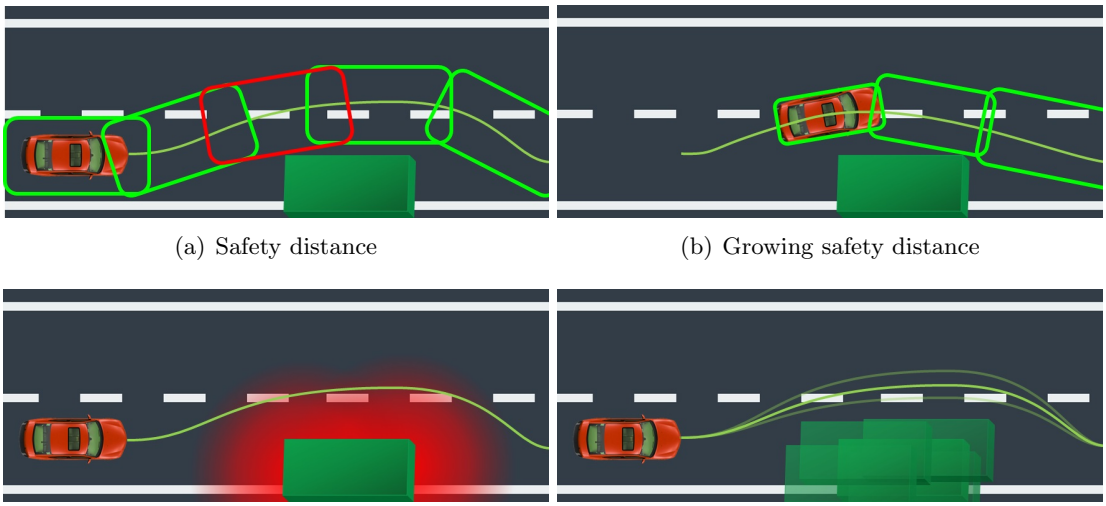

(a) Safety distance (b) Growing safety distance

(c) Potential fields (d) Planning with uncertainty

Figure 2.1: Different methods for avoiding a collision with an obstacle caused by sensor and actuator errors. Methods based only on safety distances are vulnerable to noisy inputs. Lower safety distances for near positions can lead to unnecessary closely approaching the obstacle. Potential fields are complex to parameterize correctly and planning with uncertainty requires high computation power.

to find a comfortable path but prevents collisions caused by sensor or actuator inaccuracies. This distance can be chosen based on test experience. The red rounded rectangle in Figure 2.1(a) depicts another disadvantage of this method: On the shortest path computed in the planning operations, the safety margin touches the obstacle. Any controller or measurement error can lead to the safety margin colliding with the obstacle. If the vehicle searches another path starting at this colliding position, the planning system fails. Increasing or reducing the safety distance does not solve the problem, because on the shortest path the safety margin always touches the evaded obstacle.

Werling [25] addresses this problem by starting with no safety margin and enlarging it over time or driven distance as depicted in Figure 2.1(b). This approach enforces plans that keep a safety distance in the future, but leaves the start position valid, even if sensor noise lets an obstacle suddenly appear closer. Figure 2.1(b) also illustrates a disadvantage: The planned trajectory for the near future can make the vehicle approach the obstacle without need. This is depicted by the second safety shape, which touches the obstacle although it is smaller than the corresponding safety shape in Figure 2.1(a). A good parametrization has to ensure that the reduced safety distance is still large enough and grows fast enough to accommodate sensor inaccuracies. This increases the challenge to find the right safety distances mentioned above. Furthermore, users can perceive the trajectory as unnecessarily dangerous.

A classical approach for avoiding the perceived risk is to penalize closeness to obstacles [26]. This penalty creates potential fields around static obstacles [27] as depicted in Figure 2.1(c). The planning algorithm tries to avoid the areas with high penalty depicted by the red gradient.

The approach can also be applied to dynamic obstacles [28]. One disadvantage is that potential fields can push the vehicle away from its goal [29] and completely block narrow passages [30]. This problem can be solved by adjusting the potential fields in these regions [31]. Another challenge is that the potential fields only penalize but do not forbid getting close to an obstacle. Hence, engineers have to choose the right parameters for preventing collisions even more carefully than for safety margins.

Some planning concepts address this challenge by incorporating uncertainty as depicted Figure 2.1(d). They consider the position of static obstacles as uncertain (transparent copies of green box), which can result in the collision being already inevitable [32] when the correct position is measured. A state from which a collision is inevitable is called "inevitable collision state" [33]. Robots avoiding these "inevitable collision states" remain safe even if obstacles appear suddenly. Patil et. al. [34] consider motion uncertainty and extend their work with a version optimized for higher state dimensions [35]. Lenz et. al. [36] simultaneously take into account sensor and actuator inaccuracies maximizing the probability of collision freedom. Uncertainty of traffic participants can also be regarded while planning [37]. One disadvantage of doing so is the need of high computation power. In order to reduce the computation time, researchers use simplified abstractions of the vehicle and the environment. Thus, these functions also have to be configured with sufficient safety margins in order to achieve collision freedom. These safety margins need to be tested in simulation and physical test-drives.

In summary, all methods described above require additional mechanisms for actually ensuring collision freedom for a specific vehicle and parametrization.

2.2 Formal Verification of Planning Concepts

Formal verification is one mechanism aiming to ensure collision freedom for planning and control systems. Carreno et. al. [38] regard a collision-avoidance system for airplanes on two parallel runways. The authors verify that the collision warning system issues a warning no later than four seconds before the collision occurs. For the verification, they use PVS (Prototype Verification System) [39] to model both the warning system and the allowed trajectories. For autonomous driving, there is a large number of different scenarios. Therefore, Althoff uses reachability analysis [40]–[42] to verify the planned path online in any current situation as depicted in Figure 2.2. The green path is the path to be verified for collision freedom under all expected inaccuracies. If the analysis cannot verify it to be safe, the autonomous vehicle follows the red path to a previously verified safe stop. The verification uses a simplified model of the vehicle that the authors validate by comparing it to a more complex model in simulation. One disadvantage of verification is that it limits the types of sensor and actuator errors to be modeled. For example, delays are difficult to represent. Errors are often modeled as a linear function of the current state of the vehicle. Delays are either not linear, or not a function of the current state. Therefore, further effort

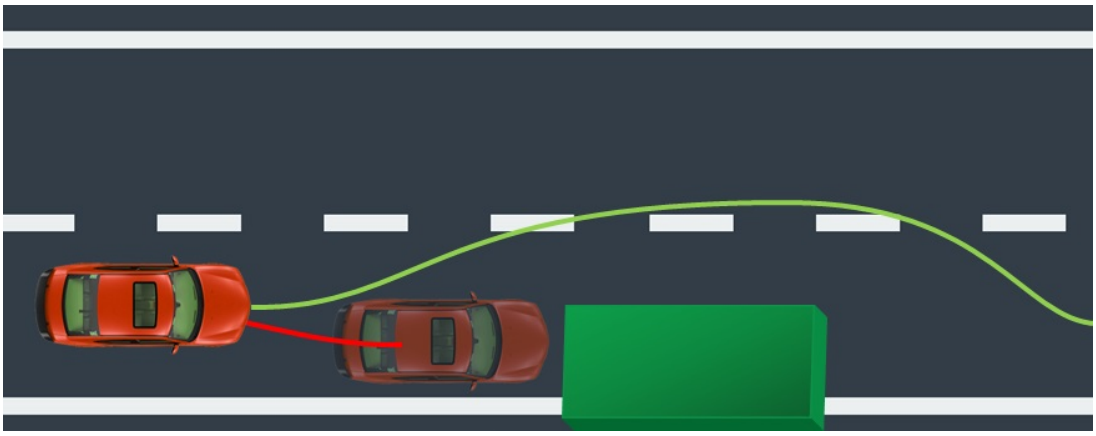

Figure 2.2: Online verification of path-planning results: If the path cannot be verified as safe, the emergency stop (red) is executed.

is necessary to represent delays. New error patterns observed in physical test-drives are also difficult to represent in the formal model. A systematic test method as presented in this thesis can support the representation of such patterns by giving a reference of what the verification models should cover. Additionally, dynamic tests are still necessary to find out whether the actual implementation reacts fast enough to new information. It also helps to avoid uncomfortable safe stops.

2.3 Testing in a Simulation Environment

The disadvantages of formally verifying the planning concepts are addressed by testing the complete autonomous driving system in a simulation environment. Research groups and automotive companies use this technique extensively. For this reason, there is a lot of research, practical experience and tool support available for setting up a simulation environment. The existing work supports different strategies of testing in simulation:

- Simulation based on realistic models
- Simulation with hardware components (HIL)
- Commercial simulation software
- Simulation with driver interaction

The following two sub sections explain these strategies.

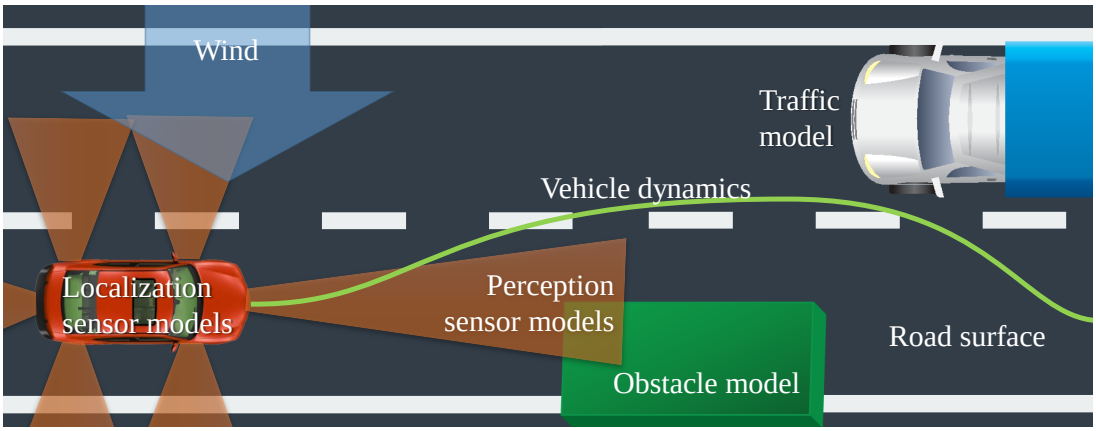

Figure 2.3: Models involved in an autonomous driving simulation: There are localization and mapping sensor models including obstacle models, vehicle dynamic models including the effect of the road surface and wind, and models of traffic participants.

2.3.1 Realistic Models for Simulation

Simulation cannot be identical to the execution in a physical environment: There is always a gap between those two–the reality gap [43]. A simulation without a reality gap requires perfect models. Figure 2.3 shows the models that are involved in an autonomous driving simulation.

Sensor models specify how the vehicle perceives its environment. The main sensors are for mapping the environment and localizing the car. Ultrasonic sensors, laser scanners, radars and cameras are the major contributors for mapping algorithms. On the one hand, models of these sensors help to increase the mapping performance [44], [45]. On the other hand, ultrasonic sensor models [46]–[48] and camera models [49] are used to test autonomous vehicles. Global Navigation Satellite Systems (GNSS) [50], [51], environment features detected by camera [52], [53] and odometry [54] are the basis of localization concepts. Each concept has different error characteristics that have to be modeled. Additionally, vehicle dynamic and actuator models like Vedyna [55] precisely model the behavior of the vehicle depending on the road model [56]. Some researchers also learn models during the execution of the autonomous system [57], [58] in order to improve the decision-making performance. The models can also include environment events like wind coming from the side (large blue arrow in Figure 2.3). Finally, the traffic interacting with the autonomous vehicle can be simulated using traffic simulation engines like Sumo [59].

One limiting factor of tests in simulation environments is computation power. For this reason, research groups try to accelerate the simulation by parallelizing simulation flows [60] and reducing the complexity of the simulation that consists of many parts [48], [61].

Mature vehicle simulations can reduce development cost. For this reason, several commercial simulation software systems are available. Examples are Virtual Test Drive of Vires[1] presented

[1] `http://www.vires.com/docs/VIRES_VTD_Details_201403.pdf`

in [62], the Pre-Crash Scenario Analyzer (PRESCAN)[2] from Tass International presented in [63] and CarMaker of IPG Automotive[3]. Research teams are also working on integrating existing simulation components into a larger framework [64].

Hardware in the Loop (HIL) tests can further reduce the reality gap by using physical hardware for parts of the simulation. In this setup, parts of the system are included as real hardware. This can include electronic control units to run the software, and parts of the actuators and sensors. For example, the HIL tests can use the physical camera in combination with a computer screen [65] instead of a camera model. As an alternative, the VEHIL setup [66]–[68] models traffic participants as physical elements by using a base moving at the relative speed of the vehicle. This way, it can integrate physical radar sensors and laser scanners into the HIL setup.

2.3.2 Simulation with Driver Interaction

The HIL setup does not include a physical representation of the human sitting in the car. In the physical world, the human influences the system by interacting with its interface or intervening in critical situations. For the autonomous driving system, this adds additional nondeterminism. Driving simulators add this missing human element. Sensors and software systems require only a simulation of aspects they need for their core function. In contrast, a human behaves differently if the simulation does not feel real. Thus, a driving simulator has to recreate the physical world as realistically as possible. This includes vision, acoustics, the cabin interior and inertial effects of the vehicle movements. The latter aspect is the most challenging one. A widespread version of driving simulators mimic vehicle dynamics by moving a cabin, the driver sits in. A hexapod can rotate this cabin and simulate accelerations [69], [70]. Additional rails in one [71], [72] or two [73], [74] directions simulate long motions potentially with high acceleration in those directions. A cost and space efficient alternative to hexapod systems is using a robot arm [75].

Instead of using an indoor device, the Vehicle in the Loop (VIL) concept [76]–[78] uses physically moving vehicles and simulates the driver's vision. The vehicles move on a testing ground without obstacles. Inside the car, the passenger does not see the exterior, but a simulation. The virtual car moves in this simulation, interacts with traffic participants and encounters dangerous events while the physical car safely moves in an empty plane producing the same inertial effects. This setup is also used for testing autonomous driving systems without driver interaction in a realistic but safe environment [79].

The mechanisms described in the previous sub sections are not sufficient for generating the same behavior as in physical tests. In particular, they do not consider nondeterminism of sensors, actuators and traffic. Instead, they can be used as a basis to improve the simulation for the approach presented in this thesis.

[2] `https://www.tassinternational.com/prescan`
[3] `http://ipg.de/de/simulationsolutions/carmaker/`

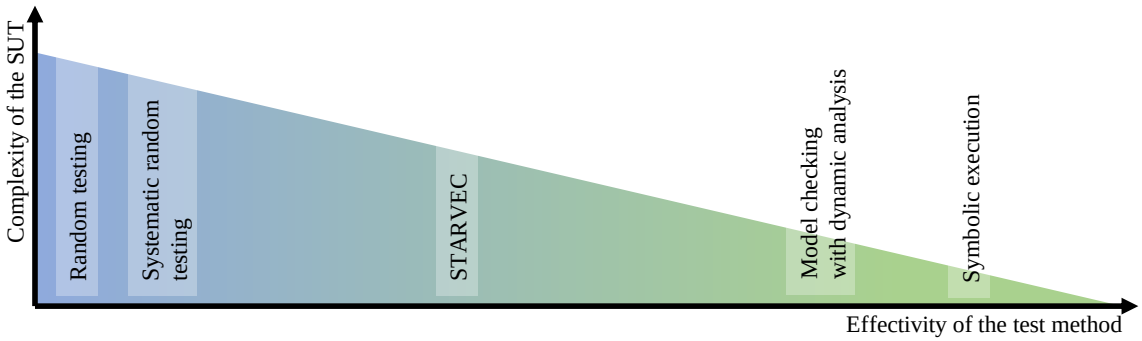

Figure 2.4: Classification of test methods according to the maximal possible complexity of the SUT and the effectivity in finding faults. Random testing can be applied to complex systems but misses many faults, whereas symbolic execution is limited to less complex systems but finds a large portion of existing faults.

2.4 Simulation with a Set of Possible Events

From the perspective of the planning and control algorithm in an autonomous vehicle, the vehicle and its environment behave nondeterministically. Nondeterministic input is a well-studied problem in software engineering. Typically, the nondeterminism is the input of a user or another system. Robust and secure applications have to ensure their functionality for arbitrary input. Symbolic execution is a successful approach for finding defects like access violations in software systems. The concept replaces real values of inputs and variables by symbols and branch conditions by constraints [80]. This way, it can execute a range of possible input values at once. A constraint solver generates actual inputs leading to a software error. Researchers have successfully applied symbolic execution to basic libraries of operating systems [80] and to generating exploits [81]. However, it suffers from the path explosion problem and generates constraints that can become hard to solve [82]. This makes it difficult to apply it to complex programs. For the programs analyzed by symbolic execution, the input is usually limited to a small size, which reduces the analysis computation requirements.

Figure 2.4 classifies test methods according of the maximal possible complexity of the SUT (System Under Test) and the effectivity of the test method in finding faults. This plot classifies symbolic execution as effective in finding faults. It does not reach the maximal effectivity because only restricted input spaces are checked. The low value in the vertical axis indicates that it can handle only a limited complexity of the tested software.

In order to cover problems that are more complex, the authors of [83] combine model checking with dynamic analysis. Similarly to the approach presented in this thesis, they use both sound and unsound abstractions for the decision whether the analysis has already visited a state. If the analysis has visited a state that is mapped to the same abstraction, it also considers the regarded state as visited. This allows model checkers to test complex software efficiently. Figure 2.4 lists the approach further to the left, as it might overlook some bugs due to the unsound abstractions. The unsound abstractions trade some effectivity for the ability to cope with higher

complexity. Model checking can also be used to ensure that a test method reaches high coverage according to some metrics. Some research teams [84], [85] generate test cases based on Linear Temporal Logic and model checking.

Collisions caused by planning and control software are still too complex for the abstractions mentioned above. Therefore, a typical approach in the automotive industry is to add random noise to sensor measurements. Testing tools like Exact [86], or Time Partition Testing (TPT) of PikeTec [87] support simulation with such noise. Frameworks like Open Robinos [88] can also add noise. Random testing is applicable to programs of any complexity and is thus listed with a high value in the vertical axis in Figure 2.4. The disadvantage is that they only test a very small subset of possible inputs and are hence not as effective in finding bugs as symbolic execution. In order to use this subset efficiently, researchers try to create a noise distribution that is close to reality [89], [90]. The authors of [91], [92] apply randomized algorithms for validating the collision probability of an Adaptive Cruise Controller in a simulation environment. Using Chernoff bounds, they estimate the number of experiments necessary for a predefined accuracy and reliability. They increase the efficiency by applying importance sampling: Prior known successful or failing tests are not executed. In Figure 2.4 this systematic random testing is listed as more effective than classic random testing. It achieves effectivity by the assumption that it already knows some successful test results, which reduces the maximal complexity of the system it can analyze. In [93], the impact of sensor noise on driver assistance functions is explored using a novelty search [94]. They apply periodic or constant noise patterns and evaluate the results focusing on creating as different results as possible. As they do not compare intermediate states, their method only finds constant noise patterns leading to undesired behavior. That is, the deviation between ideal and simulated sensor measurements remains constant. In contrast, the *STARVEC* algorithm presented in this thesis finds scenarios in which fluctuating error patterns are worse than constant patterns, as shown in Chapter 6. In Figure 2.4 the approach of [93] would be close to systematic random tests.

For actual automotive software further assumptions are applicable that fill the gap between systematic random testing and model checking. The authors of [95] use rapidly exploring random trees in order to determine the worst-case performance of a control component in the presence of disturbances to state variables. The approach works for a controller with a very limited set of state variables. This thesis extends a similar approach to more complex systems and error patterns.

2.5 Testing in the Physical World

In addition to virtual testing, physical tests are necessary to validate autonomous driving systems. Typically, professional test drivers or automated test systems[4] execute defined scenarios

[4]ATG, Automated Testing Ground: `https://youtu.be/8czFgk26qZ8`

either on a dedicated testing ground like AstaZero [96] or on public roads [97]. Engineers have to reproduce the faults occurring during these physical tests in order to understand and repair the causative defect.

Reproducing faults is also a challenge for the teams that participated in the DARPA Urban Challenge [98] and implement autonomous vehicles. They deal with faults by recording communication data when it occurs and replay the data in order reproduce it. Two of the eleven finalist teams explicitly describe how they reproduce failures [99], [100] and seven mention that they are able to record and playback communication data [101]–[107] most likely also used for reproducing faults. The remaining two teams do not explain how they deal with such problems [108], [109].

However, these logs can become very large and are not always sufficient for reproducing failures due to nondeterminism and missing initialization sequences. Some research groups reduce the size and the time necessary for replaying the communication logs by removing or shortening unnecessary parts [110], [111]. Instead of using communication signal logs, the input arguments of single functions are stored by [112]. If a fault occurs within this function, the authors can quickly replayed it with little effect of nondeterminism. Instead of a communication log, [113] uses general log messages emitted at any position in the code in order to reproduce the execution path leading to the fault. [114] automatically enhances log outputs in order to increase the performance of this method. If no logs are available, program crash dumps can guide randomized testing [115] trying to reproduce the fault. However, these methods do not robustly reproduce any faulty behavior caused by the complex inputs of planning and control systems. Section 5.3 shows how fault reproduction can be performed more robustly for automotive applications.

2.6 Sources for Test Scenarios

Both simulated and physical tests require defined test scenarios, which are extracted from

- requirement documents,
- problem understanding for creating parameterizable scenarios or
- gathered data.

Requirement documents are the first source for defining test scenarios. They should list the different types of scenarios to be expected. For each of these scenario types, there should be a test case either derived manually or supported by systematic specifications [116].

In addition to requirement documents, autonomous driving engineers understand the potential scenarios the function should support. By using this understanding, they can create test scenarios that cover as many relevant cases as possible. The authors of [117], [118] present a method for generating test cases for a parking system by evaluating the results of each test run. Using

a heuristic, they try to push the test executions toward collisions by altering the starting conditions, for example the shape of obstacles.

The third source of relevant scenarios is gathered data. Accident databases like the German GIDAS (German In-Depth Accident Study) database [119] provide such data. These databases contain information about the accident causes, which has been gathered by specialized teams after severe accidents. Other countries maintain similar databases. The efforts of [120] harmonizes these databases. As it contains particularly dangerous and difficult scenarios, the data from these accident databases is relevant for test cases. The authors of [121], [122] reproduce these scenarios and the street geometries of the accident in a simulation environment. The reconstruction can be enhanced by using three-dimensional geographic data for modeling the terrain characteristics. The reproduced scenarios are used to evaluate the expected performance of new driver assistance functions with additional sensors [123].

Alternatively, engineers can extract the data from physical test-drives. Wachenfeld et. al [124] propose to equip consumer vehicles with the necessary sensor and computing power to gather real world scenarios and perform short simulation sequences. As the scenarios are extracted from the real world, they have the same random distribution as in the real world. In frequently started short simulation sequences, an ADAS (Advanced Driver Assistance System) can take over control of the simulated vehicle. The shortness of the simulation increases the realism. If the ADAS causes a collision in the simulation, engineers can address the problem. The physical vehicle remains safe because a human controls it.

Scenario generation can also be supported by using laser scanners as a reference sensor system for recording real world scenarios [125] or running simulations parallel to actual task executions in order to detect faults [12]. Finally, there are public databases for relevant scenarios like Kitti for vision benchmarks [126] or the Next Generation Simulation Program [127] for traffic scenarios. This thesis contributes to the state of the art by proposing a method for collecting scenarios of almost-accidents during any physical vehicle drive. These almost-accidents only remained collision free, because the sensor and actuator inaccuracies did not affect the vehicle more strongly than they did.

Chapter 3

Modeling the Environment of an Autonomous Vehicle

The algorithm presented in this thesis searches for undesired behavior of an autonomous driving system in a simulation environment. For this purpose, it must be possible to produce the undesired behavior in a simulation environment. This chapter investigates how to design a simulation environment that supports the generation of physically possible behavior. First, Section 3.1 describes how a simulation environment can represent physical scenarios. It divides the simulation into an ideal behavior and separately handled inaccuracy models. Section 3.2 discusses modeling the ideal behavior. The description of inaccuracy models that enable the simulation environment to approximate physical behaviors follow in Section 3.3. These inaccuracy models have to be configured based on data from physical vehicles described in Section 3.4. Using the simulation, engineers can search for undesired behaviors as defined in Section 3.5.

3.1 Representing Physical Vehicle Scenarios in a Simulation Environment

The first step to simulate undesired behavior that is possible in reality is to ensure a correspondence between simulation and the physical world. The design of the simulation environment has to ensure this correspondence. This section starts with describing the physical world as a mathematical set of states and a transition function in Section 3.1.1. Section 3.1.2 describes the simulation system the same way. Finally, Section 3.1.3 investigates how these two systems relate to each other.

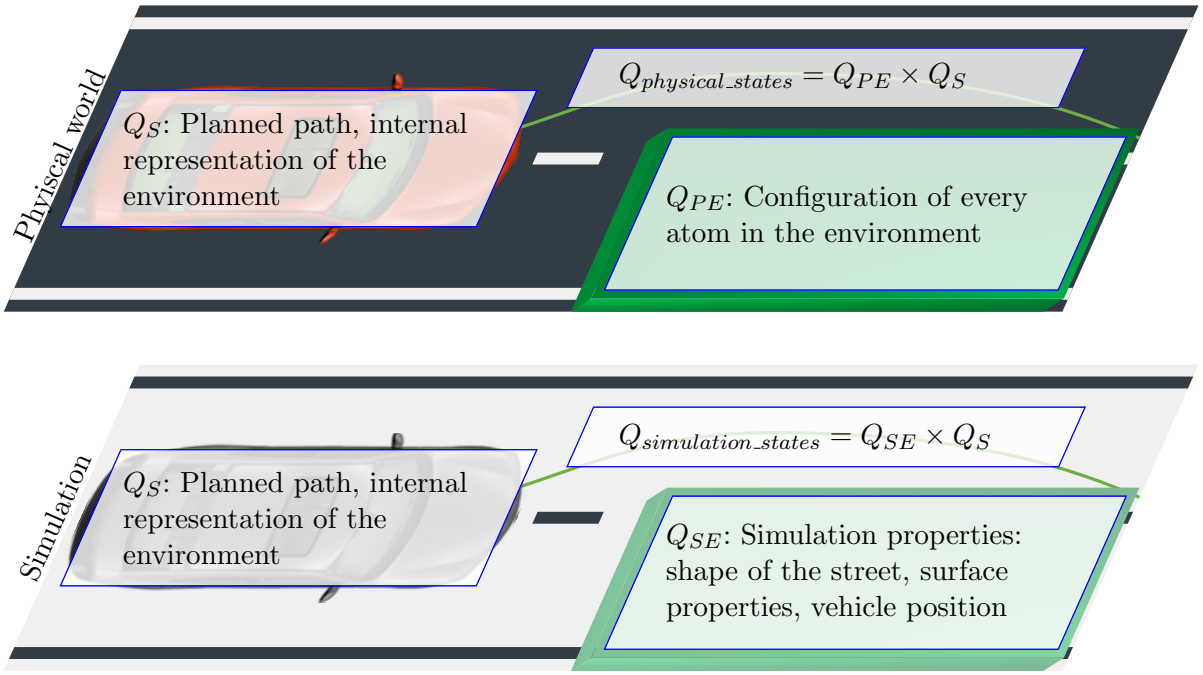

Figure 3.1: States in the physical world and states in the simulation world consist of the vehicle software state plus the state of the remaining world or the remaining simulation.

3.1.1 Modelling the Physical World

From a mathematical perspective, the state of the physical world is an element of the set of all possible physical states $Q_{physical\_states}$. The behavior of the physical world can be regarded as a function $F_{physical\_world}$ that determines the state of the world after a specified time $t \in \mathbb{R}^+$ has passed. If the physical world is known perfectly, this function can be approximated as deterministic.

$$F_{physical\_world} : Q_{physical\_states} \times \mathbb{R}^+ \to Q_{physical\_states} \tag{3.1}$$

As the focus of this thesis lies on representing the behavior of a vehicle, it is reasonable to divide the physical states into the states of the software system Q_S and the states of the physical environment Q_{PE}:

$$Q_{physical\_states} = Q_{PE} \times Q_S \tag{3.2}$$

This partition is also depicted in Figure 3.1. The state of the software system Q_S consists of all information stored by the software. This includes the path it plans to follow and the internal representation of the environment. The state of the physical environment Q_{PE} contains

everything else, including the configuration of every atom in the environment. As explained in the next section, the simulation environment can be split up similarly.

The software system consists of runnable entities, each of which has a cycle time. The runnable entity reads its input, performs computations and writes its result to the output ports after its cycle time has passed. Computations taking longer than the specified cycle time either are handled inside the runnable entity by storing intermediate values as an internal state or represent a software fault. This kind of fault can be detected by timing analysis tools and is not considered in this thesis. Most computations finish before the cycle time ends. Idle waiting time can extend these computations to take exactly as long as the cycle time. The remaining case are computations taking exactly as long as their allotted cycle time. Because of the discrete cycle times of the runnable entities, a time discrete finite state machine can represent the whole system:

$$\begin{aligned} \Delta_{physical\_world}(s_{pw}) &:= (F_S(s_{pw}), F_{PE}(s_{pw})) \\ s_{pw} &:= (x_{PE}, x_S) \\ F_S(s_{pw}) &:= F_S(x_S, y(x_{PE})) \\ F_{PE}(s_{pw}) &:= F_{PE}(x_{PE}, u(x_S)) \end{aligned} \tag{3.3}$$

where $\Delta_{physical\_world}$ is the transition relation. s_{pw} is the state of the physical world, which consists of the state of the physical environment x_{PE} and the state of the vehicle software x_S. F_S is the transition function of the software system, which depends on the current state of the vehicle software and the perception $y(x_{PE})$ of the environment state x_{PE}. F_{PE} is the transition function of the environment that depends on the current actions $u(x_S)$ of the software system and the current state of the environment. The state of the environment x_{PE} may contain the history of previous actions that affect the environment with some delay. The following sections use this representation to compare the transitions in the physical world to the transitions in a simulation system.

3.1.2 Modeling the Simulation System

The equivalent system can be defined for a simulation system by a set of simulation states

$$Q_{simulation\_states} = Q_{SE} \times Q_S \tag{3.4}$$

where Q_{SE} is the set of states of the SE (Simulation Environment) and Q_S is the set of software states as defined in the previous section. Similar to Equation 3.3, the transition function

Δ_{sim_world} of the simulation system can be represented as:

$$\begin{aligned} \Delta_{sim\_world}(s_{sw}, e) &:= (F_S(s_{sw}, e), F_{SE}(s_{sw}, e)) \\ s_{sw} &:= (x_{SE}, x_S) \\ F_S(s_{sw}, e) &:= F_S(x_S, y_{sim}(x_{SE}, e)) \\ F_{SE}(s_{sw}, e) &:= F_{SE}(x_{SE}, u(x_S), e) \end{aligned} \tag{3.5}$$

where s_{sw} is the state of the simulated world, e is an event, F_{SE} is the transition function of the simulation environment, x_{SE} is the state of the simulation environment and y_{sim} is the simulated perception. As before, the software system is represented by its transition function F_S, its state x_S and its currently performed action $u(x_S)$.

In contrast to the function representing the physical environment, Equation 3.1.2 explicitly includes events e that occur during a simulation step. These events represent nondeterministic behavior of the vehicle and the environment. Such nondeterministic events exist, because the simulation system does not model the physical world perfectly. Not modeled parts are assumed nondeterministic.

The transition function of the software F_S is the same as for the physical world. The perception y of the physical state x_{PE} is replaced by the simulated perception y_{sim} of the simulated world, which depends on the current event e. Similar to the transition function F_{PE} of the physical environment, the transition function F_{SE} of the simulation environment depends on the current state x_{SE} and the current input u. Additionally, it depends on the nondeterministic event e.

Equation 3.6 splits the transition function F_{SE} into the ideal behavior as described in Section 3.2 and deviations to the ideal model as described in Section 3.3. The split version of F_{SE} is:

$$F_{SE}(x_{SE}, u, e) = F_{SE,ideal}(E_x(x_{SE}, e), E_u(u, x_{SE}, e), u) \tag{3.6}$$

where $F_{SE,ideal}$ is the ideal behavior of the vehicle according to the vehicle model described in Section 3.2. Additionally to the current state and the applied action, it depends on the requested actions because the simulation state is modeled to contain a history of requests. E_x is the error applied directly to the simulation state as defined in Section 3.3.5 and E_u is the error applied to the input values as defined in Section 3.3.2. E_u may depend on the current simulation state including the history of previously applied actions.

Similarly, y_{sim} can be split into an ideal perception model $y_{sim,ideal}$ and deviations to the model:

$$y_{sim}(x_{SE}, e) = E_y(y_{sim,ideal}(x_{SE}), e) \tag{3.7}$$

where E_y is the inaccurate perception defined in Sections 3.3.3 and 3.3.4.

$F_{SE,ideal}$ and $y_{sim,ideal}$ can be computed by existing simulation tools like the ones mentioned in Section 2.3. The approach presented in this thesis makes no assumptions about the complexity of the simulation tool, i.e. it can be arbitrarily complex.

3.1.3 Correspondence between the Physical World and the Simulation

The goal of the simulation is to model the physical environment. Hence, every state s_{pw} in the physical world has a representation s_{sw} in the simulated world:

$$s_{sw} = R_{phys \rightarrow sim}(s_{pw}) \tag{3.8}$$

The ability to represent a physical state in a simulation environment does not imply the ability to represent a behavior. A behavior can be described as a sequence of states $(s_{pw,0}, s_{pw,1}, ..., s_{pw,n})$. This sequence can be mapped to a sequence of simulation states based on Equation 3.8. A simulation execution also visits a set of simulation states. In theory, a simulation execution that visits exactly the mapped states might exist. In practice, this is usually impossible for two reasons: Firstly, the simulation might run in an incompatible frequency. Secondly, numerical errors lead to slight deviations even if the simulation is almost perfect. Instead, the simulation can approximate a physical behavior by executing an approximated sequence. Each state of the approximated sequence has to be similar to a state of the physical sequence that is mapped using Equation 3.8.

Figure 3.2 visualizes the approximation. The upper part of the image represents the physical execution. It corresponds to the execution in the simulation environment in the lower part of the image. The small blue circles represent states in the physical and the simulated world. The physical states have a representation in the simulation environment represented by the vertical lines. However, these states are not identical to the states of the simulation sequence. Therefore, the represented physical states are mapped to the closest simulated state indicated by horizontal lines. Multiple physical states can be mapped to one simulation state. In Figure 3.2, $s_{pw,5}$ and $s_{pw,6}$ are mapped to $s_{sw,6}$. Some simulation states can have no physical state mapped to them, as $s_{sw,5}$ in Figure 3.2. If the distance to the closest simulation state indicated by the horizontal lines is short enough, the simulation sequence approximates the physical sequence.

This can also be formally measured: A sequence of n states observed in the physical vehicle $(s_{pw,0}, s_{pw,1}, ..., s_{pw,n})$ (small circles in the upper image) can be approximated in the simulation environment according to a distance metric

$$\mu_{distance} : Q_{simulation\_states} \times Q_{simulation\_states} \rightarrow \mathbb{R}_0^+ \tag{3.9}$$

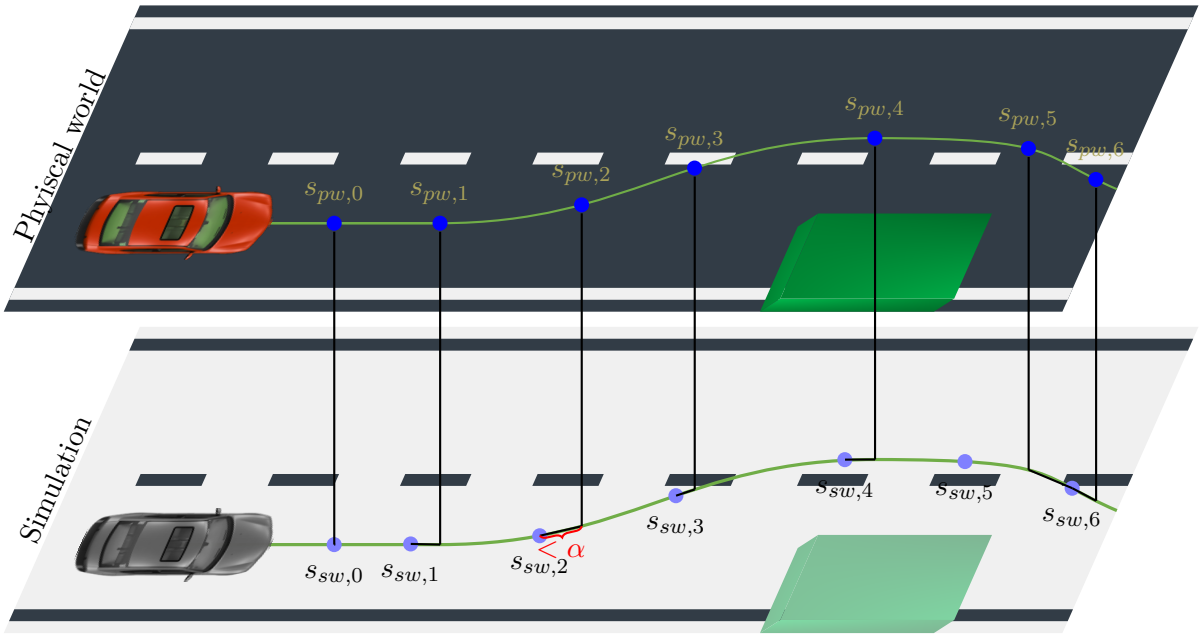

Figure 3.2: Representation of a physically driven sequence (upper part) in a simulation environment (lower part). Each physical state can be represented in the simulation (vertical lines) and is mapped to a simulated state (horizontal lines). The distance between the representation and the mapped state should be small ("$< \alpha$").

and an accuracy $\alpha \in \mathbb{R}$ (vertical lines) if the following conditions apply: Firstly, there is a sequence of m simulation states $(s_{sw,0}, s_{sw,1}, ..., s_{sw,m})$ and m simulation events $(e_0, e_1, ..., e_m)$ and a monotonous function $f_{mapping} : \mathbb{N}_0 \to \mathbb{N}_0$. Secondly, this sequence can be executed in the simulation system:

$$\forall i \in \{0, 1, ..., m-1\} : s_{sw,i+1} = \Delta_{sim\_world}(s_{sw,i}, e_i) \tag{3.10}$$

Thirdly, each state of the physical sequence is approximated by a state of the simulation sequence:

$$\forall i \in \{0, 1, ..., n\} : \mu_{distance}\Big(R_{phys \to sim}(s_{pw,n}), s_{sw,f_{mapping}(n)}\Big) \leq \alpha \tag{3.11}$$

The approximation error α and the mapping function $f_{mapping}$ are intended to compensate discretization effects but not significant deviations like model inaccuracies. This notion of approximation implies that an abstract error in the simulation environment can approximate a different error occurring in the physical world. For example, the physical vehicle accelerates with a delay of 0.1 s. In this example, the simulation environment does not model delays, but only offsets of up to 0.1 $\mathrm{m\,s^{-2}}$. However, this simulation environment might still be able to approximate physical vehicle sequences using the acceleration offsets. Section 3.3.2 further discusses this flexibility.

The whole simulation environment has a high recall if it can approximate all sequences observed on a physical vehicle as further discussed in Section 3.3.1.

A simulation sequence is physically possible if there is a corresponding sequence of states $(s_{pw,0}, s_{pw,1}, ..., s_{pw,n})$ that can be observed in the physical world. The simulation sequence has to approximate the representation of the sequence of physical states according to Equation 3.8. In practice, it is usually impossible to replay a sequence observed in a simulation environment in the physical world. Instead, software engineers can argue based on experience and for a single example whether it is reasonable to assume that a simulation sequence is physically possible.

Physically impossible sequences are a result of imprecise error models. Modeling extreme inaccuracies as events makes it simpler to create a simulation environment that can represent all sequences executed by a physical vehicle. However, this simulation environment will produce many sequences that are not physically possible. Such sequences are only a problem if a conclusion is based on these sequences. The approach presented in this thesis produces example sequences for detected undesired behaviors. Engineers can use these sequences to discuss for a single example whether it is physically possible. If the sequence is physically impossible, the simulation system can be refined to avoid such sequences while remaining able to represent all sequences observed in the physical vehicle. This is more efficient than eliminating all physically impossible sequences from the simulation system.

To summarize, the simulation environment should be able to approximate all physical behavior sequences. This can be ensured by designing the inaccuracies to the environment perception, the actions on the environment and the simulation state itself accordingly. Inaccuracies leading to physically impossible behaviors are only a problem if these behaviors are relevant. In this case, the inaccuracy models have to be adapted accordingly. An example definition of a simulation that can approximate physical behaviors is listed at the end of Section 3.3.2.

3.2 Vehicle and Environment Model

As explained in the previous section, the simulation environment is divided into a deterministic simulation and some nondeterministic error events. This section discusses the deterministic simulation. The simplest simulation environment that is able to represent all physical behavior patterns contains only a single simulation state. All physical states are mapped to this state. Hence, all physical state sequences can be mapped to sequences in the simulation. However, such a simulation would also be able to represent relevant but impossible physical sequences. For this reason, the simulation should at least model the basic geometry and dynamics of the vehicle.

The standard tool for modeling a vehicle used for static planning algorithms is the simple single-track model [128]:

$$\begin{pmatrix} \dot{x} \\ \dot{y} \\ \dot{\theta} \end{pmatrix} = \begin{pmatrix} v \cdot cos(\theta) \\ v \cdot sin(\theta) \\ v \cdot tan(\Psi)/L \end{pmatrix} \tag{3.12}$$

where x and y are the position, θ is the orientation, v is the speed, Ψ is the steering angle and L is the distance between the axles of the vehicle.

For low speed scenarios, the simple single-track model performs already similar to the actual vehicle if all actuators perform ideally. As the evaluations in this thesis are performed on low speed scenarios, they are based on a similar single-track model. As discussed in the previous section, this model is still able to represent all physical scenarios including high-speed scenarios if the inaccuracy models are designed accordingly. Section 3.3 describes these models. Similarly to the very simple model described at the beginning of this section, the simple single-track model can be insufficient for some applications. It can create deviations between simulation and reality that result in collisions in simulation and that are therefore relevant. However, these collisions are not physically possible. Thus, a suitable model for the scenarios to be tested must be chosen. For example, the simulation approaches described in Section 2.3.1 can be used for modeling the vehicle accurately. Furthermore, car manufacturers have developed their own models, which are particularly accurate for the properties important for specific development projects. Any of these simulation environments can be used together with the *STARVEC* framework presented in this thesis. The simulation environment is only required to be able to transmit its current vehicle state and allow setting the current vehicle state. Attaching any simulation environment is possible, because the concept directly executes the simulation without interfering with the actual model computations. The proposed error models only adjust the inputs and the outputs of the simulation tool.

3.3 Modelling Inaccurate Sensors and Actuators

The previous section introduced nondeterminism for closing the reality gap between simulation and the real world. Figure 3.3 illustrates some sources of nondeterminism. The nondeterminism covers

- inaccuracies of sensors and actuators,
- deviations between the used simulation model and an ideal model,
- variations to the scenario like different ground or changing wind conditions and
- additional nondeterministic events as described in Section 4.5.

The corresponding nondeterministic models are described in the following. First, Section 3.3.1 introduces the concept of precision, recall and efficiency advocating to aim for high recall.

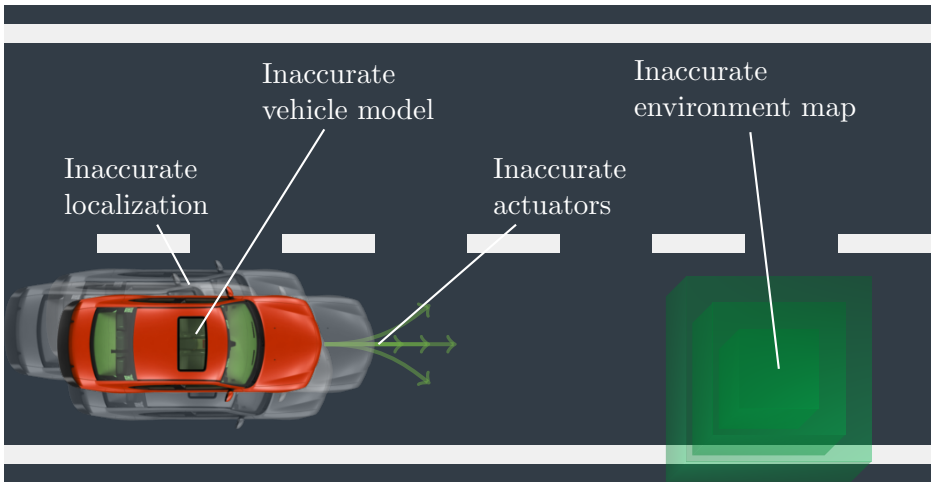

Figure 3.3: Sensors, actuators and the vehicle model are inaccurate.

The following sub sections describe the different kinds of inaccuracies. They cover actuator inaccuracies in Section 3.3.2, positioning inaccuracies in Section 3.3.3, mapping inaccuracies in Section 3.3.4 and model inaccuracies in Section 3.3.5.

3.3.1 Precision, Recall and Efficiency

The sensor and actuator inaccuracy models must represent the reality as well as possible. The models receive parts of the simulation state as input and compute possible behaviors as output. As these models include nondeterminism, multiple resulting patterns are possible. For example, a gas pedal model receives the current acceleration command as input and generates possible resulting vehicle velocities as output. The quality of the model can be represented based on three metrics: The model should achieve high

- recall,
- precision, and
- efficiency.

Recall is the "proportion of all the relevant documents in the collection that are in the result set" [129]. In the context of this section, the result set is the set of generated behaviors and the relevant set is the set of physically possible behaviors. Hence, high recall means that actions that can be observed of physical sub systems can also be generated by their simulated counterpart. The gas pedal model mentioned above has a high recall if the observed velocities in the physical world are included in the model output. A trivial gas pedal model achieving 100% recall emits the full velocity range as output. If the whole simulation has a high recall, undesired behaviors that can occur in reality can also be reproduced in simulation. Precision is the "proportion of documents in the result set that are actually relevant" [129]. In the context of this section,

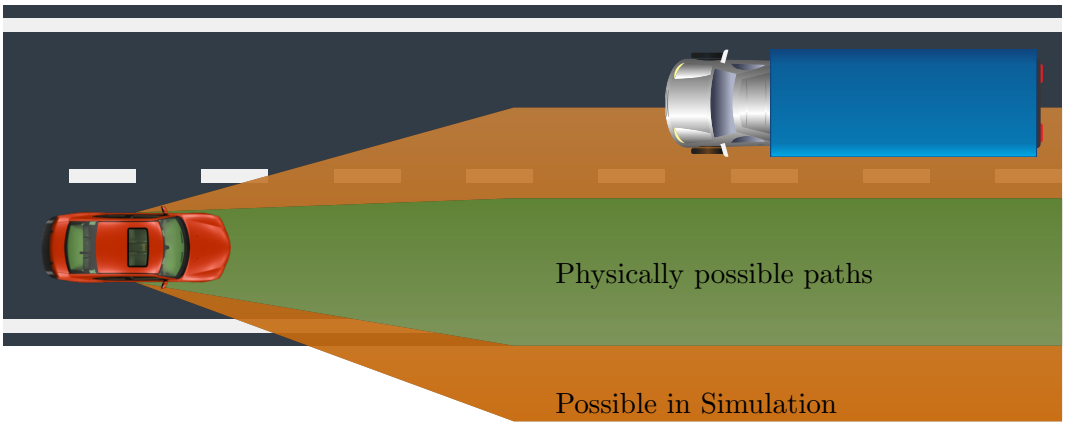

(a) High recall, low precision

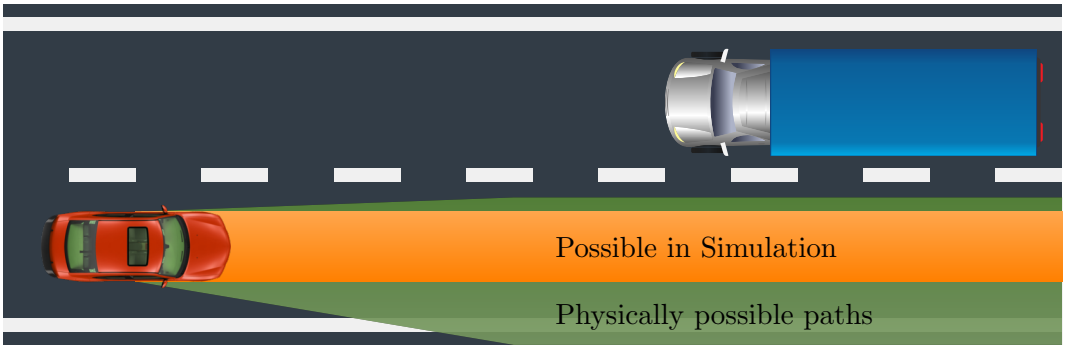

(b) High precision, low recall

Figure 3.4: Recall vs. precision: Figure 3.4(a) shows that low precision can lead to accidents that are predicted but physically impossible. Figure 3.4(b) depicts a physically possible unintended lane departure that the simulation does not predict.

high precision means that the inaccuracy model does not allow more deviation from the ideal behavior than the physical world does. A gas pedal model allowing exactly one resulting velocity for any requested acceleration achieves high precision.

Figure 3.4 illustrates the effects of precision and recall. The green and orange shapes depict the area that the red ego vehicle might cover in the future. Both shapes are broader than the vehicle, because sensor and actuator inaccuracies can lead to different behaviors covering different areas. The green shape contains all physically possible paths that a perfect simulation would predict. The orange shape depicts the behaviors predicted by the imperfect simulation. Figure 3.4(a) shows the effect of high recall, but low precision. The simulation (orange shape) predicts all behavior patterns that are possible in the physical world (green shape). However, the simulation additionally predicts patterns that are not physically possible including a frontal collision with the approaching truck. A test method using this simulation would falsely classify the autonomous driving system as unsafe. In contrast, Figure 3.4(b) depicts a simulation that achieves high precision by assuming ideal behavior of sensors and actuators. This simulation correctly predicts

that no collision with the truck is possible, but fails to predict than an unintended lane departure is possible. A test method that uses this simulation cannot find any errors of the autonomous driving system, although an error is possible.

The third metric is efficiency. Efficiency includes test computation efficiency and model validation efficiency. Test computation efficiency means that the model enables the test algorithm to be efficient. The test method presented in this thesis is more efficient if the model output is described by few parameters. For example, the acceleration inaccuracy can be modeled to result in a range between a minimal and a maximal possible acceleration, which corresponds to a single parameter to be varied. Other test methods may have other requirements for the models. Hence, the test computation efficiency depends on the used testing concept. The second part of efficiency is model validation efficiency. High model validation efficiency means that only a low amount of physical vehicle drive data is necessary for determining inaccuracy boundaries. Section 3.4 explains this process. A model that computes the output based on the input plus a value between a minimal and a maximal offset can be validated efficiently. Each data point of a physical test-drive directly contributes to all model parameters: the minimal and the maximal offset. A model containing many special cases cannot be validated efficiently. Each data point of a physical test-drive only contributes to the currently active special case. This requires a large amount of data in order to have sufficient information for each model parameter.

The first goal of creating a model is to achieve high recall. This corresponds to the concept of over-approximation often used for verification [130]. If the test algorithm then classifies the autonomous driving system as safe, the precision of the model is sufficient. If it finds weaknesses that seem physically impossible, engineers should increase the precision, possibly at the cost of efficiency.

3.3.2 Actuator Inaccuracies

The main vehicle actuators are the acceleration (gas pedal, brake) and the steering (steering wheel) actuators. Hence, the action $u(x_S)$ in Equation 3.1.2 can be written as:

$$u(t) := u(x_S(t)) = \begin{pmatrix} a(t) \\ \Psi(t) \end{pmatrix} \tag{3.13}$$

where $x_S(t)$ is the state of the software at time t, $a(t)$ is the requested acceleration at time t, $\Psi(t)$ is the requested steering angle. A more precise model might include additional actuators like light switches or gear selection.

The first input is the acceleration. Figure 3.5[1] shows some of the factors influencing the performed acceleration. Each of these factors can have a complex influence on the actually performed acceleration as expressed in Equations 3.14-3.17.

$$a_{act}(t) = F_{wheel}(f_{torque}(t), s_{pw,t}) \tag{3.14}$$
$$f_{torque}(t) = F_{motor,brake}(c_{commands}(t), s_{motor}(t)) \tag{3.15}$$
$$c_{commands}(t) = F_{ECU}(f_{torque,desired}(t), s_{ECU}(t)) \tag{3.16}$$
$$f_{torque,desired}(t) = F_{acccontr}(a_{des}(t), s_{acccontr}(t)) \tag{3.17}$$

The actually performed acceleration $a_{act}(t)$ depends on the road conditions, the state of the wheels, the dynamic state of the vehicle and many other influences. Equation 3.14 summarizes that as a function F_{wheel} of the applied torque $f_{torque}(t)$ and the state of the physical world $s_{pw,t}$. In exceptional cases, the acceleration may have no direct correlation to the applied torque. Such cases can be modeled separately. For normal operation, Equation 3.18 simplifies the complex correlations to a nondeterministic function $\hat{F}_{wheel}$. It implements a factor between a minimum $c_{w,min}$ and a maximum $c_{w,max}$, an offset between $-o_w$ and o_w and a delay Δt_w to the ideal translation of torque to acceleration. However, neither the maximal factors, nor the maximal offset or the delay is known.

$$\hat{F}_{wheel}(f_{torque}(t)) \in [c_{w,min}; c_{w,max}] * F_{w,ideal}(f_{torque}(t - \Delta t_w)) + [-o_w; o_w] \tag{3.18}$$

The state of the motor itself is complex, too. It consists of the state of the throttle, the state of the cylinders, of the direct injection motors, the emission control systems and other factors summarized as $s_{motor}(t)$ in Equation 3.15. The ECU (Engine Control Unit) controls these states and the behavior of the motor by commands $c_{commands}$. The state of the motor and the commands of the ECU define the resulting torque by some unknown function $F_{motor,brake}$ as described in Equation 3.15.

The ECU defines these commands by its implementation F_{ECU}. Additionally to implementing the desired torque $f_{torque,desired}$, it aims at smoothing the vehicle motion, reducing emissions, extending the motor life and several other goals influencing its internal state $s_{ECU}(t)$ in Equation 3.16. The smoothing mechanisms lead to inertia effects and the torque not being implemented at the requested time. However, the engine controllers are designed to converge towards the desired torque. That is, after some time $\Delta t_{ECU} \in [\Delta t_{ECU,min}, \Delta t_{ECU,max}]$ (with a constant request) the

[1] Public domain icons from `https://commons.wikimedia.org/wiki`: Digifant.jpg, Servofreno_seccionado.jpg, Throttle_body.jpg, and Sparkplug.jpg

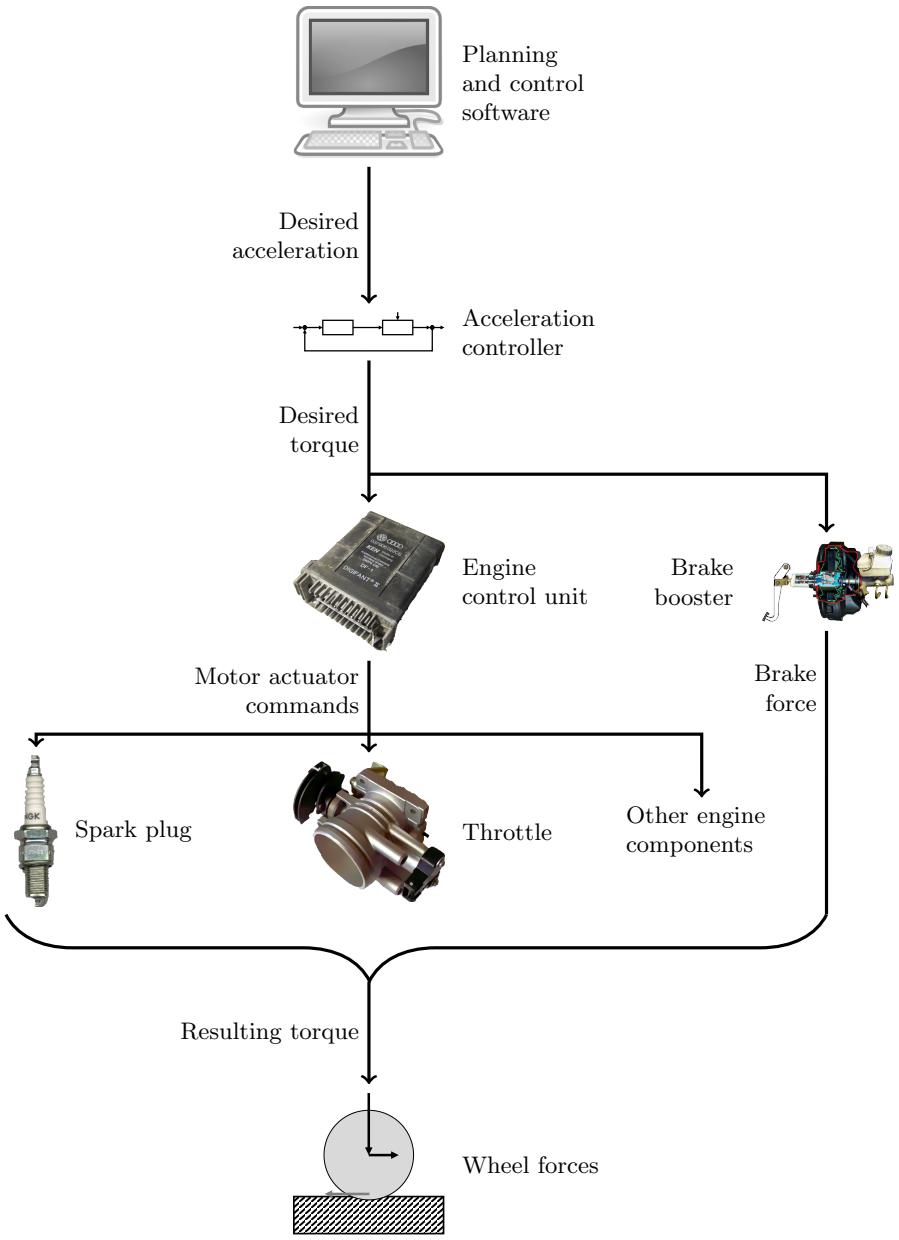

Figure 3.5: Components influencing the performed acceleration: the acceleration controller converts the desired acceleration to a desired torque, which it passes to the engine and the brake control units. These units generate commands for their hardware components leading to a resulting torque and a resulting acceleration.

engine performs a torque that differs from the desired torque by less than some offset o_{ECU}:

$$\hat{F}_{ECU} = f_{torque,desired}(t - [\Delta t_{ECU,min}, \Delta t_{ECU,max}]) + [-o_{ECU}; o_{ECU}] \tag{3.19}$$

The offset and the delay depend on the implementation of the ECU and the performance of the physical translations and are hence not known.

Finally, some current serial production cars have an additional acceleration controller. It computes the desired torque $f_{torque,desired}(t)$ based on the desired acceleration $a_{des}(t)$ and its internal state $s_{acccontr}$ as listed in Equation 3.17. As for the engine control unit, this controller aims at multiple goals including smooth behavior of the vehicle. It is also designed to converge towards the requested acceleration. Hence, after some time with a constant desired acceleration, the performed and the desired acceleration are similar:

$$\begin{aligned} a_{act}(t) &\in [a_{\min}(t); a_{\max}(t)] \\ a_{\min}(t) &= min_{t_{\text{ref}} \in [t-d_{\max};t]}(a_{\text{des}}(t_{\text{ref}})) - o_{\max} \\ a_{\max}(t) &= max_{t_{\text{ref}} \in [t-d_{\max};t]}(a_{\text{des}}(t_{\text{ref}})) + o_{\max} \end{aligned} \tag{3.20}$$

$a_{act}(t)$ is the performed acceleration at time t, $a_{\min}$ and $a_{\max}$ are the minimal and the maximal acceleration possible due to the nondeterminism. $d_{\max}$ is the maximal delay and $o_{\max}$ is the maximal offset between the requested and the performed acceleration.

The acceleration controller does not converge for accelerations that are requested for a very short period of time. If the acceleration requests alternates between a very low and a very high value, the performed acceleration is somewhere in between, but gets neither near the low, nor the high request. This behavior is also included in the approximating equation 3.20. The original Equations 3.14-3.17 are very complex, and contain many unknown values. Therefore, it is reasonable to directly estimate the few parameters of the approximated equation instead of the many parameters of the original equations. Due to the non-determinism, the behavior of the complex original equations is included in the approximated equations.

A more radical approximation would model only offsets to the desired acceleration instead of offsets plus delays:

$$a_{act}(t) \in [a_{\text{des}}(t) - o_{\max}; a_{\text{des}}(t) + o_{\max}] \tag{3.21}$$

With $o_{\max}$ being the maximal allowed offset to the steering angle. This model is still able to perform all behaviors possible by Equations 3.14-3.17. In a project connected to this thesis, physical vehicle tests were performed. In these tests, a strong influence of delays to the performed

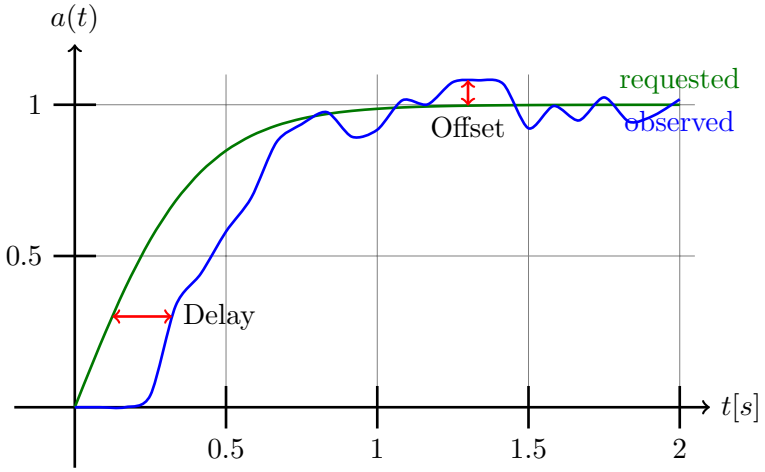

Figure 3.6: Effect of offsets and delays to the observed output. For rapidly changing inputs, the delay is the dominating pattern, for almost constant inputs, the offset dominates.

accelerations could be observed. Figure 3.6 illustrates the different effects of delay and offset to the performed acceleration. The depicted maximal offset is as low as $0.05\,\mathrm{m\,s^{-2}}$, but there is a constant delay of 0.2 s. Modeling this delay as offset results in a maximal offset of about $0.5\mathrm{m\,s^{-2}}$, which is reached at $t = 0.25\mathrm{s}$. This means a very low precision of the model. Therefore, the suggested model for acceleration inaccuracies consists of an offset interval and an interval between zero and the maximal acceleration delay $d_{\max}$ as shown in Equation 3.20.

This model allows efficient testing as the output can be described by a single parameter that defines which acceleration between the minimum and the maximum is executed. Small variations of these parameters lead to small changes of the vehicle behavior. The model also allows efficient model validation as it includes no special cases. Special cases can be necessary for some situations. For example, some vehicles show higher offsets when starting from zero velocity. Additionally, quick changes to the acceleration request can lead to overshoots in the performed acceleration [131]. Modeling such special cases increases the precision of the model at the cost of efficiency as proposed at the end of Section 3.3.1.

Section 3.1.3 demands that there is a correspondence between the physical world and the simulation. For a behavior in the real world, there should be a representation in the simulation such that Equation 3.11 holds. If we regard an example in which only acceleration errors are relevant, the inaccuracy model defined in this section fulfills this demand with:

- $\mu_{distance}(s_1, s_2)$ is the Euclidean distance between the vehicle centers of states s_1 and s_2.
- The simulation states consist of the vehicle position, velocity and acceleration.
- $R_{phys \to sim}$ maps these continuous physical values to the nearest floating point numbers.
- The discretization is chosen to be $\alpha/2$.

With these definitions, the simulation can approximate any acceleration behavior of the physical world if the maximal acceleration offsets and delays are sufficiently high.

The combination of offset and delay can also model other temporal effects like inertia effects. The steering inaccuracy is very similar to the acceleration inaccuracy with a different relation between offset and delay.

In summary the inaccurate action E_u in 3.6 can be described as:

$$E_u(u, x_{SE}, e) := \begin{pmatrix} a_{act}(t) \\ \Psi_{act}(t) \end{pmatrix} \tag{3.22}$$

Where $a_{act}(t)$ is the performed acceleration defined in Equation 3.20. The actual value is chosen as defined by the current nondeterministic event e. Analogously, $\Psi_{act}(t)$ is the performed steering angle.

3.3.3 Positioning Inaccuracies

Autonomous vehicles use two different systems for estimating the position and the motion of the vehicle: vehicle odometry and external position information. The vehicle odometry uses wheel motion and inertia measurement sensors for estimating the relative motion of the vehicle. Its accuracy decreases with the distance traveled due to undetected drifts and slips [129]. Therefore, a second system measures globally correct positions. This system can be based on a Global Navigation Satellite System [50], artificial or natural landmarks [52] or other concepts. The estimations of the system can jump, because of the incorporation of new information like another satellite or a detected landmark. Autonomous planning and control systems can access information from both systems.

Figure 3.7 shows exaggerated inaccuracies of these two positioning systems. The upper image (Figure 3.7(a)) shows inaccuracies of the global positioning system. The deviation drifts away from the true position, but every time the positioning system detects a new landmark or satellite, it jumps back to the approximated true position. Some localization systems avoid these jumps by replacing them with slow drifts back to the true position. The lower image (Figure 3.7(b)) shows inaccuracies of the odometry. The position estimations are smooth, but the deviation to the true position has no upper limit.

The model for global position inaccuracies used in this thesis is a drift of the position and the orientation of the vehicle. For example, the estimated x position $x_{\text{estimated}}(t)$ is computed as:

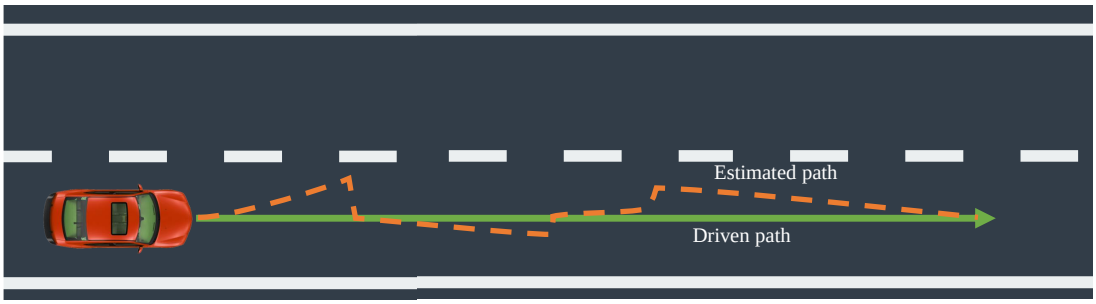

(a) Global positioning inaccuracy

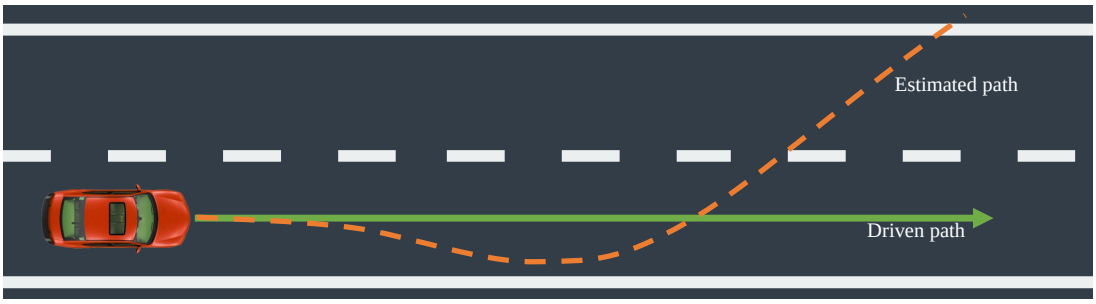

(b) Inaccuracy of the odometry

Figure 3.7: Inaccuracies of positioning sensors. The top image shows typical global positioning inaccuracies including jumps. The lower image shows inaccuracies of the odometry without jumps but high final inaccuracies.

$$
\begin{aligned}
x_{\text{estimated}}(t) &= x_{\text{real}}(t) + x_{\text{offset}}(t) \\
x_{\text{offset}}(t) &= \begin{cases} x_{\text{new}}, & \text{if new position is measured} \\ x_{\text{offset}}(t - \Delta t) + x_{\text{drift}}(t), & \text{else} \end{cases} \\
x_{\text{drift}}(t) &\in [x_{\text{drift,min}}; x_{\text{drift,max}}] \\
x_{\text{new}} &\in [x_{\text{new,min}}; x_{\text{new,max}}]
\end{aligned} \tag{3.23}
$$

where $x_{\text{real}}(t)$ is the actual x position of the vehicle and $x_{\text{offset}}(t)$ is the measurement offset to the real x position. x_{new} is the measurement error after reading new positioning data. It can be wrong by a value between a minimum $x_{\text{new,min}}$ and a maximum $x_{\text{new,max}}$. In the experiments in Section 6, this interval is modeled to be empty. x_{drift} is the velocity at which the measured x position may deviate from the real x position and can be between a minimum $x_{\text{drift,min}}$ and a maximum $x_{\text{drift,max}}$. Additionally, the absolute offset is limited to a maximal value.

The inaccuracy of the odometry is similar without the option to jump back to a new measured value. The odometry model has been implemented together with delays and inaccuracies of the velocity measurement in [131] and is tested in the evaluation chapter.

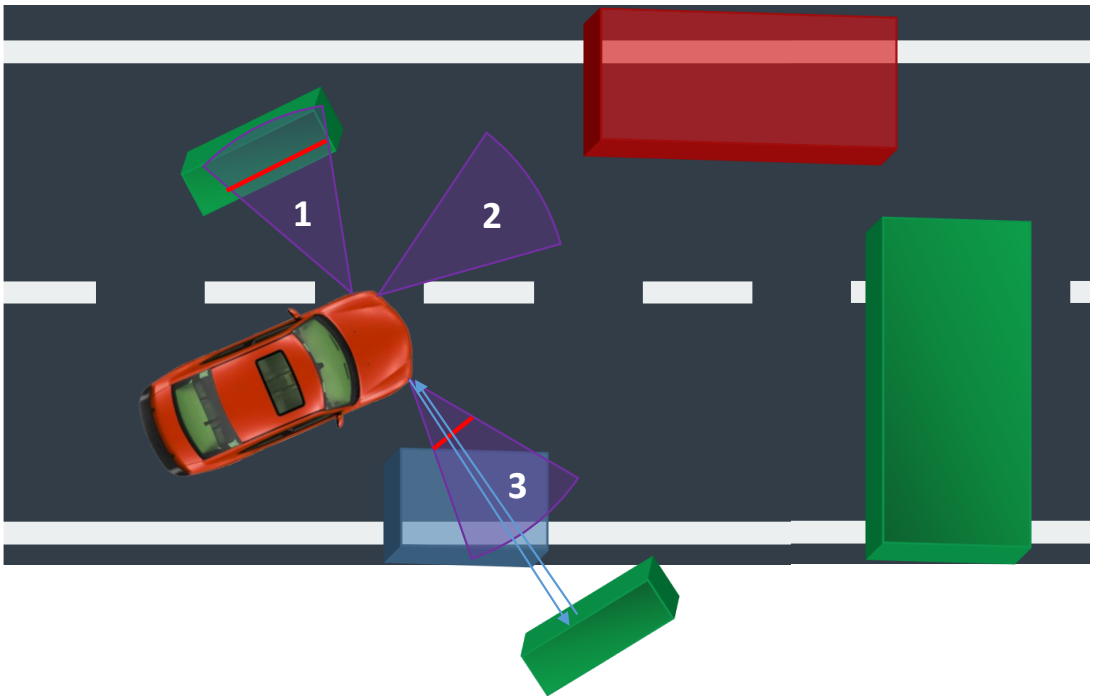

Figure 3.8: Inaccuracies of ultra sonic sensors. The upper left green box is detected at an inaccurate position due to ambiguous measured maxima (1). The red box is not detected due to insufficient sensor range (2). The bottom green box is out of the sensor range (3) but leads to a not existing obstacle (blue box) being identified.

3.3.4 Mapping Inaccuracies

Autonomous vehicles perceive their environment based on various sensors including radar, ultrasonic, laser scanners and centrally stored maps.

Ultra sonic sensors generate acoustic signals that are reflected by obstacles in the environment. Figure 3.8 depicts three sources of errors of ultrasonic sensors: inaccurate measurements, sensor capability limits and wrong signal assignment. They are related to effects visible in the raw sensor signals depicted in Figure 3.9.

The first error source is inaccurate measurements. As depicted in Figure 3.9 the regarded signal does not instantaneously change from zero to maximum. Additionally, sensor noise surrounds the increase. Therefore, the return time of the acoustic signal cannot be determined precisely. This leads to obstacles being detected at positions that deviate from reality. Accordingly, in Figure 3.8 the detected obstacle (red line) of the top left sensor (cone 1) does not exactly match the perimeter of the corresponding real obstacle (green box).

The second error source are sensor capability limits. One such limit is the minimal and maximal sensor range. Ultrasonic sensors cannot detect obstacles closer than some minimum because the emitted signal blinds the sensors for some time as depicted in Figure 3.9. Moreover, they cannot detect obstacles that are further away than some maximum, because the reflected signals get

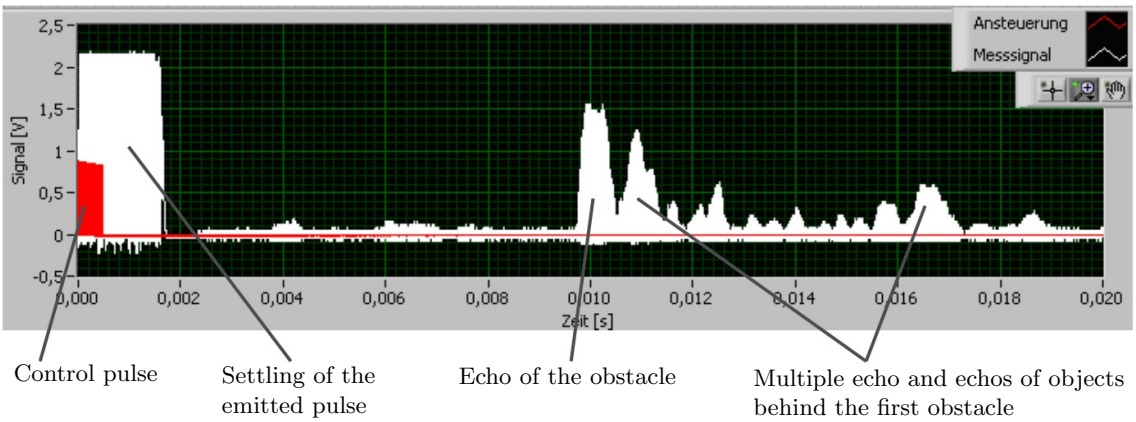

Figure 3.9: Visualization created by [132] of measurements of an ultrasonic signal showing settling time, noise and multiple echoes.

too weak. Furthermore, obstacles have different signal reflection properties possibly leading to objects not being detected. In Figure 3.8, the front sensor (cone 2) does not detect the top right obstacle (red box).

Finally, previously emitted signals can be echoed late and related to a later measurement. For example, an object outside the theoretical sensor range can reflect the signal particularly well leading to its echo being detected in the next measurement cycle. Alternatively, the echo can be reflected multiple times and therefore return to the sensor too late. Such effects can lead to an obstacle detection without a corresponding obstacle in reality. In Figure 3.8, the blue obstacle at cone 3 is detected due to such mechanisms.

Radar and laser sensors can produce false and inaccurate measurements due to similar reasons. For example, laser sensors can misinterpret measurements of the ground plane as obstacles.

Sensor fusion algorithms can correct some of the sensor measurement errors by evaluating several measurements of the same position. For example, occupancy grids divide the space in separate cells [133], [134]. For each cell c_i, they accumulate the existence probability p_j of several measurements. These measurements originate from different sensors and different measurements of the same sensor. The measurements can have different weights w_j based on their age and the sensor type:

$$P(c_i) = \frac{\sum_j w_j \cdot p_j}{\sum_j w_j} \tag{3.24}$$

Due to the fusion of several sensor signals, a single false measurement does not lead to an error in the environment map. However, false measurements caused by the physical properties of the measured object can still lead to errors in the fused map. Additionally, the sensor fusion

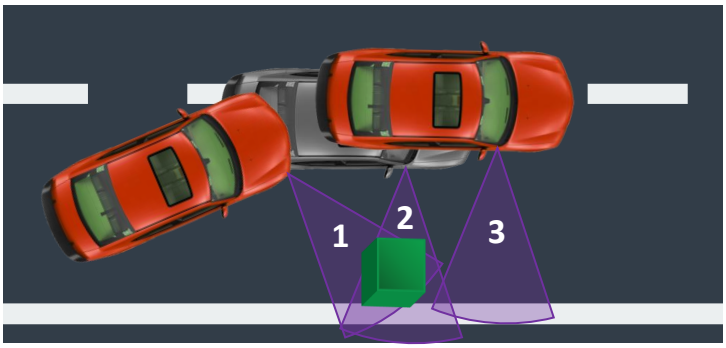

Figure 3.10: Mapping error caused by a positioning error: Measurement 1 correctly identifies an obstacle. Measurement 3 correctly identifies free space. The wrong estimation of the vehicle position leads to measurement 3 being interpreted as cone 2. As a result, the obstacle is considered not to exist anymore.

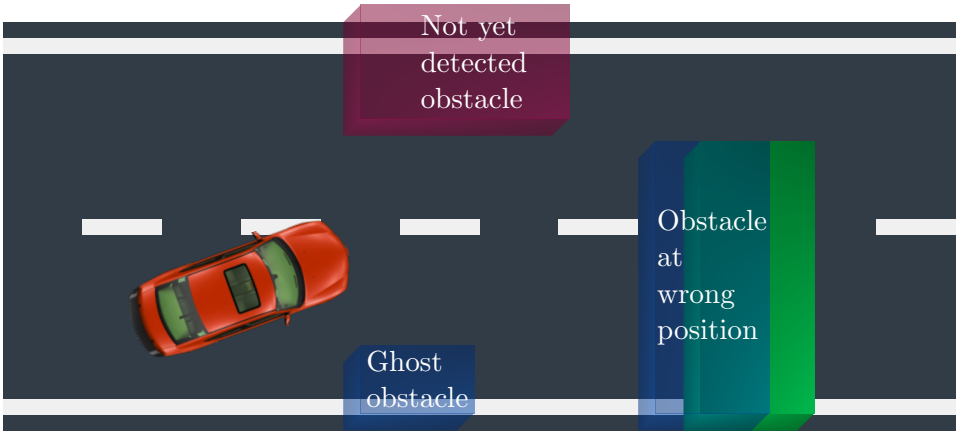

Figure 3.11: Inaccuracies of the environment map include obstacles detected at the wrong position, not detected obstacles and detected but not existing obstacles.

algorithm depends on a correct estimation of the vehicle motion. Figure 3.10 depicts a scenario in which correct sensor measurements but false ego position estimations lead to mapping errors: First, measurement 1 correctly identifies an obstacle. Next, measurement 3 correctly identifies free space. The wrong estimation of the vehicle position leads to the assumption that the cone of measurement 3 is actually at position 2. Hence, the position at which the obstacle has been identified is measured to be empty. As a result, the sensor fusion algorithm either classifies the obstacle as a measurement error, or as not existing anymore.

In total, the fused map data contains inaccuracies that are similar to the inaccuracies of the single sensors. Figure 3.11 shows possible inaccuracies of the environment map at this abstraction level. The transparent blue boxes are measured obstacles, the red and the green boxes are real obstacles. The left blue box represents a measured obstacle that does not physically exist. It makes the vehicle execute an unnecessary evasive maneuver. The right blue box is the inaccurately measured representation of the physical green obstacle. Engineers have to consider such offsets when choosing the safety distances of the planning algorithm. Finally, the red

obstacle is not detected at all in the current time step. The later it is detected, the higher the risk of a collision.

Some of these inaccuracies have been implemented for the *STARVEC* algorithm in the Master Thesis [131]. Inaccurate position measurements can be represented by adding offsets to the positions of measured obstacles. Obstacles that are measured but do not exist can be represented by adding obstacles to the measurements. However, this only tests some positions for ghost obstacles, rather than all possible positions. Not detected obstacles are removed from the fused map. The not detected obstacles can be a pre-defined set of potentially not detected obstacles or a rule, for example a maximal sight radius. In Chapter 6, inaccuracies corresponding to not detected obstacles and inaccuracies corresponding to displaced obstacles are evaluated. Figure 3.11 only includes inaccuracies of the static environment map. Dynamic obstacles are dealt with in Section 4.5.

Together, the positioning inaccuracies described in Section 3.3.3 and the mapping inaccuracies described in this section form the inaccurate environment perception $y_{sim}(x_{SE}, e)$ defined in Equation 3.7.

3.3.5 Model Inaccuracies and Scenario Specific Nondeterminism

Additionally, to the sensor and actuator inaccuracies listed above, the model of the vehicle itself is not perfect. The deviation from the physical vehicle can also be modeled as nondeterminism. Instead of changing the sensor measurements or actuator behavior this nondeterminism directly changes the state of the vehicle. The same concept of precision and recall discussed for sensor and actuator inaccuracies also applies to model errors: If the model of the vehicle is very inaccurate–for example it only models driving straight ahead–very high model inaccuracies have to be assumed. The result is to falsely classify the autonomous driving system as unsafe. Model uncertainty also covers variations to street surface conditions.

Model inaccuracies also cover deviations between a model designed for low speed motions and a vehicle driving fast. For low speed motions, the single-track model is very accurate. For high-speed scenarios, the vehicle may for example drift laterally. Using an inaccurate model leads to high inaccuracy boundaries as described in Section 3.4. High inaccuracy boundaries lead to collisions being predicted in simulation that are not actually physically possible. In such cases, the developers have to switch to a more complex model that more adequately represents the vehicle behavior. If the high inaccuracy boundaries do not lead to undesired behavior, it is not necessary to improve the model. Hence, the boundary at which it is necessary to switch to models that are more complex depends on the use cases of the developed software system.

Finally, there can be scenario specific nondeterminism. The example of traffic participants is discussed in Section 4.5. Other examples would be sensor failures, or driver interventions for which the performance of the planning system is tested.

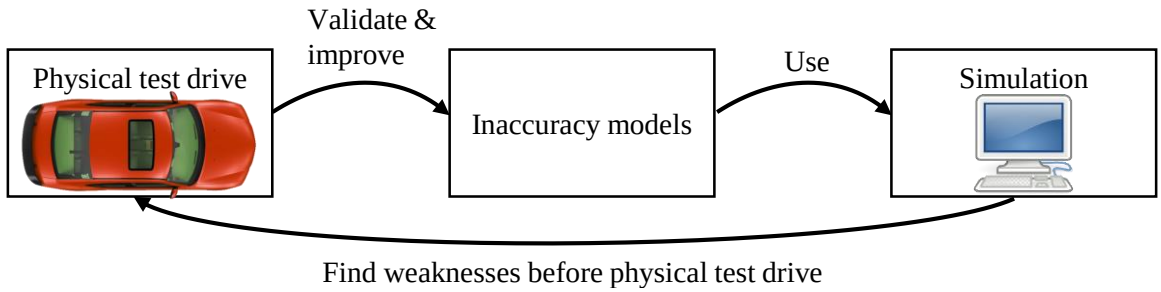

Figure 3.12: Extracting inaccuracy models from physical test-drives: Physical test-drives improve (arrow "validate and improve") the inaccuracy models that are used (arrow "use") for simulation. Simulation eliminates some weaknesses before they are detected in physical test-drives.

In summary, the inaccurate actuators defined in Section 3.3.2, the inaccurate perception defined in Sections 3.3.3 and 3.3.4 and the inaccurate model defined in this section contribute the three nondeterministic elements defined in Section 3.1.2. The deterministic part of the simulation is the used simulation environment itself and may be based on the simple model provided in Section 3.2.

3.4 Determining Inaccuracy Boundaries

The possible effects caused by the inaccuracy models described in the previous section depend on the boundaries of the defining parameters. For example, the gas pedal model depends on the maximal delay and the maximal offset to the acceleration request. Choosing the right boundary is the precondition for creating a model with a high recall. The boundaries can be determined based on data from physical test-drives as depicted in Figure 3.12. Physical test-drives improve the inaccuracy models that the simulation uses. In return, the simulation prepares physical test-drives by eliminating weaknesses of the planning and control system. This way the next set of physical test-drives can focus on the remaining errors.

As explained in the previous sections, engineers should choose inaccuracy boundaries aiming to achieve high recall. This means that every data point that is received from test-drives has to be a possible result of the inaccuracy models. However, there is not only one choice of possible inaccuracy boundaries. As explained in Section 3.3.2, the delay shown in Figure 3.6 can be assumed zero or small at the cost of very high boundaries to the acceleration offset. Determining the boundary values is a multi-objective optimization problem: minimizing the maximal delay without increasing the maximal offset is not possible. Such problems can be solved either interactively or based on a cost function [135]. For solving it interactively, first the Pareto front of possible solutions is computed or approximated. Figure 3.13 shows one example for a Pareto front computed by [131] based on the results of physical vehicle experiments. If a higher maximal delay is assumed, the resulting maximal offset decreases.

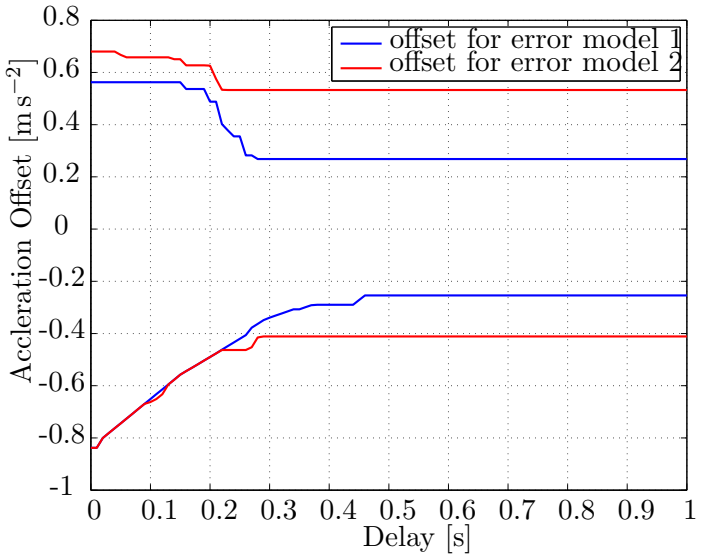

Figure 3.13: Pareto front of possible offset and delay parameters extracted from physical vehicle drive data by [131]. By assuming a high delay, lower maximal offsets can be concluded. The experiment was conducted with two different error models.

Among the solutions of the Pareto front, the software engineer chooses the best solution. As all solutions maximize the recall, the best solution is the one that also maximizes the precision. That means the best solution leads to as few as possible different behaviors of the vehicle in the simulation environment. For determining the best solution based on a cost function, engineers have to assign weights for boundary changes to each parameter. Using these weights, the optimization algorithm can automatically choose the best result from the Pareto front. Instead of weights, the cost function can also be based on metrics estimating the precision resulting of the boundary values.

If the computed boundaries result in very imprecise inaccuracy models, the inaccuracy model might not be complex enough. In this case, the complexity of the model has to be increased. For the acceleration error, the added complexity can be to distinguish a special situation for stopped vehicles as explained in Section 3.3.2. Too many special situations can result in overfitting the model to the available data. The more special situations are distinguished, the more data is necessary for deriving the inaccuracy boundaries. One method for reducing the effect of overfitting is to add error margins to the inaccuracy boundaries. This error margin can be proportional to the statistically computed standard deviation of the average of computed boundaries. A larger data set that is relevant for the regarded boundary reduces this standard deviation. This way, the recall is increased and more data increases not only the recall but also the precision.

Engineers can apply the optimization approach for determining the actuator and position sensor inaccuracy boundaries. For the offsets in the mapping errors and the distance for which it can happen that obstacles are not be detected, they can apply a similar method. For the Tesla

Autopilot, systematically gathering this data might have resulted in an error model stating that a relevant obstacle is sometimes detected only in the very last moment. Such an error model can trivially lead to a collision that the *STARVEC* framework would also detect. This could demonstrate the need to improve the sensor fusion system, which might have prevented the fatal Tesla accident [136]. In addition to not detected obstacles, there can be measured but not existing obstacles. The positioning of such ghost obstacles can either be included in the scenario description or be performed randomly.

3.5 Finding Undesired Behaviors

The simulation including models for sensor and actuator inaccuracies can generate different behaviors of the vehicle. This is the precondition for finding undesired behavior. This section starts with a definition of undesired behaviors in Section 3.5.1. It concludes with the definition of the problem in Section 3.5.2 that is addressed by the approaches presented in the next chapter. The relevant question is whether there is an undesired behavior among the set of possible behaviors generated by the simulation.

3.5.1 Definition of Undesired Behavior

First, undesired behavior has to be defined. The most common undesired behavior searched for are collisions with some static or dynamic obstacle. However, the car manufacturer might consider many other behaviors undesired. For example, it can consider uncomfortable or non-elegant behavior as described in Section 4.4 undesired. For the purpose of an automatic analysis, the system analyst has to formally specify what behavior they consider undesired.

In mathematical terms, this specification is a function:

$$f_{undesired\_physical\_behavior} : (Q_{physical\_states})^n \to \mathbb{B} \tag{3.25}$$

where $Q_{physical\_states}$ is the set of all possible physical states as defined in Section 3.1.1. The function $f_{undesired\_physical\_behavior}$ states whether a given sequence of n physical states shows an undesired behavior. For analysis purposes, it is reasonable to define this function in the simulation state space:

$$f_{undesired\_simulation\_behavior} : (Q_{simulation\_states})^n \to \mathbb{B} \tag{3.26}$$

Using the function $R_{phys \to sim}$ defined in Section 3.1.3 this function can also be applied to sequences of physical states.

The undesired behavior of colliding with an obstacle mentioned above can be identified by deciding for a single state whether it is undesired. This kind of undesired behavior can be defined as a function:

$$f_{undesired\_simulation\_state} : Q_{simulation\_states} \rightarrow \mathbb{B} \tag{3.27}$$

A simulation sequence is undesired if it contains an undesired state.

In the concept presented in this thesis, the undesired behavior can be represented as a software component taking any information available in the simulation as input and triggering an event if it detects an undesired state. The concept considrers such a component as part of the simulation environment maintaining an internal state. Additionally, Section 4.4 describes a method for specifying $f_{undesired\_simulation\_behavior}$ in CTL (Computation Tree Logic).

3.5.2 Problem Definition

The goal of this thesis is to efficiently determine if an autonomous driving system can show undesired behavior in the physical world. On the one hand, this requires modeling the behavior of the vehicle such that all physical behaviors can be represented and the precision is maximized. The previous sections addressed this task. On the other hand, this requires using this model for efficiently finding undesired behaviors in a simulation environment.

Using the definitions of Sections 3.1 and 3.5.1, the algorithm solving the latter step can be specified as:

Algorithm	Find undesired behavior
Input:	$s_{sw,init}, E_{events}, \Delta_{sim\_world}, f_{undesired\_simulation\_behavior}$
Output:	For each detected undesired behavior: sequence of events $(e_1, e_2, ..., e_n)$ resulting in the undesired behavior

where $s_{sw,init}$ is the initial state of the simulated world and E_{events} is the set of all possible events. Δ_{sim_world} is the transition function defined in Section 3.1.2 that determines the next resulting state for a given current state and an active event. $f_{undesired\_simulation\_behavior}$ is the specification of the undesired behavior defined in Section 3.5.1. The output consists of the events $e_1, e_2, ..., e_n \in E_{events}$. The corresponding states can be computed based on Δ_{sim_world}.

As the simulation is specified to be executed in discrete time steps (compare Section 3.1.1), the number of possible behaviors with a limited maximal length is finite. However, it grows exponentially with the length of the simulation: In each simulation step, any of the $n := |E_{events}|$ possible events can be applied. After m steps, there are n^m possible behaviors.

Chapter 4

An Efficient Approach for Testing with Inaccuracies and Nondeterminism

This chapter presents several aspects of a new concept for efficiently searching the space of possible behaviors for undesired behaviors. First, the basic concept is described and motivated in Section 4.1. Next, it is extended to perform more efficiently in most scenarios in Section 4.2. Using a system that is based on the created method, scenarios from real world test-drives are imported and analyzed as described in Section 4.3. In both, real world scenarios and simulation scenarios, complex temporal behaviors can be searched for as described in Section 4.4. Finally, Section 4.5 applies the presented concepts to the interaction with traffic participants.

4.1 A Concept for Efficiently Covering the State Space

This section presents the primary concept of the *STARVEC* algorithm. Some of the findings in this section have already been published in [137]. It starts with the basic concepts of testing the implemented software and covering the geometric state space in Section 4.1.1. Next, Section 4.1.2 explains how storing simulation states and uniformly covering the reachable state space reduces the complexity of the task. Finally, Section 4.1.3 explains how the simulation state of the whole planning and control system can be stored and loaded.

4.1.1 Basic Concepts

The concept presented in this section is based on two ideas:

1. Planning and control algorithms are quickly adapted to new problems. Therefore, the implemented code rather than an abstract concept should be tested.
2. Planning and controlling of a vehicle is a geometrical problem, thus geometrically similar positions typically lead to similar behavior.

The first idea is to execute the implemented software directly. During the development of an autonomous driving system, many small problems occur and have to be resolved. For example, in an industrial project connected to this thesis, the team working on the planning and control software implemented special strategies for some special cases. One example of such a strategy applies if the computed trajectory needs to be adapted due to controller errors while following a very sharp curve. These special cases quickly lead to deviations between a simplifying abstraction designed to increase computation efficiency and the actual implementation. Additionally, designing good abstractions often requires more time than the implementation itself. For these reasons, abstractions should be developed as soon as the actual concept is stable for a long period. Software updates can challenge this stability even after serial production has started. Furthermore, testing the implemented code also allows using any implementations of sensor and actuator deviations. Many abstraction concepts require these deviations to depend only on the current state of the vehicle or some helper variables. Deviations that depend on the history of states–like delays–are difficult to represent. The concept presented in this thesis allows implementing errors like the delays described in Chapter 3.3.

The second idea is that autonomous planning and control tasks are geometrical problems for which similar positions lead to similar behavior. In particular, this is true for reactive high frequency controllers that compute their behavior based on the planned and the current position. Planning components can compute a different path for slightly different positions. However, this is usually only true for one direction. That is, if two points A and B are geometrically close to each other, a vehicle at a Point C between A and B will probably behave similar to being at A or similar to being at B.

4.1.2 Reducing the Complexity

The sensor and actuators are modeled to be nondeterministic as described in Section 3.2. In theory, the behavior can change at any time leading to an infinite set of possible behaviors. For this reason, the time and the error models are sampled, such that there is a finite set of d error characteristics that can change after a finite amount of time t_{step}. If there are d different error characteristics, and the simulated scenario takes up to $l \cdot t_{step}$ seconds, there are up to d^l possible

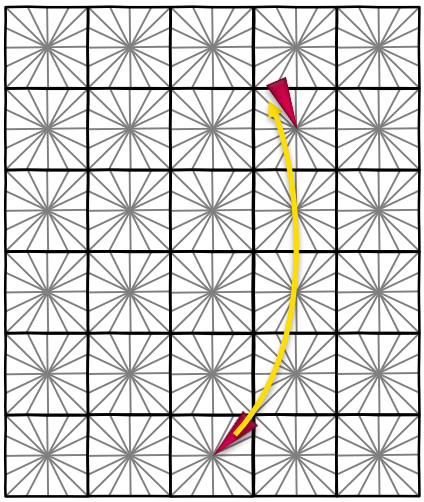

Figure 4.1: Example of (coarse) geometric discretization. The top red cone and the state after executing the yellow path are in the same grid cell and considered similar.

different states this time. Executing all of them requires a simulation time of:

$$t_{simulation,full} = O\left(d^l\right) \tag{4.1}$$

The simulation time grows exponentially with the duration of the test sequence.

The algorithm searches for undesired behaviors like collisions or uncomfortable driving. These are externally visible geometric behaviors. There are exponentially many possible paths, but large sub sets of them are geometrically almost identical. For these almost identical paths, different future behavior is mostly due to sensor and actuator inaccuracies rather than different planning results. Groce and Joshi [83] have regarded a similar problem trying to cover different behaviors related to memory accesses. They applied "sound and unsound abstractions" [83] considering paths only as different if they perform different memory accesses. This way, they are able to achieve a good coverage of different behaviors connected to memory access. The same approach can be transferred to autonomous driving systems by considering states only as different if they are geometrically different according to some geometric grid as depicted in Figure 4.1. If the test process encounters any state that it has already visited according to this metric, it does not continue the simulation. This means, it does not add the state to the queue of states that it plans to expand further.

Figure 4.2 depicts a schema of the resulting execution rule. It starts by storing the current simulation state (Top left box). At this point, storing a state means to store the applied sensor and actuator inaccuracies in order to be able to reproduce the state. Accordingly, restoring in the next step means to apply the stored sensor and actuator inaccuracies until the analysis reaches the stored state. Later in this section, this is replaced by actually storing the state itself. For the restored state, an error type is applied that has not been applied yet ("Apply

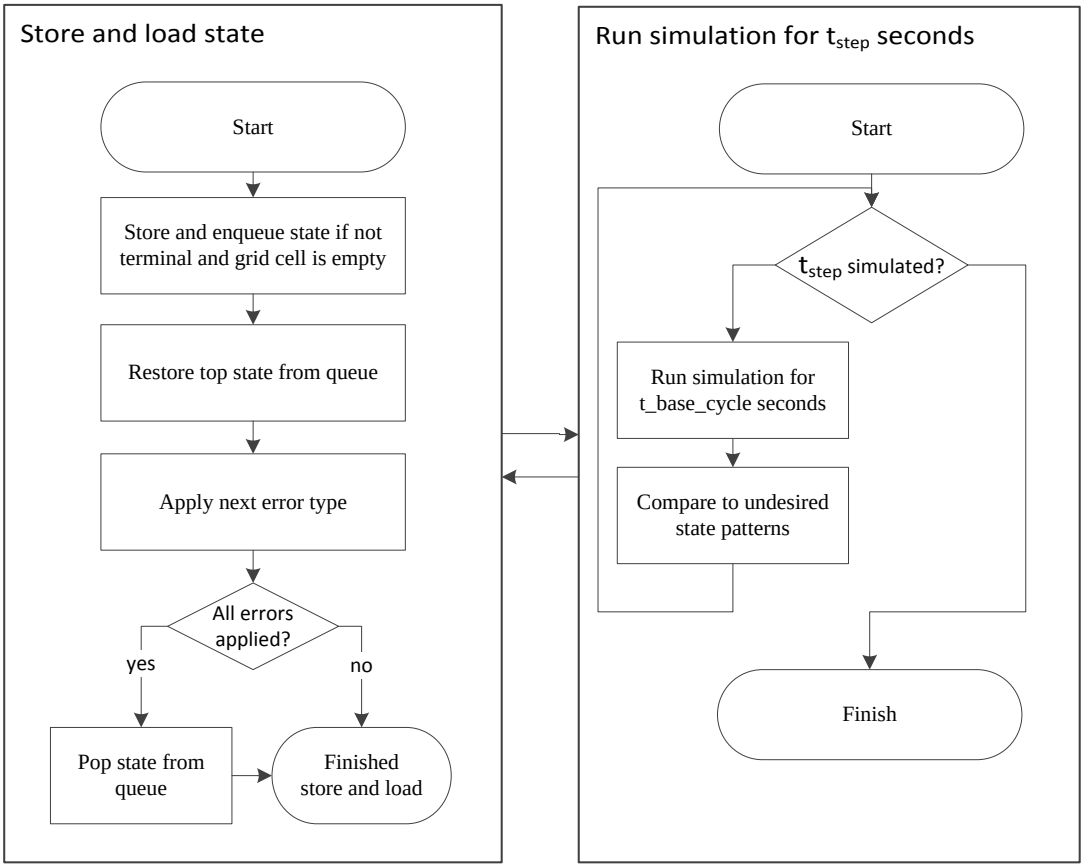

Figure 4.2: Overview of the *STARVEC* algorithm for finding error pattern combinations leading to undesired states. Loading states and applying new inaccuracy patterns alternates with executing a short part of the simulation sequence.

next error type"). If all error types have been applied to this state, it is removed from the state queue, else it remains in the queue in order to be restored again. Next, the test supervisor starts with the restored state and the applied error pattern to execute the simulation environment for t_{step}. During that time, the simulation is continuously checked for collisions or other undesired behaviors.

This approach reduces the complexity of the testing task. A typical scenario includes moving from one position to another. If no sensor and actuator inaccuracies occur, the vehicle will execute one path that will be referred to as reference path. Sensor and actuator inaccuracies lead to deviations from the reference path by a limited range. For example, they can result in controller errors by some decimeters, but typically not multiple meters. This limited range combined with a finite grid density leads to a finite amount of possible states around each point of the reference path. If K is the maximal number of grid borders in one dimension for one position along the ideal reference path and $N_{dimensions}$ is the number of observed geometric dimensions, this leads to $K^{N_{dimensions}}$ possible states for each point along the reference path.

Executing a single simulation step for all possible states at one point of the reference path with all error characteristics requires $d \cdot K^{N_{dimensions}}$ execution steps. Additionally, the path leading to these nodes has to be executed, requiring between one and l steps depending on the distance to the scenario start. This process has to be repeated for each of the l points along the reference path resulting in a complexity of

$$t_{simulation,grid} = O\big(K^{N_{dimensions}} \cdot d \cdot l^2\big) \tag{4.2}$$

K and $N_{dimensions}$ do not depend on the length of the scenario. Hence, the abstraction reduces the complexity from exponential in l (compare Equation 4.1) to quadratic in l.

This complexity can be further reduced by storing and reloading the state of the whole simulation including the planning and control software. The technical details of storing and loading states are explained in the next section. Using this capability, reaching any of the final states requires only reaching the predecessor states plus d simulation steps for each final state, which are up to $K^N_{dimensions}$. The same applies for the predecessor states regarding their predecessors. This process has to be repeated up to l times until the initial states are reached. Thus, the complexity is reduced to linear in l:

$$t_{simulation,grid} = O\big(K^{N_{dimensions}} \cdot d \cdot l\big) \tag{4.3}$$

In practice, finding undesired behavior typically does not require the worst-case execution time. Hence, the observed computation speed gains are lower than theoretically possible. However, the experiments in [137] show that a significant speed up is reached for relevant scenarios.

4.1.3 Loading and Saving the State of a Software Component

The presented algorithm must be able to store and load the state of the simulation environment including the planning and control system. It can do this based on a serialization library. For example, Sumaray and Makki [138] compare "XML, JSON, Thrift, and ProtoBuf". For serializing (storing) the state of a whole software component, the storing code must require as little implementation overhead, as possible. C++ libraries for XML (Extensible Markup Language) and JSON (JavaScript Object Notation) need explicit implementation of each value to be stored including referenced classes and cannot cope with private data members. ProfoBuf additionally requires writing a specification file for the serialized data. In contrast, Boost Serialization[1] serializes referenced classes identically to basic data types. Boost Serialization copes with calling the right serialization function of referenced classes and ensures serializing multiply referenced classes only once. It can also access private data members.

For this purpose, the software developer needs to enhance the classes with two lines of code for declaring the serialization function and registering the class. The actual serialization code is stored in a separate source file. It mainly contains a list of the members of each class embedded into the boost serialization syntax. The library supports different serialization formats including XML and a compressed binary format. The implementation created for this thesis stores the serialized states to the hard drive instead of keeping it in the main memory. This way, the size of the main memory does not limit the execution. Furthermore, the state of the whole test system can be loaded after terminating the process and potentially changing the source code of the test component.

It has been demonstrated that it is feasible to implement and maintain the code for serialization of a complex software project. The demonstrated example is the planning and control framework developed during this dissertation. The computational overhead for loading and saving states is small compared to the time necessary for the actual simulation. In order to minimize the storage requirements, the serialized data is compressed using the ZLib standard [139]. Figure 4.3 compares the overhead caused by the test supervisor algorithm and the actual simulation time. The overhead consists of the time necessary for loading and saving states, evaluating whether a state shows undesired behavior and choosing which state to expand next. In total, the computation time used for the actual simulation is significantly higher than the time used for overhead. Optimizing the storing procedures can further reduce the overhead. In addition to the computation time, the testing framework requires 23 kB per stored state on average. It stores one state per simulated second.

Another precondition of using the presented test supervisor is the ability to run the simulation for a specified time. That means there has to be a scheduler component that can trigger the execution of both the simulation environment and the planning and control components. In

[1] `www.boost.org/libs/serialization/doc/`

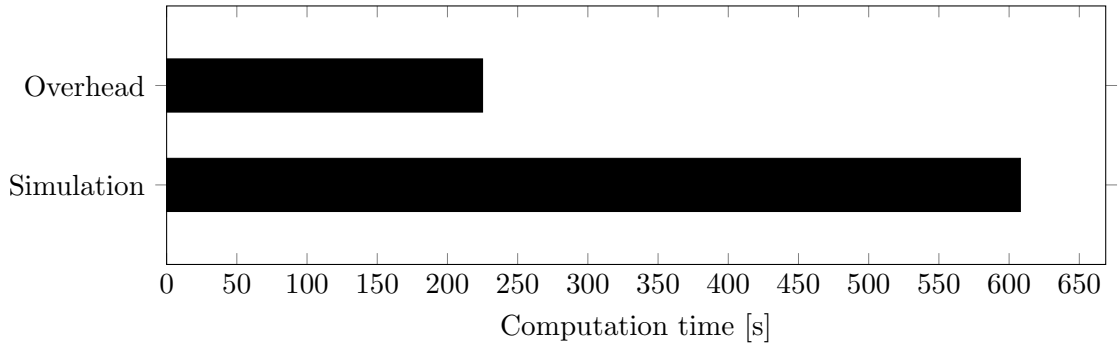

Figure 4.3: Comparison of the computation time used for simulation vs. overhead of the presented testing algorithm: The simulation time dominates the total computation time.

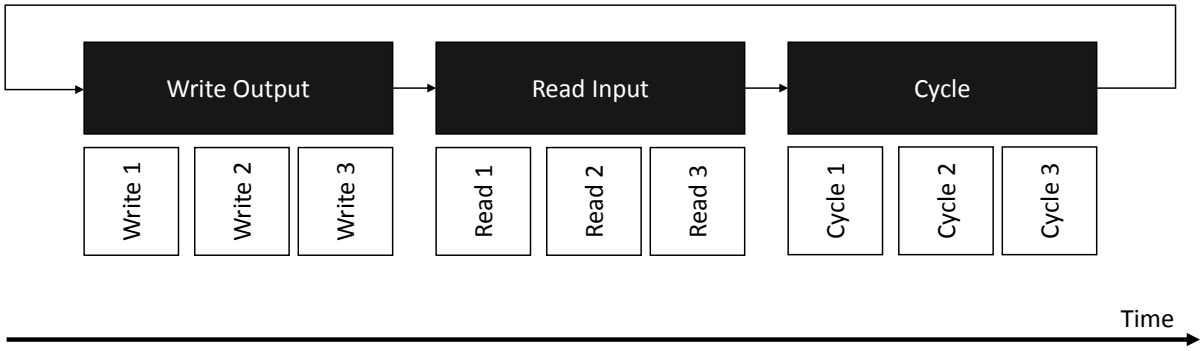

Figure 4.4: Serial execution of software components: In each step, components 1, 2 and 3 are executed serially.

order to create deterministic results, it should also trigger the data transmission between the tested components. Figure 4.4 shows the execution model applied in the implementations for this thesis. In each simulation cycle, the current time is increased and the active components are determined. A component is active if the current simulated time is a multiple of the component's cycle time. In the example, components one, two and three are active. First, all components write their current output, that is the output that has been computed in the previous cycle. This corresponds to each component requiring its full cycle time for its computation. Next, each components reads its input data and finally, each component performs its main computations in its periodically called cycle method. These strict execution orders enforce the same deterministic behavior even if the simulation is executed faster than in real time.

In order to speed up the computation, the execution of the read, write and execute methods can be performed in parallel, as depicted in Figure 4.5. If separate simulated clocks are used for each component, the cycle execution of a component may take longer than one cycle time of component with the highest frequency. The execution may take until the component is triggered to write its output data. The long execution time does not change the behavior of the complete system. This way, several cycles of a high frequency component like a controller can be executed during the computation time of a low frequency component like a planner.

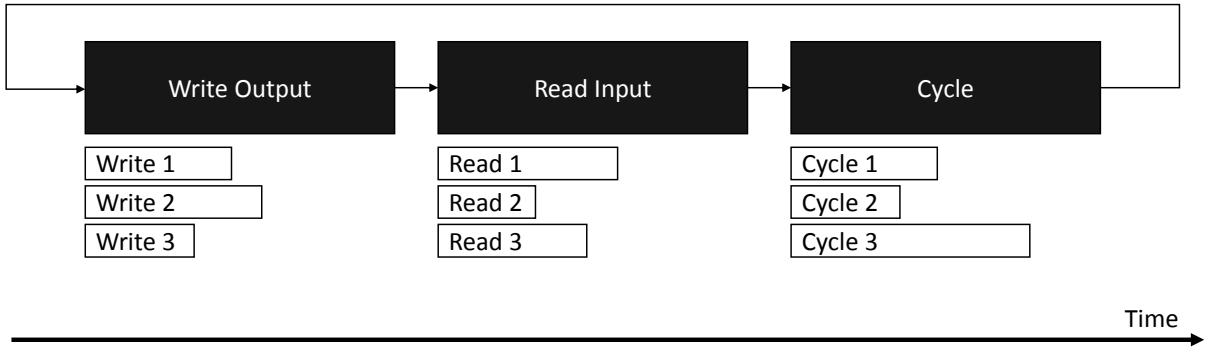

Figure 4.5: Parallel execution of software components: In each step, components 1, 2 and 3 are executed in parallel.

The execution model leads to some data being transmitted but not read yet in each point in time. Therefore, the buffered data has to be serialized in addition to the actual state of the software components.

In summary, the proposed method reduces the complexity for finding undesired behaviors caused by sensor and actuator inaccuracies from exponential in the length of the simulation l to linear. It accomplishes this by discretizing the space of geometric states and exploiting the ability to save and load states.

4.2 Optimizing the Search Efficiency

The method described in the previous section reduces the worst-case complexity for finding undesired behaviors. However, it requires specifying the size of the grid and takes the worst-case execution time even for finding undesired behaviors that occur often.

Thus, the method is extended by two concepts:

- Replacing the geometric discretization grid by novelty search
- Choosing the applied error characteristic randomly until all characteristics have been applied

These concepts are presented in Sections 4.2.1 and 4.2.2. Section 4.2.3 extends the pure geometric grid to a grid containing arbitrary user defined states. Some concepts of the described test method have been introduced in [140] as the *STARVEC* algorithm.

4.2.1 Expanding the Most Novel State

The first concept mentioned in the introduction to this section is novelty search. Instead of ignoring states that are in a grid cell in which another state has already been expanded, all states

are kept in a priority queue waiting for expansion. Figure 4.6 shows an exemplary situation. State 1 has been expanded 7 times resulting in states 2-8. States 6 and 8 have already been

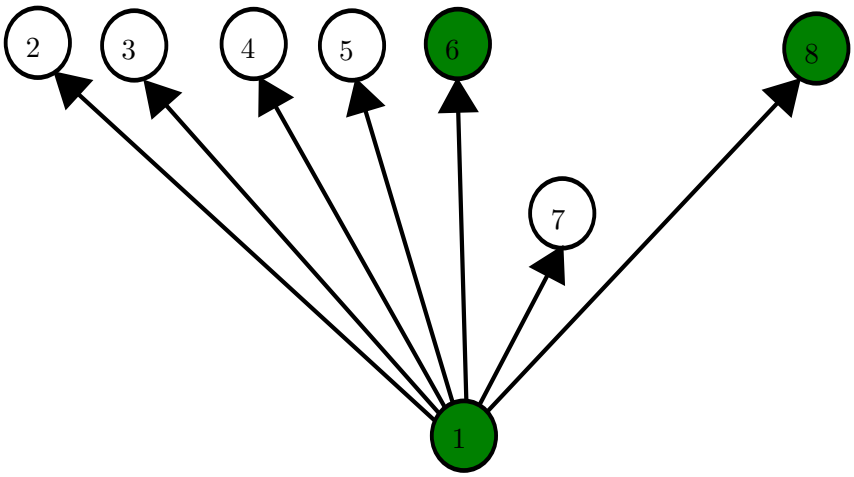

Figure 4.6: Example set of expanded (green) and not expanded (white) states. Node 7 has the highest distance to any neighbor. Node 2 has the highest distance to the nearest expanded neighbor.

expanded, too. The resulting priority queue is depicted in Figure 4.7. The priority of each state

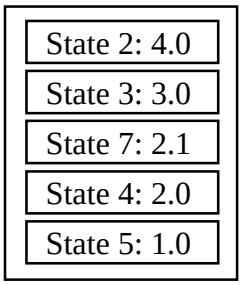

Figure 4.7: Priority queue of the *STARVEC* algorithm. The priorities correspond to the distances to the nearest expanded neighbor in Figure 4.6.

is proportional to the distance to the next fully expanded state. The distance is the Euclidean distance in a state space that corresponds to the grid introduced in Section 4.1.2: The state space contains one dimension for each regarded state variable. In Figure 4.7, State 2 has the highest priority, as its nearest expanded state (State 6) has a distance of 4.0. For the distance computation, only expanded states rather than all reached states are considered. This aims to distribute the expanded states in the state space evenly. Considering all reached states would result in expanding State 7 leaving the left half of the state space without expanded states.

The exact formula for computing the priority $p(s)$ is shown in the following equation (Equation 4.4):

$$p(s) = min_{s' \in Q_{explored\_states}} \big(dist(s, s')\big) \tag{4.4}$$

where $Q_{explored\_states}$ is the set of the already explored simulation states and $dist(s, s')$ is the Euclidean distance between states s and s' in the space of the grid introduced in Section 4.1.2. The term $min_{s' \in Q_{explored\_states}}(dist(s, s'))$ is approximated using the library FLANN (Fast Library for Approximate Nearest Neighbors) [141].

At all times, the highest priority in the queue is the largest distance from any not expanded state to its neighboring state. One could fit a grid-like structure to the state space with each cell having a radius lower than this distance. Each cell containing a state also contains at least one expanded state. This way, the advantages of the grid-based approach described in the previous section still apply. However, this virtual grid becomes continuously denser, resulting in a fast and increasingly dense coverage of the state space. The concept is similar to the concept of RRT (Rapidly-exploring Random Tree)[142]. For this task, Novelty Search performs better than RRT, because most states in the state space are not reachable by only altering error characteristics. This significantly slows down an RRT based approach as discussed in the evaluation in Chapter 6.

4.2.2 Prioritizing Unexpanded States

The second concept mentioned in the introduction to this section is to randomly choose from the error characteristics planned to be applied. Each error characteristic is a combination of configurations of the error models as described in Section 3.3. In some situations, only a few of the error models significantly influence the behavior of the vehicle. In these cases, a limited number of randomly chosen successors is likely to contain all configuration combinations of these few error models. The limitation to the number of chosen successors reduces the negative impact of error models with little influence. This speeds up the search process if large sets of error characteristics are defined.

The successor limitation is reflected in the priority formula shown in Equation 4.5.

$$p(s) = w(s) \cdot d_{mod}(s) \tag{4.5}$$

where $w(s)$ is the weight of a state and $d_{mod}(s)$ is the modified distance to its nearest expanded neighbor. As the successor limitation leads to states not being fully expanded, the distance to the nearest expanded neighbor is replaced by a radius. Within this radius, the total number of expansion has to exceed a threshold:

$$d_{mod}(s) = min\Big(\Big\{r \in \mathbb{R}^+ | \Big(\Sigma_{\{s' \in Q_{explored\_states} | dist(s,s') < r\}} n_{succ}(s)\Big) > n_{threshold}\Big\}\Big) \tag{4.6}$$

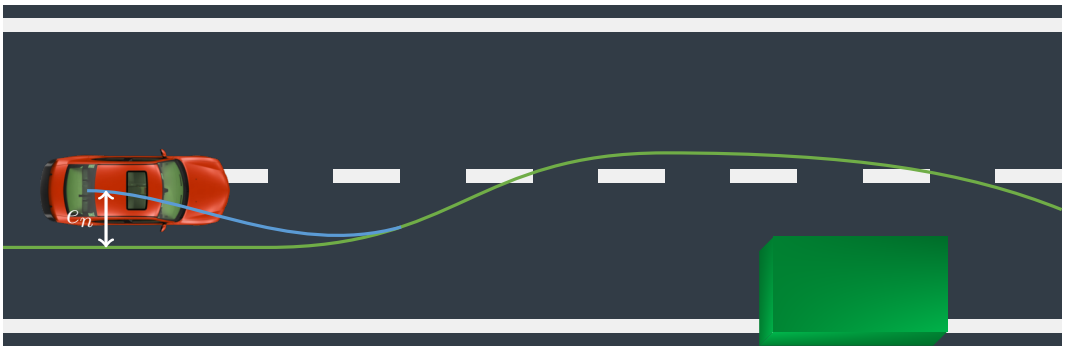

Figure 4.8: Planning concept that uses the green path as reference. If the controller error e_n is too high, the planner computes a trajectory (blue path) that smoothly returns to the reference path.

where $Q_{explored\_states}$ is the set of already explored simulation states, $n_{succ}(s)$ is the number of successor states of state s and $n_{threshold}$ is the number of expansions that needs to be exceeded within the computed radius.

The weight is computed as:

$$w(s) = (w_{successor} \cdot n_{succ}(s) + 1)^{-1} \tag{4.7}$$

where $w_{successor}$ is a weight factor penalizing the number of successors.

4.2.3 Generalization of the Grid Concept

The previous sections focus on improving the efficiency. This section additionally increases the applicability of the concept by allowing custom state dimensions. The basic concept described in Section 4.1 projects the state of the vehicle to a geometric grid. This grid includes external features like the position, orientation, acceleration or velocity of the vehicle. In addition to these external features, the future trajectory of the vehicle depends on the internal state of the planning algorithm.

One planning concept is to first create a collision free path and use a controller to follow the initially planned path. In this case, the state of the planning component mainly consists of constant parts like the initially planned path and externally visible parts like the current environment map and the perceived vehicle state. In this case, the grid that consists of dimensions that correspond to physical states is a good abstraction of the simulation state.

Another planning concept is depicted in Figure 4.8. The planning and control system follows an initially planned reference path (green path), but some sections of the path are adapted continuously. For example, [25] continuously adapts the velocity, reacts to new obstacles and high controller deviations. The resulting trajectory (blue path in Figure 4.8) in each adaptation depends on the start position of the replanning procedure. This start position is not necessarily

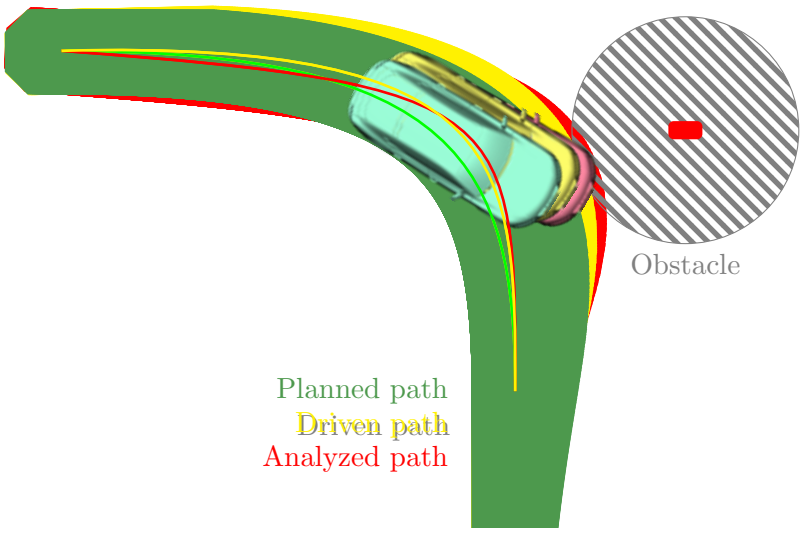

Figure 4.9: Passing an obstacle scenario: The actually driven path (yellow) deviates from the planned path (green). The worst-case path (red) can be found using the *STARVEC* algorithm.

identical to the vehicle position. [25] uses the planned vehicle position instead, except if the controller deviation is higher than a specified margin. For this method, the current state of the vehicle in combination to the current distance to the replanning start point is a good abstraction of the simulation state. The distance to the replanning point equals the controller error (e_n) after replanning.

In order to incorporate such internal states, the user of the *STARVEC* algorithm can supply a list of variables that are used in addition to the vehicle state. For each of the variables the user specifies a weight that corresponds to the distance between two similar simulation states in that dimension. The planning and control components emit the current values of these variables using a logging interface. ADTF (Automotive Data and Time triggered Framework) [143] provides the signal view interface for this purpose.

4.3 Determining Scenarios to be Tested

Some of the findings in this section have already been published in [144]. The concept described in the previous sections finds undesired behaviors based on a given scenario. Typical sources for defining the scenarios to be tested are requirement documents, expert knowledge about the problem or reconstructed scenarios from accident databases. By exploiting the latter source, situations leading to an accident for one vehicle can be prevented for other vehicles. Using the *STARVEC* algorithm additionally allows searching for almost occurred accidents. Figure 4.9 shows an example. The vehicle plans to follow the green path, but due to sensor and actuator inaccuracies it actually follows the yellow path, which also does not result in a collision with the obstacle. However, the worst-case is the red path that would lead to a collision. The depicted

obstacle can be either some static obstacle like a crash barrier or it can be a pedestrian who has an area of motion uncertainty around it. Such almost occurred accidents are more likely than actual accidents. Therefore, a system that can identify almost occurred accidents and helps repairing the causative defect can substantially reduce the number of accidents that are due to conceptual weaknesses.

First, Section 4.3.1 describes the situations in which scenarios can be stored for further analysis. Next, Section 4.3.2 discusses the equipment and techniques used for storing scenarios. Section 4.3.3 investigates how the available scenarios can be filtered for relevant situations. These relevant situations are analyzed as described in Section 4.3.4. Finally, Section 4.3.5 explains how to distribute the results of the analysis to the vehicle fleet.

4.3.1 Sources for Collecting Scenarios

There are various situations in different levels of the development process of autonomous vehicles providing scenarios worth further analysis. Scenario data can be collected from:

- test-drives executed by developers
- test-drives according to requirement specifications
- drives performed in a prototype testing program, and
- regular usage by customers

Developers regularly drive the experimental vehicle in order to test the functions they are currently working on. These test-drives are usually less systematic than independent vehicle tests but they are based on knowledge and experience that is not necessarily available during requirements specification or test-drives by independent test experts. A disadvantage of this source is that the tested autonomous driving software might still contain known defects. Such known defects can dominate and mask conceptual weaknesses to be found by scenario analysis. That means instead of finding the conceptual weaknesses, the scenario analysis only finds the known defects. In this case, the analysis does not produce relevant results.

The second group of scenario sources mentioned above are test-drives based on the requirements specification. These test-drives systematically cover the requirements and can be additionally supported by reference sensor systems or known environment maps. This way, the recorded data can be of high quality. Systems tested by professional test drivers contain less defects than the experimental system described above. Consequently, many detected problems are relevant.

After professionally testing the vehicles, but before the final customers use the product, a limited set of almost final prototypes is produced and used. These prototypes can still contain some extra devices for gathering development data, which increases the quality of the collected data. The

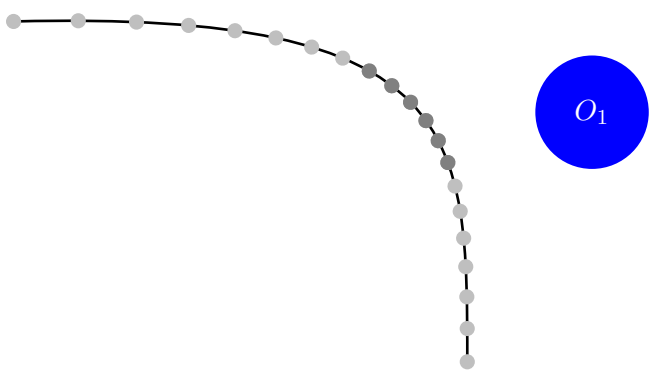

Figure 4.10: Points (gray) at which the planning and control system is saved while following the path described in Figure 4.9. The dark grey states are regarded by the analysis, as the car is close to the obstacle.

prototypes are used in a similar way as they are used by the end customers and hence create similar data before market launch.

Finally, scenarios can be gathered anonymously during usage by the final customers. Data collected from this source cannot prevent the distribution of faulty vehicles, but it can help eliminating defects before they lead to undesired behavior experienced by a customer. For example, they can include the almost-accidents described at the beginning of this section and help resolving their cause. Customer vehicles do not contain reference sensors, which reduces the quality of collected data, but they produce the largest amount of data.

4.3.2 Recording and Restoring Scenarios

During the drives used for data collection described in the previous section, the state of the vehicle and its environment is stored periodically. Figure 4.10 shows markers for each position at which the state is saved while executing the motion described in Figure 4.9.

Figure 4.11 illustrates how the scenarios are stored and loaded. Storing the state of the planning and control software is based on the same techniques as used for the *STARVEC* algorithm described in Section 4.1.3. This is depicted by the boxes of the *Planning and Control* system as input (bottom right green box) and output (top right red box) of the *Scenario Extractor*. The only difference are connections to the execution environment: The system clock is replaced by a simulated clock with the same time stamp.

In contrast, the *Simulation Environment* (top left box) has to be recreated based on the *Perceived Environment* (bottom left box). Depending on the available sensors, different information sources can be used. For some test-drives, *Ground Truth* data is available. For example, if the test-drive is executed on a test track, the exact position of the road and all obstacles might have been measured in advance. On public roads, 3D-geodata [145] from high definition maps might exist that includes the environment geometry. If no ground truth data is available or the data is not

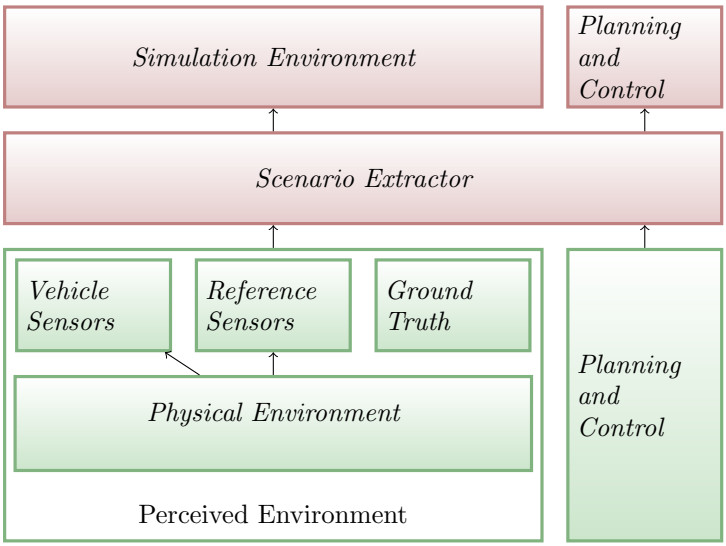

Figure 4.11: The software system and its environment during the physical drive (green) are converted to a representation in the simulation environment (red). The perceived environment can be converted based on different sensor measurements or prior known ground truth information.

sufficient, sensor data is used. This can be either data from the standard vehicle sensors or from special reference sensor systems. Compared to the vehicle sensors, reference sensor systems provide higher accuracy, as they do not have to comply with the same space or price restrictions. Typical examples are high definition laser scanners as a reference for low cost ultrasonic sensors or differential GPS systems as a reference for the vehicle odometry. If no reference sensor systems are available, the standard vehicle sensors have to be used for scenario reconstruction. In this case, the reconstructed environment does not perfectly correspond to the physical environment. However, it does correspond to how the autonomous driving system perceives the environment. The analysis might determine that the vehicle does not react appropriately to the perceived environment. In this case, it has found a scenario in which the autonomous driving system acts inadequately, which has to be resolved. The actions in the perceived environment may be inadequate, even if the actual physical scenario was safe.

The simulation environment is instantiated based on the extracted environment information. This includes setting the vehicle to its position according to localization sensors and adding static obstacles to positions according to the environment map. Dynamic obstacles can be classified and represented according to a model of their behavior. For example, a pedestrian can be modeled to be able to suddenly move two meters in any direction, forcing the vehicle to keep two meters of safety distance.

4.3.3 Identifying Relevant Situations

The computation time of the *STARVEC* algorithm is linear to the duration of the scenario. This makes it possible to analyze all recorded data in full length provided sufficient computation power per driven distance. However, this is not necessary as most situations have small collision risk. If all static obstacles are several meters away and the vehicle drives slowly, sensor and actuator inaccuracies in the past cannot lead to a collision, either. This makes it reasonable to limit further analysis to situations that appear to have a high collision risk. For example situations, in which an obstacle is very close to the vehicle. Limiting analyzed scenarios to these situations reduces the necessary computation power per driven distance as well as the amount of data that needs to be stored and transmitted. The latter factor is a limitation for consumer vehicles, for which the data needs to be transmitted using mobile network connections.

The focus of this thesis lies on inaccuracies of sensors and actuators rather than on complete sensor failures. However, for identifying relevant scenarios on consumer vehicles, failing sensors are another factor. Data from these scenarios can be used to analyze whether the fail-safe concept could have led to a collision. Another factor for identifying relevant scenarios is unexpected behavior of traffic participants. The presented concept can be applied to determine whether the situation was still safe. For test-drives of autonomous driving systems on public roads, the test driver sometimes has to intervene in order to prevent an accident. From September 2014 until November 2015, Mercedes-Benz reported 967 [146], Volkswagen reported 85 [147] and Bosch reported 625 [148] interventions during test-drives in California. Such interventions can also be used as a trigger for later analysis trying to determine whether the intervention prevented a possible accident. Google [149] uses a similar approach for filtering the disengagements reported to the traffic agency. By applying the *STARVEC* algorithm, the post analysis can find situations that are more dangerous among these disengagements.

4.3.4 Analyzing Recorded Scenarios

The restored simulation states are considered as part of a search tree as the one created by the *STARVEC* framework described in Section 4.1. Each state is assigned to its physical predecessor as a successor in the search tree and added to the queue of not expanded states. If a trigger is used for identifying relevant scenarios, only states some seconds before and after the trigger are added to the queue of not expanded states. In this case, the analysis is also limited to this period. Any simulation state of which the time stamp is higher than the end of the time frame is no further expanded. If the analysis finds an undesired behavior, the sequence leading to that behavior starts with a physical state and continues with simulated states.

4.3.5 Distributing Analysis Results

An undesired behavior found by the *STARVEC* analysis is due either to incorrect models or a weakness of the planning and control system. In the first case, the detected sequence is an example that can be used for investigating possible model improvements. As discussed in Section 3.4, it might be possible to create a more complex model that does not exhibit the actions leading to the detected undesired behavior. For example, the behavior of the model in special situations like accelerating from zero velocity can be implemented. This requires sufficient physical test-drive data showing the behavior of the vehicle in that special case.

The second case is a weakness of the planning and control system. The consequences of this weakness depend on the source of the scenario. If the source was an early test-drive, developers need to regard the scenario and eliminate potential errors. If the source is a vehicle owned by a customer, a quick reaction is necessary. Possible reactions are

- adapting parameters of the vehicle software,
- deactivating the executed function at one geographic position, or
- globally deactivating the executed function.

The reaction to adapt parameters is reasonable if the undesired behavior is a collision due to unexpectedly high controller deviations. In this case, the safety distance parameters can be increased covering these deviations. The parameter adjustment can be performed either manually or automatically. After adjusting the parameters, all other known scenarios should be reanalyzed. The disadvantage of increasing safety distances is that this can decrease the overall function performance. For example, a parking assistant would require larger parking lots. The parameter adjustment can also be a temporary solution until the planning and control software is conceptually improved and able to cope with lower safety distances.

Another possible reaction is to deactivate or constrain the corresponding function for a specific geographic position. For example, if the controller deviations are due to bad road conditions, other vehicles can be warned to drive more carefully at one specific bend. This way, the analysis does not only evaluate autonomous vehicles, but also the environment and the infrastructure.

Finally, if the analysis uncovers a safety risk that cannot be resolved by applying the reactions listed above, the function can be deactivated globally. If this happens, the responsible engineers have to work on a solution that enables the autonomous driving system to cope with that situation in order to reactivate the function quickly.

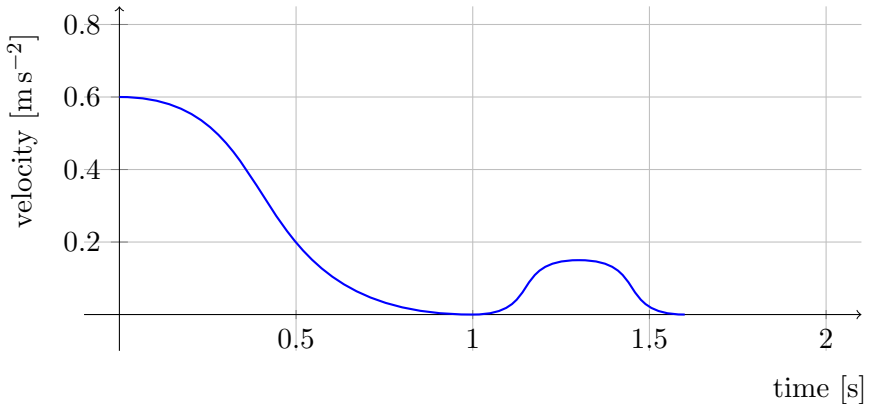

(a) Example velocity plot

CTL: $\neg\mathbf{EF}(v > 0.3 \wedge \mathbf{E}[v > 0\,\mathbf{U}\,v = 0 \wedge \mathbf{E}[v \geq 0\,\mathbf{U}\,v > 0.05]])$

(b) CTL formula

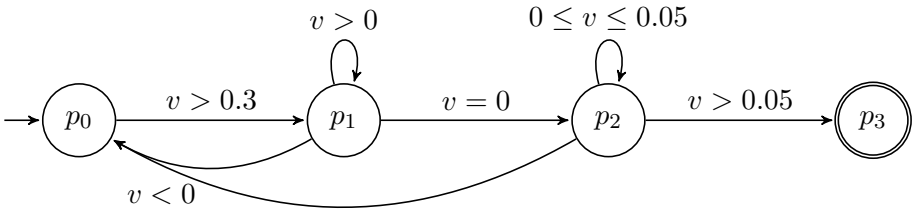

(c) Pattern state machine

Figure 4.12: Stopping before the goal position and restarting in the same direction expressed as a state machine, an example velocity plot and a Computation Tree Logic formula.

4.4 Searching for Temporal Behavior Patterns

Some of the findings in this section have already been published in [150]. The simplest undesired behavior that can be searched for are collisions. Behaviors that are more complex can cover a time span rather than a single point in time. For example, a car might drive slalom or repeatedly start and stop needlessly. These patterns cannot be detected by comparing a single state to a specification of undesired states. Instead, a sequence of states can be compared to a specification of undesired sequences.

Figure 4.12 shows different representations of the same undesired behavior of starting and stopping without need. The first representation is not formal, but a plot of the velocity signal that an engineer recognizes as an example of this pattern. The second representation is CTL, which is typically used for model checking. The goal of model checking is to determine whether "a given automaton satisfies a given temporal formula" [151]. It is performed by several freely available tools like NuSMV (New Symbolic Model Verifier) [152]. Using these tools requires only

connecting the *STARVEC* algorithm with model checking tools as described in Section 4.4.1. An alternative to these tools is the problem specific implementation of Breadth First Search described in Section 4.4.2. It uses the third representation shown in Figure 4.12(c).

4.4.1 Combining STARVEC and Computation Tree Logic

The system for which temporal logic specifications should be checked consists of the planning component, the deterministic part of the environment and the nondeterministic events. The typical model checking approach starts with creating a model of each component. Next, this model is represented in a model checking tool like NuSMV. Using this representation, the tool applies the specification to the model. As stated in Section 4.1.1, the goal is to check the actual implementation of the planning component. However, the whole software code of the planning component is too complex for automatically generating a model of the source code for which a model checker can produce results in reasonable time. Instead, the *STARVEC* algorithm creates a search tree connecting possible reachable states. This tree can be regarded as a model of the possible behavior of the planning software. As explained in Section 4.2, not expanded states are considered to be similar to their nearest expanded neighbor states. If an expanded state and all its neighboring not expanded states are treated as a single state, the search tree becomes a general graph. The transition guards of this graph are the active nondeterministic environment events leading from the source of a transition to its target state. This graph can be converted to a NuSMV compatible representation.

Listing 4.1 shows the structure of such a transition table. It computes a new value for the macro NEXT_STATE_ID. First, it checks whether the variable sub_step is below NUM_SUB_STEPS. As the environment event changes only after a specified time, for example one second, several simulation steps have to be completed before reaching a new state. These sub steps have to be represented in the NuSMV model, as the undesired behavior might happen in one of these steps. Therefore, the counter sub_step counts from 0 to NUM_SUB_STEPS and restarts with 0. The state id can only change after executing NUM_SUB_STEPS sub steps. If the state id changes, the new state is determined based on the current state (*state_id*) and the currently active environment event (*error_number*). Some environment events lead to the same target state, because not expanded states are represented by their nearest expanded neighbor. Some states lead to the special state TERMINAL_STATE. The simulation is not continued at these states, because either an undesired behavior is detected, or a simulation end condition is reached.

This transition table is one central element for combining NuSMV with *STARVEC*. It is generated based on the *STARVEC* search graph. In addition to the transition table, a property table is necessary. It lists for the combination of each defined property with each state, sub step and environment event whether this property is true or false. As NuSMV cannot access the simulation states directly, it depends on these properties being defined and extracted. The syntax of the property tables is similar to the transition table shown above. The extracted properties

Listing 4.1: NuSMV transition table: the id of the next state is computed based on the current state and the number of the current error pattern. The active state only changes if sub_step equals NUM_SUB_STEPS.

```
1  NEXT_STATE_ID :=
2   case
3    sub_step < NUM_SUB_STEPS - 1 : state_id;
4    sub_step = NUM_SUB_STEPS - 1 :
5     case
6      state_id = 0 :
7       case
8        error_number = 0 : 1;
9        error_number = 1 : 1;
10       error_number = 2 : 1;
11       error_number = 3 : 1;
12      esac;
13     [...]
14     state_id = 1051 :
15      case
16       error_number = 0 : 998;
17       error_number = 1 : 566;
18       error_number = 2 : 571;
19       error_number = 3 : 571;
20      esac;
21     state_id = 1052 : TERMINAL_STATE;
22     [...]
23    esac;
24  esac;
```

can be used in CTL and LTL (Linear Temporal Logic) formulas for specifying undesired behavior (bottom right box in Figure 4.13).

Additionally, a NuSMV base model is required. The base model combines the transition table, the property table and the temporal logic specification. It is constant for all search graphs and is shown in Listing A.1 in the appendix. The main parts of it are a definition of the NuSMV state variables and state transitions.

Both the transition table and the property table can become very large. In the worst-case, the property table can contain one line for each combination of state, sub step, environment event and defined property. The transition table can contain one line for each combination of state and environment event. Three measures are applied to reduce the number of lines:

1. If all successors of a state are identical, the inner case clause (line 8-11 in 4.1) is omitted.
2. All states preceding a special state are integrated into a single case using the NuSMV set construct: *state_id* in {2, 3, 4, 6}.
3. The set constructs are shortened by combining directly succeeding ids: *state_id* in {2..4, 6}.

Together, these measures reduce the size of the transition table by about 70%. Similar reductions can be applied to the property table.

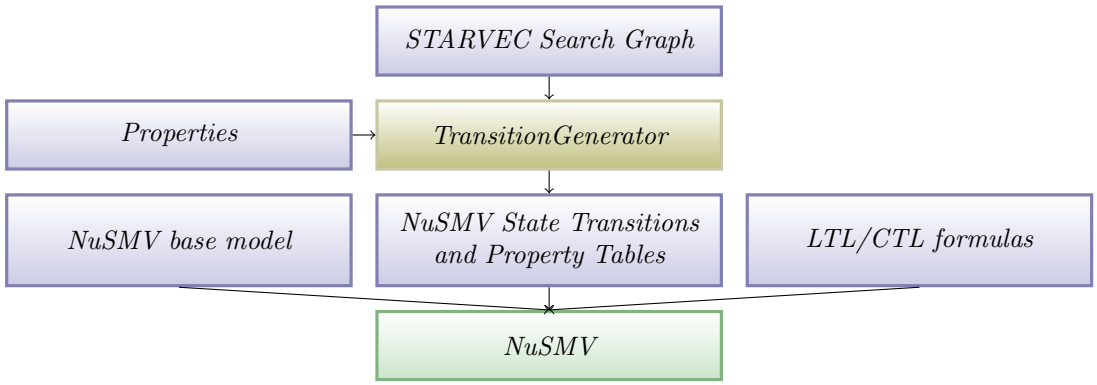

Figure 4.13: Steps for generating a NuSMV model from test data: The *STARVEC* search graph is converted to NuSMV transition and property tables. These tables are the basis for checking CTL formulas.

Using the resulting optimized transition table, NuSMV can search for patterns like the formula shown in Figure 4.12(b). NuSMV is a tool for proving properties of a model like the one described by the transition table created in this section. If the Boolean formula describing the property is not satisfied, NuSMV generates a counter example. For the present application, the counter example is one instance of the undesired behavior of the autonomous driving system. Accordingly, the property to be proven is that the system cannot exhibit the undesired behavior. Therefore, the CTL formula in Figure 4.12(b) starts with the negation operator "¬" followed by a specification of the behavior. **EF** (Exists Finally) means that there exists a path for which eventually some property is fulfilled. In this case, the property is the occurrence of the undesired behavior starting with the velocity being larger than $0.3\,\mathrm{m\,s^{-1}}$. The remaining operators are **EU** (Exists Until) operators. They state that there exists a path for which a property holds until another property holds. First, the velocity is positive until it is zero. At this point, it stays larger or equal to zero until it is larger than $0.05\,\mathrm{m\,s^{-1}}$.

In summary, CTL can be used for specifying temporal patterns of undesired behavior. The model generated by the *STARVEC* analysis can be converted to a representation that NuSMV can check against such a specification.

4.4.2 Fast Pattern Search Based on Simple Automata

An alternative is to define the pattern of an undesired behavior as a deterministic automaton. The transitions of the automaton are guarded by logic conditions on some variables. These variables are a subset of the ones tracked in the checked model. If the accepting state of that automaton is reached, it means that the behavior has occurred. BFS (Breadth First Search) can determine if this state is reachable within the checked model. The checked model is the combination of the automaton above and the model used for extracting the NuSMV transition tables.

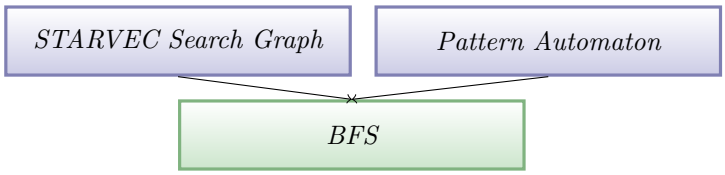

Figure 4.14: Steps for generating the input of the Breadth First Search (BFS): It directly uses the *STARVEC* search graph.

Breadth first search means that "the root node is expanded first, then all the successors of the root node are expanded next, then their successors, and so on" [129]. In contrast, DFS (Depth First Search) "always expands the deepest node in the current fringe of the search tree" [129]. BFS is superior to DFS in this context, as it provides the shortest path to an occurrence of the pattern, which is easier to understand.

Figure 4.14 illustrates that generating the inputs for the BFS is simpler than for NuSMV, because BFS can directly access the states in the *STARVEC* search graph. The only inputs are the *STARVEC* search graph and the pattern automaton. Property tables as described for the NuSMV model are not necessary, because the pattern automaton can contain guards directly pointing to state variables. For both the NuSMV model generation and the pattern state machine, it is necessary to list all variables that can be used for properties or guards before executing the *STARVEC* algorithm. The analysis then stores the values of these variables in each simulation step. In the worst-case, the BFS visits every combination of model state and pattern state once. Thus, its run time is linear to the size of the combined state machine.

An example for a pattern automaton is shown in Figure 4.12. The pattern can be initialized at any point during the simulation, hence p_0 is always reachable. First, the pattern searches for a velocity larger than $0.3\,\mathrm{m\,s^{-1}}$. This triggers the transition from state p_0 to state p_1. If the velocity is lower than zero at any point during the pattern comparison, the pattern state is reset to p_0. The transition from p_1 to p_2 is triggered when the velocity is zero. Finally, the velocity needs to be larger than $0.05\,\mathrm{m\,s^{-1}}$ in order to reach the terminal state p_3. Reaching p_3 means the specified pattern is detected.

4.4.3 Comparing Pattern State Machines and Computation Tree Logic

Using Computation Tree Logic for specifying undesired behaviors has two advantages over BFS:

- CTL has the higher expression power
- CTL is a standard language that many experts are able to use.

The first advantage is the expression power. A possible undesired behavior pattern might constrain all possible future scenarios. For example, an emergency brake system should be activated if the collision is inevitable for any actions of the involved vehicles. A false positive is

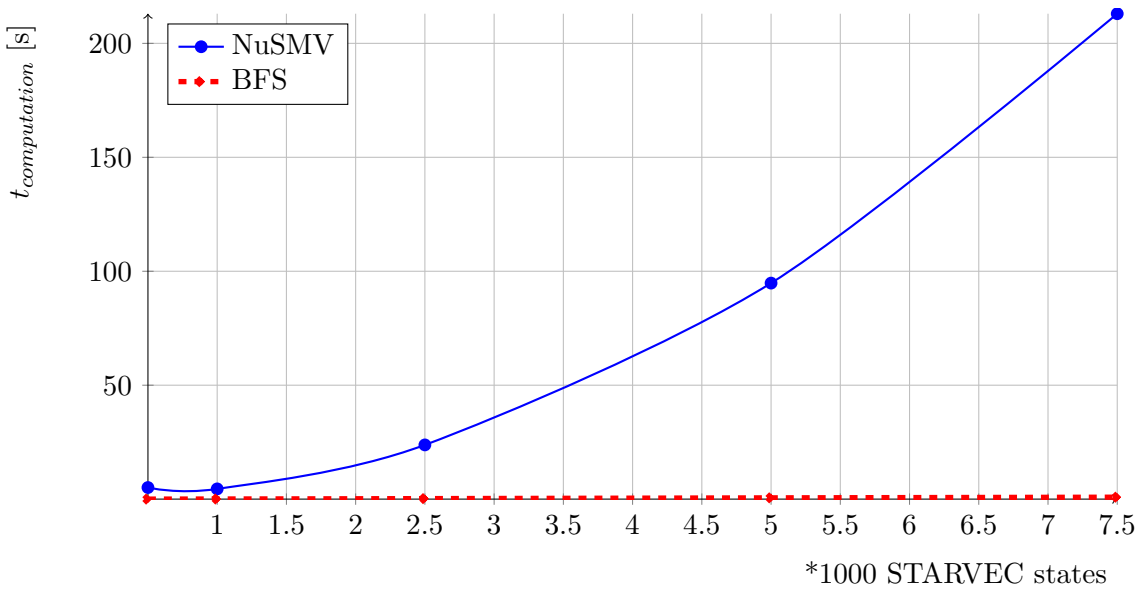

Figure 4.15: Comparison of BFS and NuSMV computation times: NuSMV is very slow for large state numbers.

the system first being activated but no collision follows. This could be expressed by both CTL and the pattern state machine. A false negative is if the system is not activated but for all possible future states, a collision occurs. As the pattern state machine determines for a single execution whether the pattern occurred, the false negative cannot be expressed using the pattern state machine. CTL can demand properties for all possible future scenarios, enabling it to express false negatives.

The second advantage of CTL are the available experts. The language is taught at universities and applied by many research groups. The involved experts are both trained to express problems in CTL and to use available tools like NuSMV. In contrast, using the problem specific pattern state machine requires the engineers to get familiar with it. However, it is easy enough for most temporal logic experts to familiarize themselves quickly.

The advantage of the pattern state machine is the computation time. As depicted in Figure 4.15 the NuSMV computation time for detecting a simple pattern increases rapidly with the number of *STARVEC* states to be covered. For 7500 states, it requires 213s, whereas BFS requires only 0.86s. For searching in 350.000 states, the BFS requires 77 seconds, which is still feasible.

Both, the BFS based method and NuSMV emit a state trace with the corresponding environment events resulting in the detected behavior. The BFS based method is integrated into the *STARVEC* framework such that this behavior can be replayed by clicking the corresponding button. Instead of sequentially loading the explored states of the state trace, the simulation is rerun with the detected environment events leading to the behavior. This way, a debugging tool can be attached to the simulation allowing more thorough analysis of the interaction of planning components and the environment. For the NuSMV based method, the emitted environment

events can also be entered into the simulation environment allowing replaying the detected behavior.

In summary, CTL beats the BFS based method concerning expression power. Most relevant behavior patterns can be expressed by both formalisms, but some corner cases can be expressed in CTL, but not using the pattern state machines. However, the BFS based method is significantly faster than the method based on analyzing CTL in NuSMV, making it the better choice for applications that do not require the corner cases. All cases that were relevant in the development of the planning and control system referred to in this thesis could be expressed using the BFS based approach.

4.5 Interaction with Traffic Participants

One of the most complex challenges for autonomous driving is the interaction with other traffic participants. They can show a large number of possible behavior patterns for which the vehicle concept and implementation has to ensure safe operation. This makes it difficult to test interacting autonomous driving systems. Errors related to a complex chain of events, which were not discovered in prior simulations, recently led to one of Google's self-driving cars bumping into the side of a bus at two miles per hour.

Section 4.5.1 describes how to model the behavior of the traffic participant as nondeterminism, for producing such complex events in a simulation environment. It concludes by describing how *STARVEC* uses this model for generating undesired behavior like collisions. Section 4.5.2 describes how to identify the collisions that are caused by the ego vehicle.

4.5.1 Modeling Traffic Participants

In Chapter 3, the *STARVEC* algorithm is used for handling sensor and actuator inaccuracies affecting the vehicle nondeterministically. Traffic participants also have multiple options in each moment. Therefore, they can be modeled similarly to sensor and actuator inaccuracies.

In the scenarios regarded in this thesis, the opposing vehicle follows a lane that the ego vehicle wants to cross or merge into. Figure 4.16 visualizes that within this lane, the opposing vehicle can drive either fast, or slowly. It can drive at a constant speed, repeatedly change its velocity or slow down to a full stop due to various reasons. These reasons do not need to be known for modeling the traffic motion, because they are modeled as nondeterminism. In the *STARVEC* framework, the nondeterministic behavior can change after a fixed time interval. For each time interval, the opposing vehicle can accelerate, decelerate or keep its velocity. Combinations of these three motion primitives lead to different motions including the options depicted in Figure 4.16. The whole range of motions is allowed. The model does not include behavior rules like maintaining a

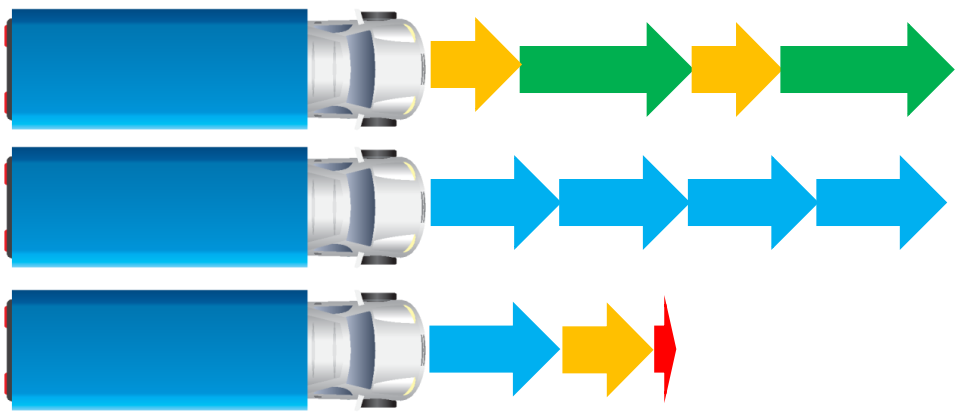

Figure 4.16: Examples of different possible speed profiles resulting in different behavior of the complete system: The vehicle can repeatedly change its velocity (top), drive with a constant velocity (middle) or decelerate to a full stop (bottom). Many other combinations are possible.

minimum distance or driving carefully. Such rules might prevent behavior patterns in simulation that do occur in reality.

The resulting behavior includes patterns that seem to be intentionally aggressive. A physical driver might have various reasons for such behavior. Therefore, the autonomous vehicle should ensure that for any behavior leading to a collision the behavior of the opposing vehicle was not acceptable and the collision was directly caused by this behavior. Instead of removing unacceptable behavior from the model of the opposing vehicle, the resulting collisions should be filtered for those caused by the ego vehicle. This approach avoids removing some unanticipated but acceptable behavior from the traffic participant model. For example, the traffic participant might overtake with little safety distance.

Based on the traffic participant model the *STARVEC* algorithm searches for different behaviors of the system the same way it does with sensor and actuator inaccuracies. In each step, a different pattern of traffic participant behavior can be selected. The resulting configurations are compared to the specifications of undesired behavior. If an undesired pattern is detected, it can be replayed and analyzed.

4.5.2 Identifying Self-Caused Accidents

In a static environment, the ego vehicle must prevent all collisions. In contrast, traffic participants might steer their car directly into the ego vehicle and make it impossible to prevent the collision. The task of a test method is to find collisions and decide whether they should have been prevented by the ego vehicle.

Figure 4.17 shows some example situations of a collision between an autonomous vehicle (red, ego vehicle) and a traffic participant (blue truck). The first sub figure (Figure 4.17(a)) depicts

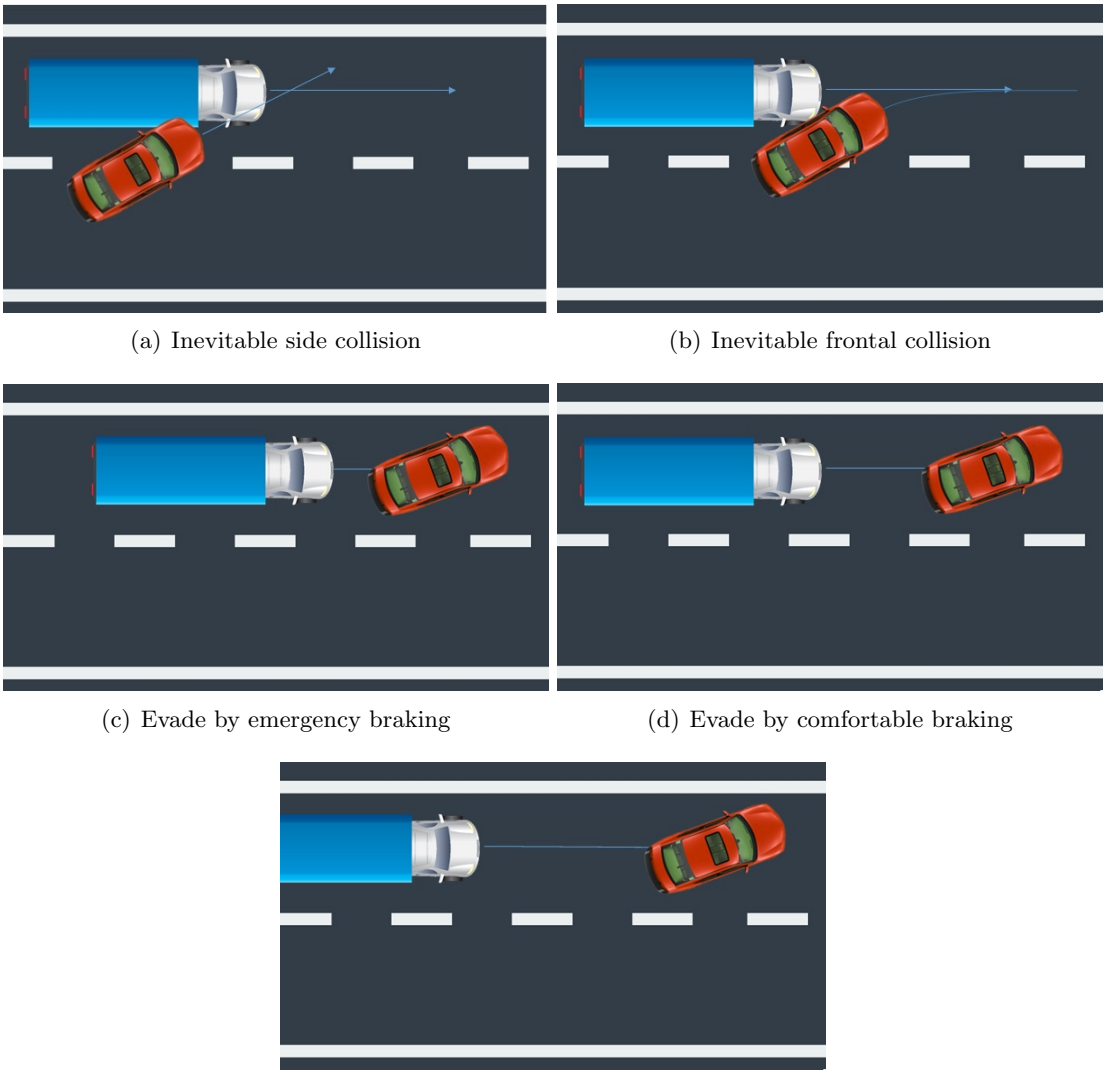

(a) Inevitable side collision

(b) Inevitable frontal collision

(c) Evade by emergency braking

(d) Evade by comfortable braking

(e) Evade by not accelerating

Figure 4.17: Different constellations of a collision between the ego vehicle and a truck. If the ego vehicle crashed into the truck, the truck could not have prevented the collision. If the ego vehicle enters the lane far in front of the truck, the truck is responsible for preventing collisions with the ego vehicle.

the ego vehicle steering into the side of the truck. The truck can only prevent this situation by not approaching the ego vehicle too closely. As the truck has the right of way, the blame for the collision can be assigned to the ego vehicle. In the second situation (Figure 4.17(b)), the truck drives into the ego vehicle. The truck has the right of way and does not need to assume that the ego vehicle will block its way. Therefore, the collision is also the fault of the ego vehicle. In the third situation (Figure 4.17(c)), the truck could avoid the collision by executing an emergency brake maneuver. The fault of the following collision can mostly be assigned to the ego vehicle, as it may not force the truck to perform such a maneuver. The truck can be partially blamed for the collision if it does not brake. The collision following the fourth situation (Figure 4.17(d)) should be avoided by both traffic participants. The ego vehicle should not force the truck to brake immediately, but the truck has to avoid a collision by braking. Finally, a collision following the fifth situation (Figure 4.17(e)) is the fault of the truck. The truck only hits the ego vehicle if it accelerates although the ego vehicle is in front of it.

The first kind of situation can be identified by checking whether the accident would occur if the ego vehicle had stopped just before the collision. If stopping can prevent the collision and the truck has the right of way, the collision is most likely the fault of the ego vehicle. The same applies if the right of way is not clear, for example in unstructured environments. The ego vehicle should follow a driving strategy such that it does not actively drive into another vehicle. If all vehicles ensured that they are only involved in collisions that cannot be prevented by stopping, there will not be any collision. Therefore, it has to be determined whether an accident would have occurred if the ego vehicle stopped. This decision can be made by moving the virtual representation of the ego vehicle to the previous position and repeating the collision check. For the scenarios regarded in the evaluation (Section 6.3.2), it is sufficient to check, which vehicle reached a critical position first.

Situations b-d ((Figures 4.17(b)-4.17(d)) can be recognized based on the concept presented in Section 4.4. The temporal sequence to search for would be

- the ego vehicle first merges into the lane of the truck,
- then collides, while
- the safety distance between the two vehicles is at no point in time sufficient and
- after a short reaction time, the pursuant vehicle decelerated constantly.

The last step of the sequence depends on the situation to search for. For situation b, the deceleration would be an emergency brake maneuver that is not sufficient. In situation c, comfortably braking and in situation d constant velocity are not sufficient for avoiding the collision.

Detecting situation e requires searching for any collision. However, avoiding this collision results in overly conservative driving of the ego vehicle. In most merge situations, it would not be able

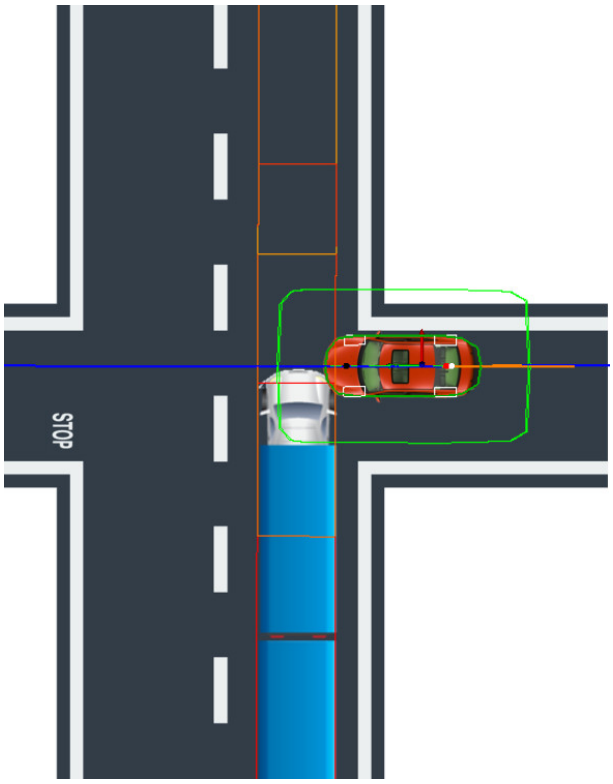

Figure 4.18: Collision of the ego vehicle in an intersection. The truck has the right of way. Hence, the collision is the fault of the ego vehicle.

to squeeze in between two other vehicles. Accepting situation d (Figure 4.17(d)) might also be considered necessary for avoiding overly conservative driving.

The collision pattern to search for depends on the tested scenario. Figure 4.18 shows a collision between the ego vehicle and a truck having the right of way. In this scenario, a collision as in situation e can be avoided without driving overly conservative: The truck may be expected to accelerate comfortably. It is still not necessary to cope with the truck accelerating at its physical limit.

In summary, determining that a collision is the fault of the ego vehicle is possible for some scenarios based on the *STARVEC* algorithm. For other scenarios, collisions that are mainly the fault of the opposing traffic participant have to be accepted in order to avoid overly conservative driving.

Chapter 5

A Framework for Testing Automotive Planning and Control Components

Based on the description of the *STARVEC* approach in Chapter 4, this chapter explains how the test framework can be integrated into a software architecture. First, Section 5.1 describes the implemented architecture of the *STARVEC* framework including the interaction with inaccuracy models and simulation components. Next, Section 5.2 explains how the benefit of the *STARVEC* approach can be maximized in the development process. As an additional advantage, Section 5.3 shows how the concept of loading and saving states introduced in Section 4.1.3 increases the efficiency of debugging. Finally, Section 5.4 outlines how the *STARVEC* algorithm can be used for online testing of self-evolving autonomous driving systems.

5.1 Software Architecture

Figure 5.1 shows the simulation architecture of the presented testing framework. As described in Section 4.1.3, the *STARVEC* framework can trigger all components involved in the simulation. For this purpose, the components are expected to implement the *TriggerableFilter* interface that requests the implementation of five functions: The three scheduling functions described in Section 4.1.3, plus the load and the save function described in Section 4.1.3. The interface is implemented by every planning component and simulation component. The simulation environment can consist of separate components for the vehicle dynamics, environment mapping and other systems interacting with the planning and control software. Additionally, there can be components that introduce inaccuracies into the system. For example, a component defining the acceleration inaccuracy described in Section 3.3.2 can expect the currently requested acceleration

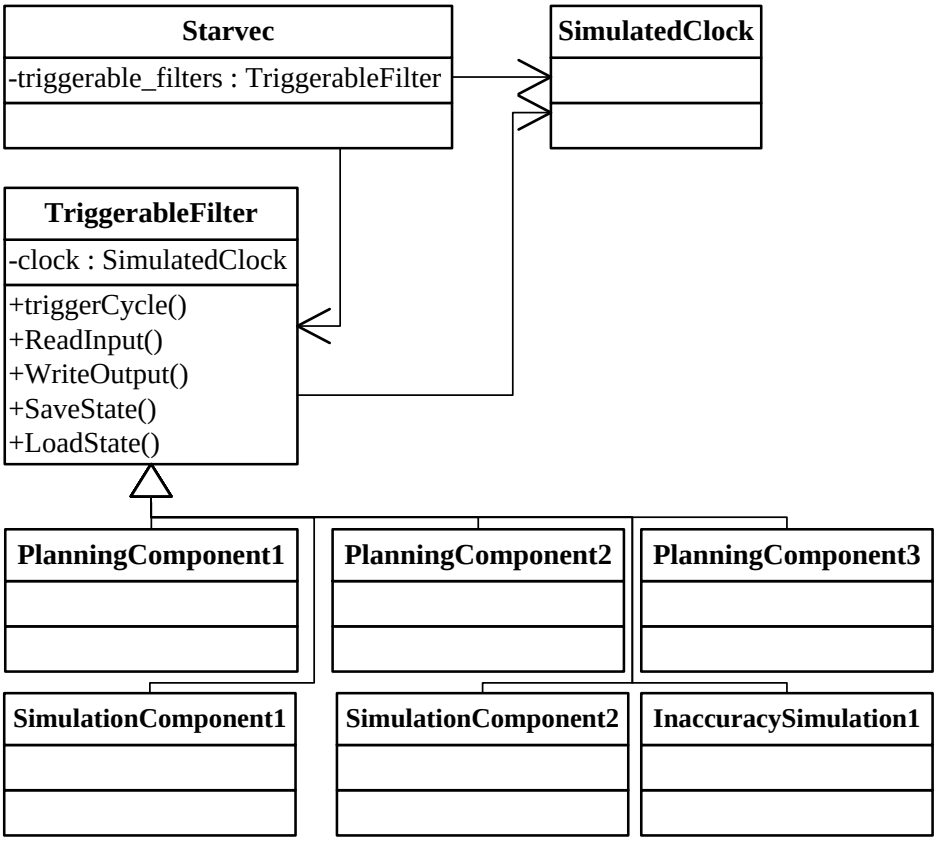

Figure 5.1: Architecture of *STARVEC* and the simulation environment. Each component implements the triggerable filter interface and registers with the *STARVEC* system.

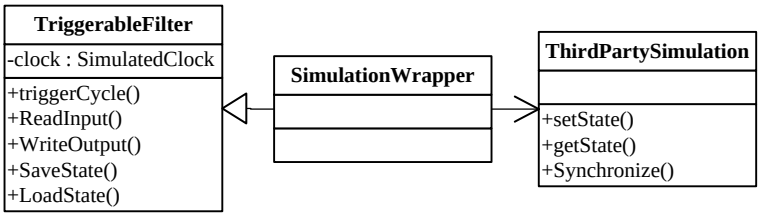

Figure 5.2: Instead of directly implementing the triggerable filter interface, a third party component can be connected to a wrapper filter implementing the interface. The communication between the wrapper and the third party component follows the specification of the third party component.

of the controller as input and emit an inaccurate acceleration to be performed by a simulation environment.

For some components, it is impossible to let them directly implement the *TriggerableFilter*-interface. An example of such a component is a third party simulation software with defined interfaces. In this case, a wrapper component connects the simulation and the *STARVEC* framework. Figure 5.2 shows such a wrapper. It implements the same TriggerableFilter interface as the other components, but instead of directly performing the corresponding actions, it forwards them to the third party simulation. If it is requested to store its state, it reads the current state of the simulation and returns the representation requested by *STARVEC*. The third party simulation might use a different concept for synchronizing with other components. This concept is also translated by the wrapper component.

The internal structure of the *STARVEC* framework is depicted in Figure 5.3. It shows the major structural parts of the implementation with some names changed for easier understanding. The *StarvecBase* mediates between the *STARVEC* algorithm, the middleware and the GUI (Graphical User Interface). The actual test concept is implemented in the class *StarvecAlgorithm*. It administrates the search tree and tells the scheduler to trigger the simulation and planning components for loading or saving states. For the decision, which state is loaded next, the *STARVEC* algorithm asks its OpenQueue which state to load. The implementation of this queue defines the test concept that is running as used in Chapter 6. The RandomQueue always returns the last stored state, which corresponds to not using the load and save state functionality. Parallel to the core concept implementation, there is a GUI component that displays information about the current execution state from the *StarvecBase* and can trigger methods in the framework.

5.2 Integration into the Development Process

Developers should apply the *STARVEC* system in parallel to the main development process. A set of test scenarios can be included in a continuous integration process or executed as regression tests at each milestone. This section first describes how developers should deal with detected

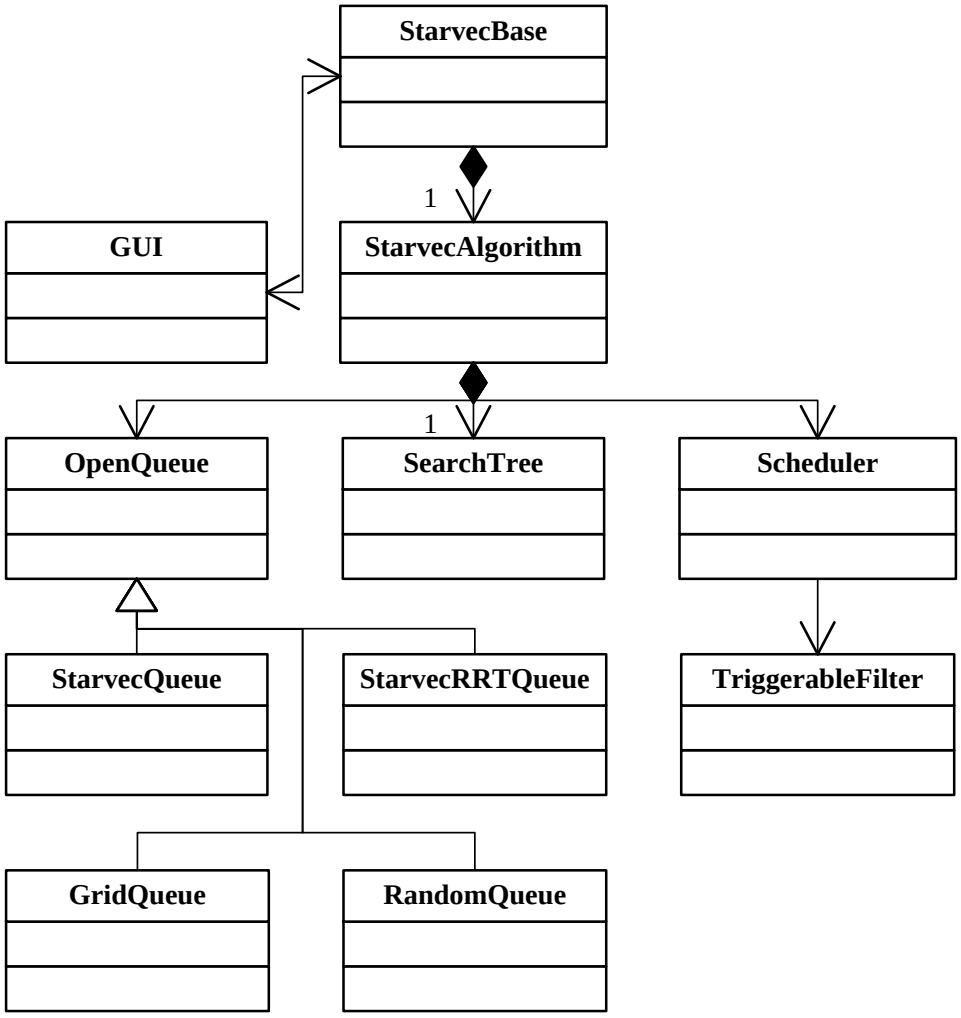

Figure 5.3: Internal architecture of the *STARVEC* system: The major components are the algorithm core ("StarvecAlgorithm"), the queue of states to be expanded ("OpenQueue"), the tree containing all explored states ("SearchTree") and the "Scheduler" communicating with the simulation components.

faults in order to benefit from that information. Next, the role of modeling inaccuracies and applying the *STARVEC* concept for discussing the consequences of faults is sketched.

5.2.1 Benefit from Detected Weaknesses

If the test method finds undesired states like a collision, the software engineer has the following options:

1. improve the planning and control system,
2. increase the safety distances, or
3. verify that such a combination of errors is impossible and change the error model.

The first solution means to handle the undesired case inside the planning function itself, which is the preferred solution. The second solution–increasing the safety distance–can solve the problem in one scenario, but it will prevent the system from working in other scenarios. Finally, if it can be verified that the combination of errors leading to the undesired state is physically not possible, the error model can be changed accordingly. For example, the software engineer might conclude that at low speeds the steering angle offset is lower than at a higher speed. The disadvantage is that adding such exceptions would add parameters to the error model. As explained in Section 3.3.1, this would make testing and model validation less efficient.

5.2.2 Inaccuracies as Base for Developer Discussions

A fault in a physical test-drive is often a consequence of inaccuracies in localization, mapping, vehicle actuators and imperfect control. Improving any of these components improves the performance of the vehicle. However, the effect of improvements in one component to the behavior of the system is often difficult to estimate. For example, there is no simple correlation between localization inaccuracies and resulting controller deviations.

Figure 5.4 shows an informal process of coping with faults occurring in a physical test-drive. It starts with the fault. This can either be a safety relevant error of the autonomous driving system, or a weakness like some function not being completed successfully. If the fault is related to controller deviations, any of the reasons listed above can be the primary cause. Therefore, the first step is to analyze the signal traces logging the performance of the involved components (second box). Based on this analysis, a counter measure has to be found. A typical counter measure is the adaptation of the component that performed worse than expected. The assignment which component is considered responsible is based on discussions and experience of previous faults. Political considerations can also be involved. Next, the assigned team tries to improve the performance of its components accordingly. If it is successful, the fault can be considered solved. Else, the discussion is repeated and the problem is reassigned to either the same or a

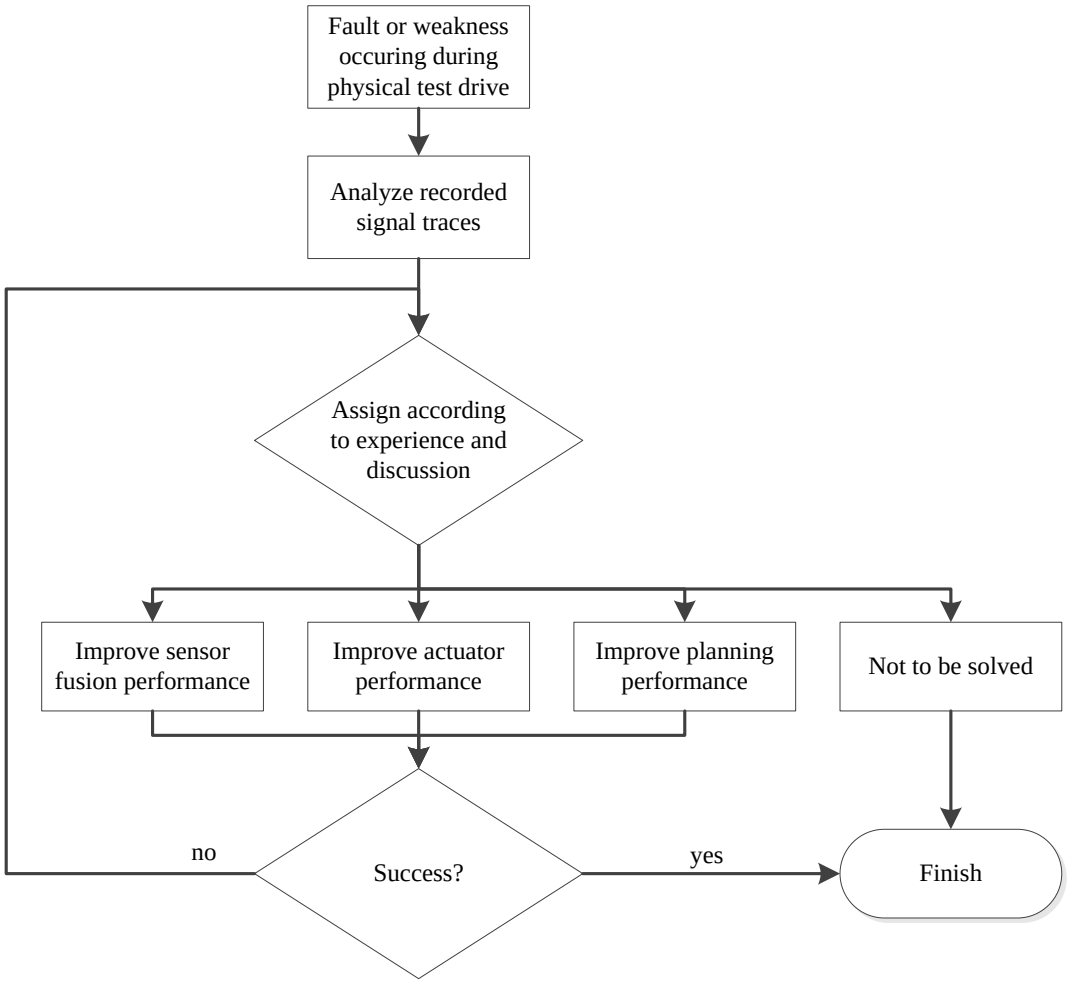

Figure 5.4: Coping with faults and weaknesses in the development process: The fault needs to be analyzed and assigned to the team developing one of the software components. In some cases, there are several options which component to adjust in order to fix the fault.

different team. It can also be considered as unsolvable with the available sensors and actuators. For example, a narrow passage can be considered as impassable.

This informal process includes no documentation about expected inaccuracies and no analysis of the consequences to other scenarios. The decision which component should be considered responsible can be wrong. In addition, it gives little information about whether a better sensor would improve the performance. Modeling sensor and actuator inaccuracies and using the *STARVEC* algorithm can improve the discussion as depicted in Figure 5.5. The green boxes can be enhanced by the *STARVEC* framework. First, the decision which component is responsible for an occurred fault can be based on a comparison with sensor and actuator models. If the sensor or actuator performance is worse than the models predict, the assumption is that the corresponding component can improve the performance for that situation. If this is impossible, the models have to be changed accordingly. This affects further tests of other scenarios and serves as a documentation of sensor and actuator performance. The changed models might also lead to predicted faults in other scenarios that have not yet been observed in physical test-drives.

If the inaccuracies are within the limits of the models, it should be possible to reproduce the fault using the *STARVEC* system. In this case, the scenario is added to the regression test set and the performance of the planning and control components is improved for this scenario. If it cannot be improved, the requirements to the sensor and actuator components are increased or the scenario is considered as not to be solved. A result of this process are valuable sensor and actuator inaccuracy models and a test set of difficult planning and control situations. Based on these artifacts, decisions about replacing, up- or down- grading sensors or actuators can be made and a first evaluation of new planning and control components can be executed fast.

5.3 Using Serialized Software Components for Debugging

The content of this section is based on the paper published in [153]. As mentioned in Section 4.1, the regarded approach requires being able to save and load the state of the planning and control system. Apart from allowing efficient testing using the *STARVEC* algorithm, this also supports debugging efforts. If a fault occurs during the development process of an autonomous vehicle, the reason of this error is often not immediately clear. Figure 5.6 illustrates the effect of a fault occurring in different steps of the development process. In order to understand and fix the corresponding defect, the fault needs to be reproduced in a simulation environment. If the fault occurs while executing a unit test it can be reproduced and fixed quickly. A fault during a full simulation or a physical test-drive can be more difficult to reproduce.

The typical approaches for reproducing a fault are based either on manual experiments or on signal traces. Both methods are often not sufficient for reproducing the objected behavior. Manual experiments cannot create the exact same situation that led to the behavior in the vehicle. However, some faults only occur in very special situations and are therefore difficult to

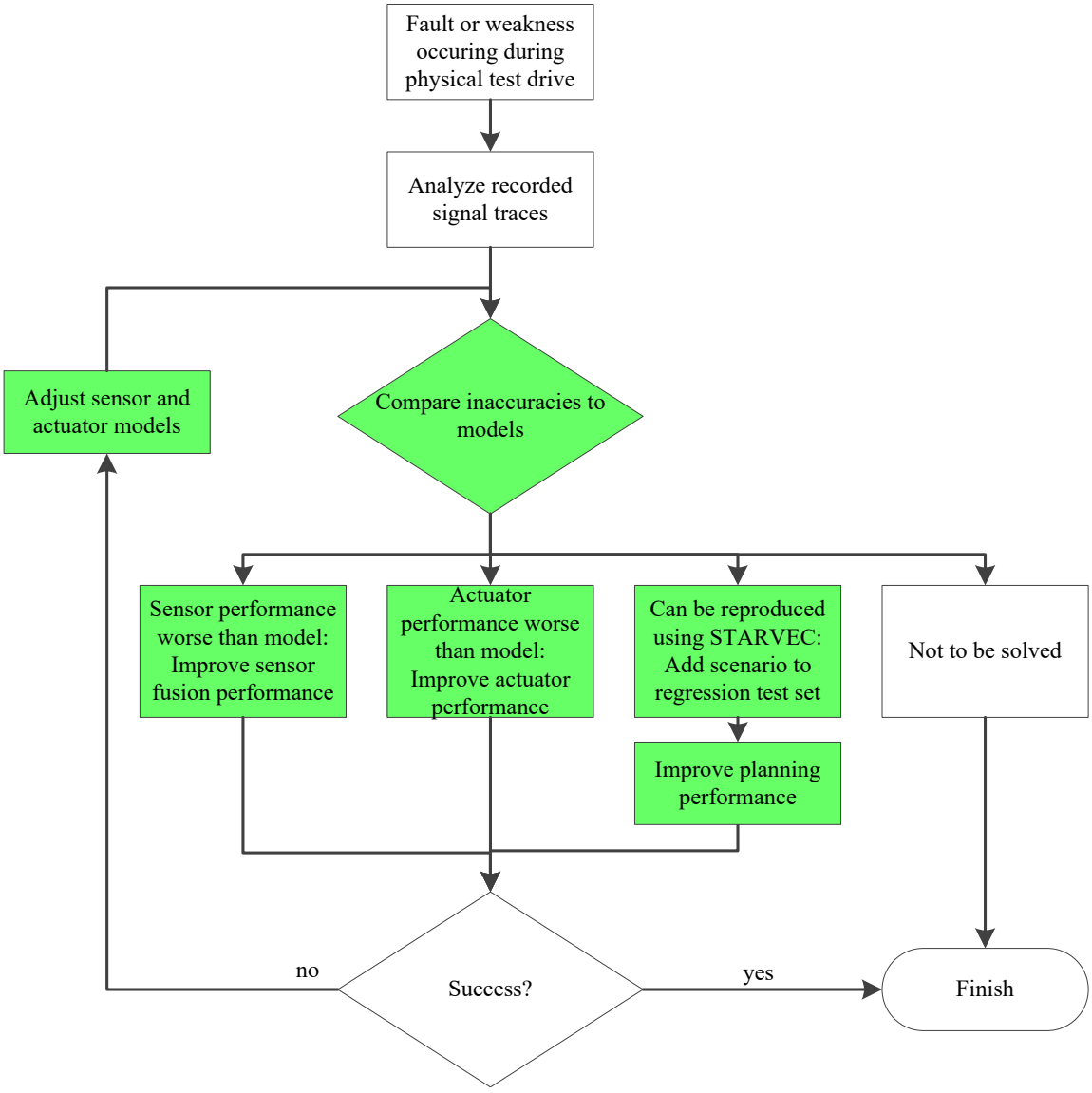

Figure 5.5: Coping with fault and weaknesses in the development process supported by *STARVEC*: The negotiated allowed inaccuracies created by each component are integrated into the inaccuracy models. This makes decisions more explicit.

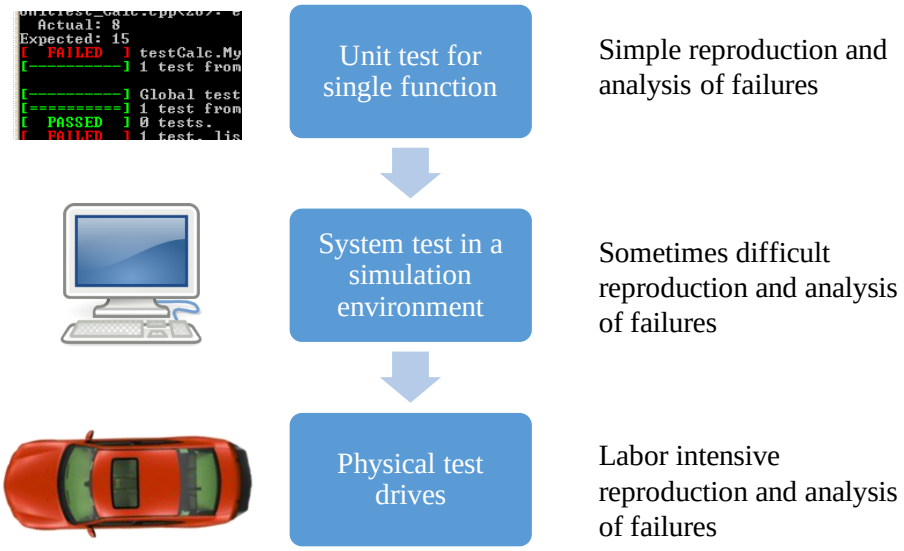

Figure 5.6: Reproducing faults in the development process: Faults detected in unit tests require little effort, while reproducing faults detected in physical test-drives are labor intensive.

reproduce manually on a workstation. The second typical approach is based on signal traces. On the one hand, they can be used to replay many computation sequences. On the other hand, they require signal data starting with the initialization of the involved component until the manifestation of the fault. This requires a large amount of data for long test-drives. Moreover, it takes much time to replay the whole signal trace. Without the start of the signal data, the regarded component might be in a different state and thus not show the observed behavior. Furthermore, nondeterminism can change the behavior of the component. The nondeterminism is either wanted like in randomized algorithms or unintended like in race conditions. This nondeterminism can happen at any time between initialization and fault manifestation and prevent the fault from being reproduced.

Exploiting the save and load operations that are also used by *STARVEC* can solve these problems. The approach deserializes the state of the planning and control system that was serialized just before the fault occurred. This way, it can execute the cycle showing the faulty behavior again with a debugger attached to it. Based on this approach, the software engineers can quickly find and fix the underlying defect. Moreover, they can test the corrected software by executing the computation cycle. For achieving this goal, serialization has to be triggered in the right moment as described in Section 5.3.1 and an environment for deserialization as described in Section 5.3.2 has to be available. Based on these prerequisites, the method can be applied efficiently as described in the case study in Section 5.3.3.

5.3.1 Triggering Serialization

The ideal moment for serialization is just before the interesting event occurs. Three mechanisms can be applied for approximating this ideal:

- manual trigger for serialization,
- serialization each time, an error message is logged
- serialization before each cycle

The manual trigger can be used to store a state that a test driver considers worth further analysis. For example, the car might refuse to continue driving without an apparent reason. If the system recognizes that something does not work, the logged error message can be used as a trigger, instead. This is particularly useful to find an example of an already known error pattern. For example, situations in which the planning component is unable to find a path. In practice, serialization is performed just before the cycle is executed, which approximates the ideal mentioned above. If no error occurs in the cycle, the serialized data is discarded. This way the exact situation in which the error occurs can be repeated. Finally, serialization in each cycle means that the serialized data is never discarded. This setting allows tracing back a faulty system state to the point in time in which it became faulty. This setting produces a larger amount of data but still less than a signal trace.

In any of the three triggers for serialization, some engineers notice that some behavior of the vehicle needs further investigation and file a ticket in a bug tracking system. To this ticket, they attach the corresponding serialized software components.

5.3.2 Simulation Environment for Reproducing Faults

In addition to the planning components serialized before a fault occurs there needs to be an environment for deserializing the component and reproducing the fault. This can be either a stand-alone environment supporting only the interfaces of one software component or a closed loop simulation of the planning components and the components interacting with it.

In the project supporting this thesis, mainly a stand-alone environment is used. A screenshot of this environment is depicted in Figure 5.7. In this application, the software engineer can control the planning component based on a GUI. The user interface contains a visualization of the planning results. This visualization is integrated in a more general visualization concept: Each component developed by the planning and control team has access to a logging and visualization interface. It uses this interface for publishing information about its computation states. In the stand-alone environment, this interface is implemented to forward the visualization to the depicted GUI. The GUI also allows controlling the inputs of the planning and control

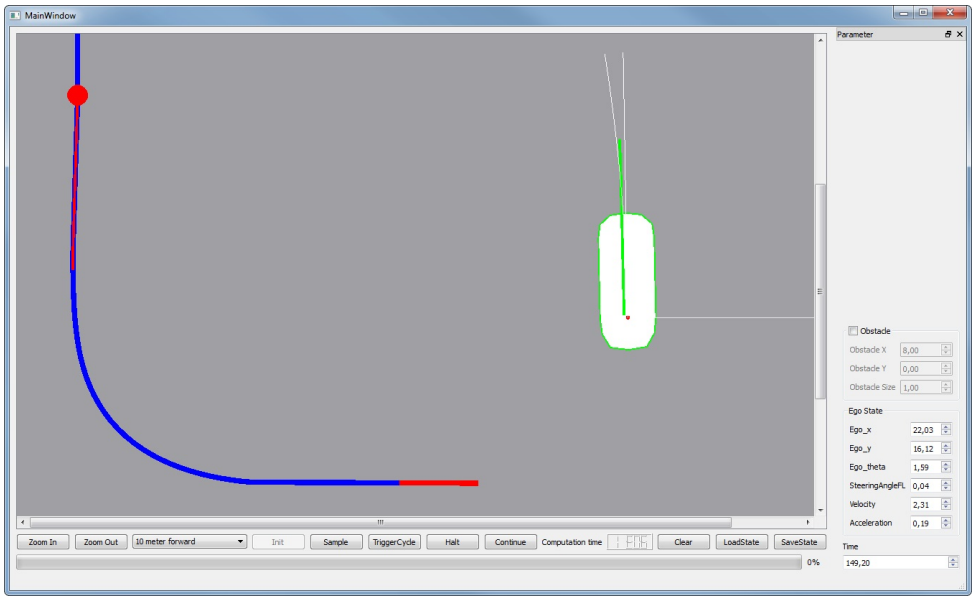

Figure 5.7: Deserialized planner in a stand-alone environment: The main area visualizes the planned path and the current position known by the planner.

component precisely. These inputs include triggering the execution of another cycle and setting the time of the simulated clock.

Loading a state of the planning and control system can also increase the accessibility of debug information. Typically, engineers use release builds for executing planning and control systems on the real car. In contrast, the stand-alone execution environment can deserialize the same planning system using a debug build. This way, standard debugging software can step through each line of code of the planning and control system. If an error message indicates the problem that should be further analyzed, tracing it down to the source code is very simple. The software engineer only adds a break point to the line of code emitting the error message. When the debugger hits the break point, the software engineer analyzes the state of the software component.

Some cases require executing the particular situation in a full simulation. This is performed by reproducing the situation as described in Section 4.3.

5.3.3 Application to an Industrial Project

The approach presented in the previous sections has been applied to an industrial software project. This Section summarizes the process and the results of an example application for tracing back a software fault to a defect and fixing the defect. Figures 5.7-5.11 visualize the single steps.

The technique was useful in a situation in which the vehicle drove less smoothly than usually. In this situation, the integration team collects the log files created by the planning and control

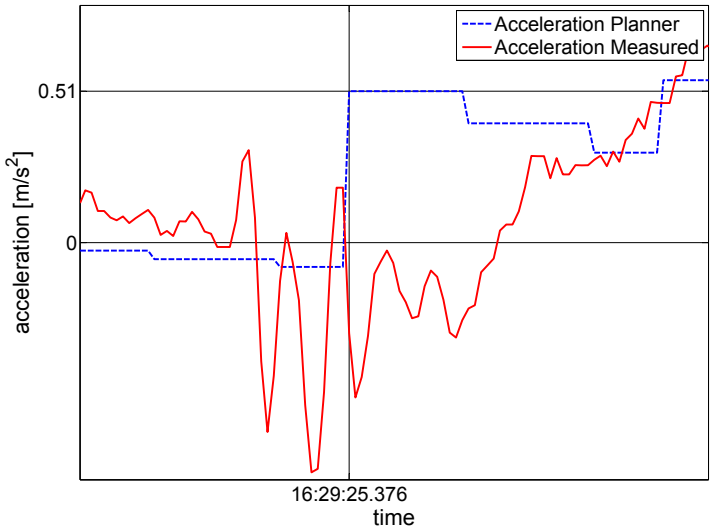

Figure 5.8: The planner assumed the wrong current acceleration: At the marked point in time, the planned and the measured acceleration should be identical.

Figure 5.9: The log message of the planning component confirms the wrong acceleration assumption (red circle).

system. They attach these log files to a ticket for the team responsible for the planning and control components asking for analysis.

First, the planning and control team identifies the objected driving situation in the recorded acceleration data. This data is part of the log files and depicted in Figure 5.8. It contains the measured acceleration and the acceleration computed by the planning component. The team knows that at the time marked in Figure 5.8, these two acceleration values are supposed to be approximately equal. However, the values differ significantly which means that the planning component computes and emits the wrong acceleration.

Next, the planning and control team analyzes the log messages created by the planning component at the regarded time. Figure 5.9 shows the log message indicating that the planning and control component assumed a wrong initial acceleration.

Hence, the planning and control team loads the state of their component that was serialized before the faulty log message was created. In this case, a stand-alone environment is sufficient for reproducing the fault. This environment is depicted in Figure 5.7. The main part of the stand-alone environment contains an illustration of the current position, the current reference path and the currently planned trajectory. For this particular loaded state, the illustration does not depict any wrong behavior.

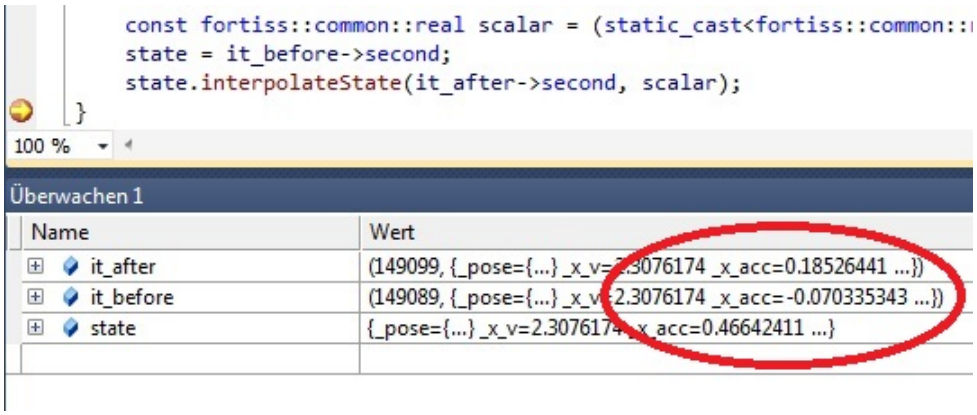

Figure 5.10: The stand-alone environment allows re-running the cycle using a debug build of the planner based on the serialized state. A standard debugging tool allows quickly finding the line of code and variable values leading to a bad acceleration interpolation.

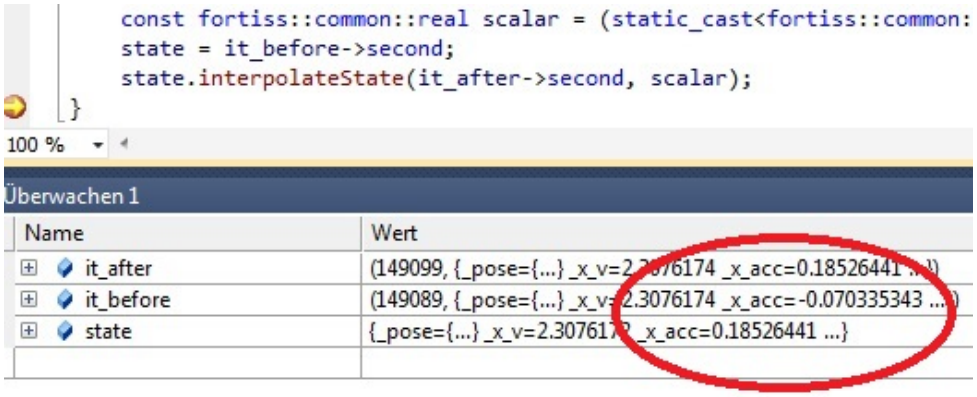

Figure 5.11: After fixing the corresponding function, the serialized situation can be repeated with a different version of the planner showing that the problem does not occur anymore.

Instead, the planning and control team uses a debugging tool to execute the planning cycle step by step. This way, they finally execute the lines of code depicted in Figure 5.10. These lines of code include the function “interpolateState” which does not return the correct result in this context. The context assumes that the interpolated value is between the two input values. The input values are 0.18 and -0.07, but the interpolated value is 0.46.

Instead of an interpolation, the regarded line of code performed an extrapolation. The problem is fixed by limiting the results to the interval between the two input values.

Finally, the improved software component is tested by executing the same serialized state with the new version of the planning system. Figure 5.11 shows that the interpolation function now correctly returns 0.18 which is in the interval of the two input values.

The regarded solution to a software defect is an example how loading and saving states improves the development process. It starts with a vague observation of the vehicle acting uncomfortably

and traces it to the incorrect implementation of an interpolation function in the source code. For preventing further problems, a unit test is added testing the regarded part of the planning component.

In the described example, a signal trace is less useful than the serialized software components:

- It would require significantly more time until the planning component reaches the exact same state as in the vehicle.
- The error was strongly related to the timing of the components: A few milliseconds difference let the problem disappear.
- A signal trace would have been very large and might not have been transferred over the internet.

The signal trace would also be larger than the serialized software components. The ADTF signal traces of a seven-minute simulation require 812 MB compared to 10 MB for the serialized states of the regarded planning and control system.

In summary, loading and saving states does not only allow efficient testing, but also efficient reproduction of faults. The proposed method has been implemented and successfully used in a software project.

5.4 Towards Self-Aware Autonomous Vehicles

In the book chapter [154], Winfield suggests to make robots self-aware by equipping them with a "What-If"-engine. This engine is basically an internal simulation of the robot and its environment and needs to be "controlled by the same Robot Controller as the real robot". It enables the robot to predict the consequences of its actions, even if the robot model, the environment simulation and the robot controller have evolved by Machine Learning and the robot has not been designed for the current situation. Winfield argues that this ability corresponds to a limited version of self-awareness and enables the robot to behave ethically. Whether this ability can be called self-awareness is controversial, but it can help a robot to cope with new situations.

The same principle can be transferred to autonomous driving as depicted in Figure 5.12. It is divided into the *STARVEC* algorithm (right box), the planning and control system to be tested (top left box) and the simulation environment for this system (bottom left box). Both interacting components: the planning and control system and the simulation environment can be based on learning mechanisms. This section first investigates how the planning system and each of the three depicted simulation components can be supported by learning techniques in sub sections 5.4.1 and 5.4.2. Next, Section 5.4.3 addresses some challenges of applying the *STARVEC* algorithm to such systems.

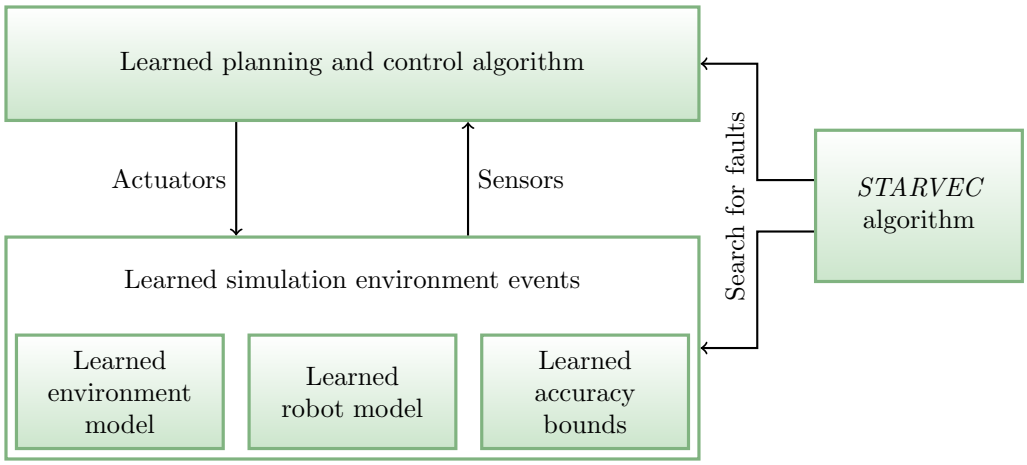

Figure 5.12: Testing learned algorithms online: All simulation elements and the planning and control algorithms can be based on learned information. *STARVEC* tests the behavior of the components rather than the internal structure and is therefore also applicable to learned components.

5.4.1 Learning for Planning and Control Systems

Several recent scientific works have investigated how to teach a robotic system to perform autonomous driving planning and control tasks based on machine learning. The developers of [155] enhance a full size road vehicle by a camera system and computer controlled steering and acceleration. They teach the system the correspondence between video images and the steering behavior of a human driver. Based on this learned knowledge, the vehicle is able to follow a road in some demonstrated scenarios. Similarly, the authors of [156] teach a model vehicle to make steering decisions based on video images. The focus of the paper is to create a system that works without lane markings and on unpaved roads.

These research projects are two recent examples of machine learning algorithms used for solving planning and control problems. The input of both systems differs from the input assumed in Section 3.3.4. The learning systems use raw video images, while the planning and control system referred to in this thesis relies on preprocessed information: the position and state of the vehicle and an environment obstacle map. The preprocessed information is more abstract, i.e. it contains less data. This simplifies the simulation of such a system. In contrast, simulating video images is more complex. This can be addressed by increasing the similarity between simulation and reality as described in Section 2.3. For classic autonomous driving systems, developers might know which part of the simulation needs to be particularly accurate. For example, a pedestrian intention recognition system might require seeing the movements of arms and legs but ignore facial expressions. Machine learning systems do not tell which part of a video image they are actually using. This makes the development of sufficiently accurate simulation systems significantly more difficult. An alternative approach is to also learn the correct simulation as described in Section 5.4.2.

Another alternative is to apply the machine learning system to the same abstract preprocessed information that the classical planning approach uses. This way it can be tested using the same simulation and the same error models as the classical planning approach.

5.4.2 Learning for Simulation Environments

As sketched in Figure 5.12, the simulation environment can also be learned based on gathered data.

The first part of the simulation to be learned is the model of the environment. For example, the authors of [157] create a machine learning algorithm that predicts how the video input of the vehicle evolves over time. It includes the video representation of other vehicles moving around the ego car.

The second box depicted in Figure 5.12 is learning the model of the own vehicle. One example of such a learning technique is presented in [57]: The software automatically learns the actuator capabilities of the robot. It does so by optimizing a set of internal models to fit to the behavior of the robot and by performing actions that distinguish candidate models. Analogously, an autonomous vehicle might for example learn that it always slightly drifts towards one side in some situations. The resulting model can be used by the simulation and hence by the *STARVEC* algorithm.

The third box in Figure 5.12 refers to automatically learning accuracy bounds of sensors and actuators. For example, the acceleration actuator might perform the requested acceleration with some maximal offset as described in Section 3.3.2. A process of determining the accuracy bounds is described in Section 3.4.

5.4.3 Applying STARVEC to Learned Systems

The *STARVEC* concept is applicable to such learned environments as it has only few requirements to the involved components. As Winfield points out, the simulation might fail "to (virtually) collide with an object" [154] and hence incorrectly classify a motion as safe. This challenge can be reduced by applying the *STARVEC* method as it detects also collisions caused by inaccuracies and nondeterminism. Currently, most research solutions for improving planning and control performance by machine learning directly apply the results to the robot and ensure safety only by human supervision. Systematically testing the behavior of the resulting planning and control component is a first step for increasing the safety of the approach. If the accuracy bounds of the sensor and actuator model is automatically determined, the robot can also reproduce observed undesired behavior in simulation. It used either almost correct sensor and actuator models or less correct ones. If it uses correct models, it is able to reproduce the behavior using the *STARVEC* algorithm and some starting situation as described in Section 4.3.

If it uses incorrect models, experiencing the undesired behavior makes it update the accuracy bounds also allowing it to reproduce the behavior.

The main challenge of applying the *STARVEC* system is its dependency on high computation power. Basically, it can be used for two use cases:

1. Assessing the safety of a maneuver before executing it
2. Testing the safety of a new set of machine learned parameters before applying them

The first use case requires fast execution of the *STARVEC* process. This either requires very high available computation power inside the vehicle. It has to be strong enough to execute several thousands of instances of the planning and control component and the environment simulation in parallel. This is technologically not possible, yet. The alternative is a high bandwidth and low latency connection to a high performance computer. With the introduction of the successors of LTE (Long Term Evolution), the fifth generation mobile network (5G) [158], such connections are possible.

The second use case is to validate evolutionary changes made by machine learning over night before applying these changes to the control system. For this use case, *STARVEC* has less strict time requirements but needs more total computation time. This can be solved either by a very powerful computer in the vehicle or by a standard mobile connection to a high performance computer.

Chapter 6

Evaluation

The *STARVEC* concept has been evaluated in multiple scenarios and compared to several state of the art algorithms. Section 6.1 describes these scenarios and the competing methods. Next, Section 6.2 shows that *STARVEC* performs better than the competing test functions in the evaluated scenarios. Section 6.3 extends the evaluation to more patterns of inaccuracy and additional nondeterministic events. Additionally to the evaluations in this Chapter, [159] successfully applies the *STARVEC* algorithm to compare the performance of a new uncertainty based control concept to a state of the art algorithm.

6.1 Test Setup

The test setup consists of the compared search algorithms, the planning and control component they are applied to and the scenarios in which they are evaluated. First, Section 6.1.1 describes the planning and control system and its major configuration parameters. Next, Section 6.1.2 presents the search algorithms that are extracted from related research and compared to the *STARVEC* approach. Finally, the scenarios in which the planning and control system is tested are defined in Section 6.1.3.

6.1.1 System under Test

The system under test is a planning and control system that consists of a static path planner (pp) based on the concept of [19] and a trajectory planner (tp) based on the work of [25]. It is an adapted version of the system presented in [160]. The static path planner creates curvature continuous paths from a start configuration to a goal configuration that do not collide with any static obstacle. The path planner collision check can be configured by a lateral ($s_{\mathrm{pp,lat}}$) and a longitudinal ($s_{\mathrm{pp,long}}$) safety distance that enlarge a shape around the vehicle. This shape may

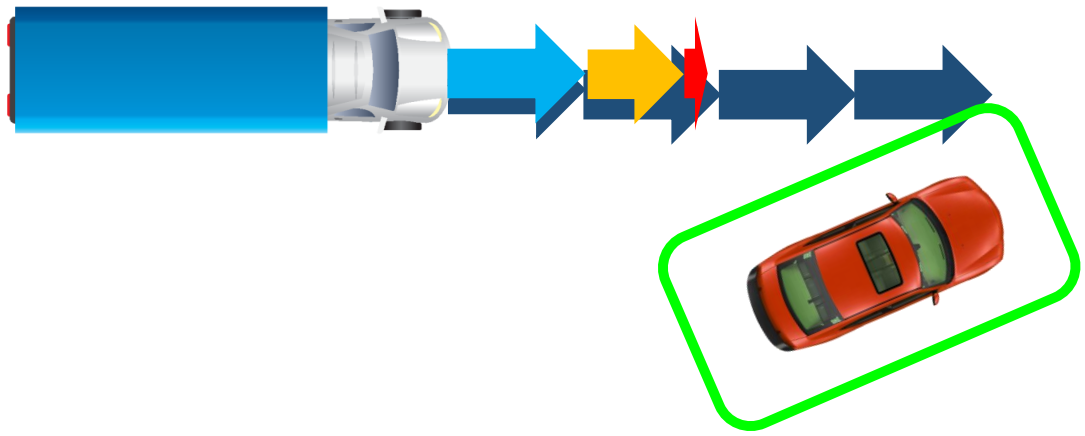

Figure 6.1: Safety margins used in the collision-avoidance system: The truck is predicted to stop (blue, yellow and red arrows) but driving constant velocity is checked additionally (dark blue arrows). The geometric safety margin (green rectangle) would collide with the latter prediction of the truck.

not collide with a static obstacle. The created paths are passed to the trajectory planner that reacts to local changes of the environment and unpredicted errors.

The trajectory planner predicts the future motions of all traffic participants and computes an ego vehicle trajectory that does not collide with any obstacle or traffic participant at the predicted positions. Two kinds of safety margins have been added as depicted in Figure 6.1:

- a geometric safety margin and
- a behavioral safety margin

The geometric safety margin corresponds to the collision checking-concept of the path planner. It is implemented by enlarging the vehicle shape by configurable safety distances (green rounded rectangle): A lateral ($s_{\text{tp,lat}}$) and a longitudinal ($s_{\text{tp,long}}$) safety distance. The purpose of the geometric safety distance is to compensate actuator and location sensor inaccuracies.

The behavioral safety margin should compensate wrong behavior predictions about traffic participants. For each traffic participant, a virtual duplicate with an increased acceleration is considered. The light blue, yellow and red arrows in Figure 6.1 represent the predicted deceleration of the truck. The dark blue arrows are the virtual duplicate that is not decelerating. This is meant to avoid collisions due to traffic participants changing their behavior to stronger accelerations. Both safety margins can be configured and are heuristic methods and no proofs for preventing collisions. If the ego car is not moving, the situation depicted in Figure 6.1 would be considered as colliding: The geometric safety margin (green rounded rectangle) collides with the behavioral safety margin (dark blue arrows) of the truck.

For the purpose of evaluation, some unsafe behavior optimizations have been added. If the traffic participant is predicted to collide despite the ego vehicle not moving, the traffic participant is assumed to stop. This way it will accelerate in front of the truck instead of blocking its way until

the truck actually stops. This behavior is similar to what the software of the Google Car assumed according to [14]. However, this collision check does not use the actual vehicle shape, but adds a safety distance s_{assume_stop} similar to the safety margins described above. This behavior also corresponds to the software of the Google Car before the reported accident [14]. It can lead to situations in which the traffic participant behaves exactly as predicted but only collides because the ego vehicle starts moving. A good test method should find these situations. *STARVEC* does find such situations as demonstrated in Section 6.3.2.

The behavioral safety margins are used for the collision checks of the trajectory planner. In order to define the actual trajectory, the system under test applies the two level concept described in [25]. It consists of a trajectory planner and a low-level controller. The input of the two level system is a reference path. This reference path is computed once by the path-planning component and is constant during the execution. The trajectory planner follows the reference path, but is allowed to deviate in order to evade obstacles or to correct controller errors smoothly. This deviation is performed in the frenet frame: All states are represented as a longitudinal position on the reference path and a lateral deviation from the reference path. In this representation, the trajectory planner finds a trajectory that minimizes the jerk in equation 6.1 relative to the reference path.

$$J = \int_0^\tau \frac{1}{2} u^2(t) \mathrm{d}t + c_{goal} \tag{6.1}$$

J is the computed cost for a trajectory. u is the control input that corresponds to the acceleration and steering of the vehicle and is expressed as the applied jerk. c_{goal} is the additional cost for deviations of the goal position to the reference path. As described above, such deviations occur due to static obstacles or high controller deviations. The cost term 6.1 is applied to both: the longitudinal and lateral motions of the vehicle. Werling has proven that the optimal solution for this minimization problem is a polynomial [25].

The result of the minimization is a trajectory, which is passed to the low-level controller. The stability of this controller has been proven asymptotically stable [25]. However, the proof does not include actuator errors as defined in this thesis.

6.1.2 Alternative Methods for Testing against Nondeterminism

The system under test presented in the previous section is evaluated against *STARVEC* and several competing concepts that are based on related work. For comparison, the competing methods are implemented inside the *STARVEC* framework as depicted in Figure 6.2. It corresponds to the schema depicted in Figure 4.2. One difference is the choice of the state to be expanded next, which degenerates to always the already active state. This way the whole

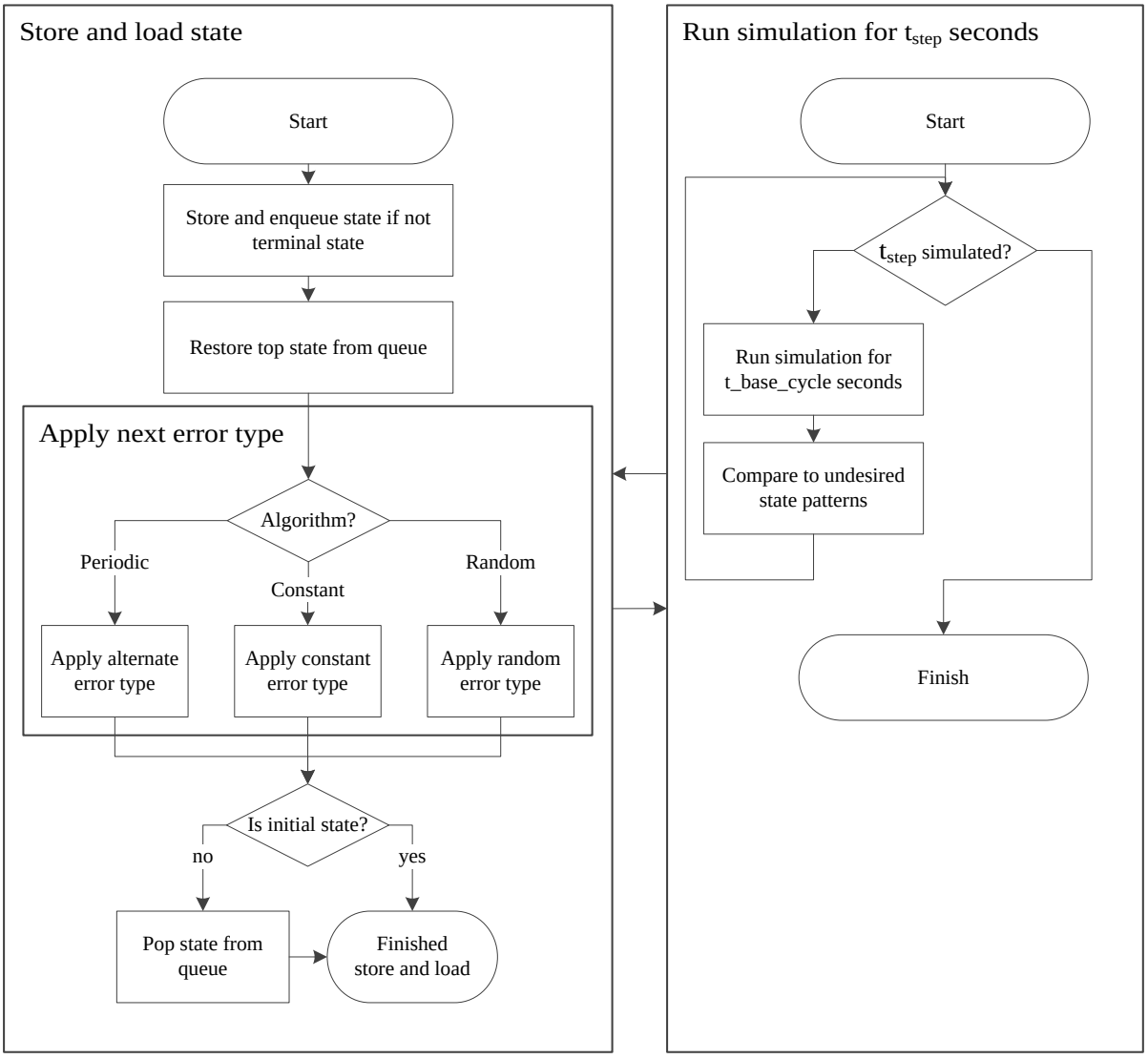

Figure 6.2: Implementation of existing test methods based on the schema depicted in Figure 4.2: The competing algorithms only differ in a custom method for choosing the next error type to be applied.

simulation sequence is executed in a row instead of splitting it into small pieces as for the *STARVEC* approach. If the current simulation sequence has finished, the initial state is chosen instead, which means a new simulation sequence is started. For this reason, the initial state always remains in the stack of states to be expanded (box "Is initial state?"). The choice of the inaccuracy pattern to be expanded next depends on the used method (compare box "Apply next error type"). Three concepts have been implemented for comparison:

- a Monte Carlo method,
- periodic inaccuracies, and
- constant inaccuracies.

The Monte Carlo based method corresponds to the state of the art in the industry as described in Section 2.4. Random noise is added to the sensor outputs and actuator inputs that are modeled as inaccurate. For the inaccuracy models described in Section 3.3, this means the applied inaccuracy pattern is chosen at random. Typically, the inaccuracy varies with a high frequency, which corresponds to a low step time t_{step} in Figure 4.2. Two versions of the Monte Carlo algorithm are implemented: one with a high frequency and one with the same frequency with which the *STARVEC* process varies the inaccuracy. As the following sections show, the low frequency version performs better in finding collisions than the high frequency version. Therefore, in this evaluation chapter, the high frequency version is referred to as Monte Carlo HF (Monte Carlo with High Frequency), the low frequency version just as "Monte Carlo".

The second and third competing method are periodic and constant inaccuracies. Ramirez et. al. [93] have applied such patterns in order to find latent behavior resulting of inaccuracies. Constant patterns means that in every step the same inaccuracy is chosen, except for the initial step in which a random inaccuracy is chosen. The corresponding box "Apply constant error type" in Figure 6.2 does nothing if the current state is not the initial state. If the current state is the initial state, it chooses a new random inaccuracy that remains constant during the new simulation sequence. This corresponds to the Monte Carlo Method with an infinite step time. In contrast, for the periodic pattern, two combinations of inaccuracies are chosen at random at the beginning. These combinations alternate in each step (box "Apply alternate error type").

In addition to the traditional test methods, a method sharing most of the source code with the *STARVEC* framework and differing only in the choice of the next node to be expanded has been implemented. The node choice is based on the RRT [142] algorithm that is widely used for solving planning problems [161]–[163]. In each step, RRT generates a random point in the configuration space for choosing the node to be expanded. Next, it expands the state that is closest to this random point. This strategy aims at quickly covering the configuration space. As explained in Section 6.2.4, this strategy has a different effect for testing, as most areas of the configuration space are not reachable. Section 6.2.4 also presents a modified version of the RRT that is more efficient for testing, which is referred to as "Optimized RRT".

In total, *STARVEC* is evaluated against five methods:

- Monte Carlo
- Monte Carlo HF
- Periodic Noise
- Constant Noise
- RRT
- Optimized RRT

Each concept is applied to the four parking scenarios and five lane following scenarios described in the next section.

6.1.3 Evaluation Scenarios

The *STARVEC* method has been evaluated with several static obstacle scenarios and some scenarios with traffic participants. Static scenarios can be categorized into those with and without direction change. Scenarios with direction change are mainly parking scenarios discussed later in this section. Scenarios without direction change typically involve following some kind of reference path. Figure 6.3 shows five examples, each representing a category of static scenarios without direction change.

The first example (Figure 6.3(a)) depicts the task of following a narrow lane with static obstacles to the left and to the right. By adjusting the lane width of the scenario, it corresponds to following any straight public street, parking garage transit lane or other straight path. The obstacles could be the border of a bridge, some flowerbeds or the walls of a narrow alley. The scenario can be varied by changing the width of the lane. For the experiments in this evaluation, the lane is 0.3 m wider than the safety shape of the path planner. Hence, an experiment with a higher safety distance also tests a wider lane.

The task changes if the lane is not straight, but follows a curve or corner as depicted in Figure 6.3(d). Such settings are common in public parking garages or in front of a private garage next to a house. As for the narrow lane, the width of the curve can be adjusted. It is three meters larger than the width of the path planner safety shape. The vehicle still drives close to the borders as it turns around the corner.

It also makes a difference if the narrow part only starts after the curve (Figure 6.3(c)) like at the entrance of a garden or an alley. For the evaluation in this chapter, the width of the target lane is set to the width of the safety shape plus 1.8 m. This width still represents a narrow target, but allows the path planner to find a path without direction change into the target lane.

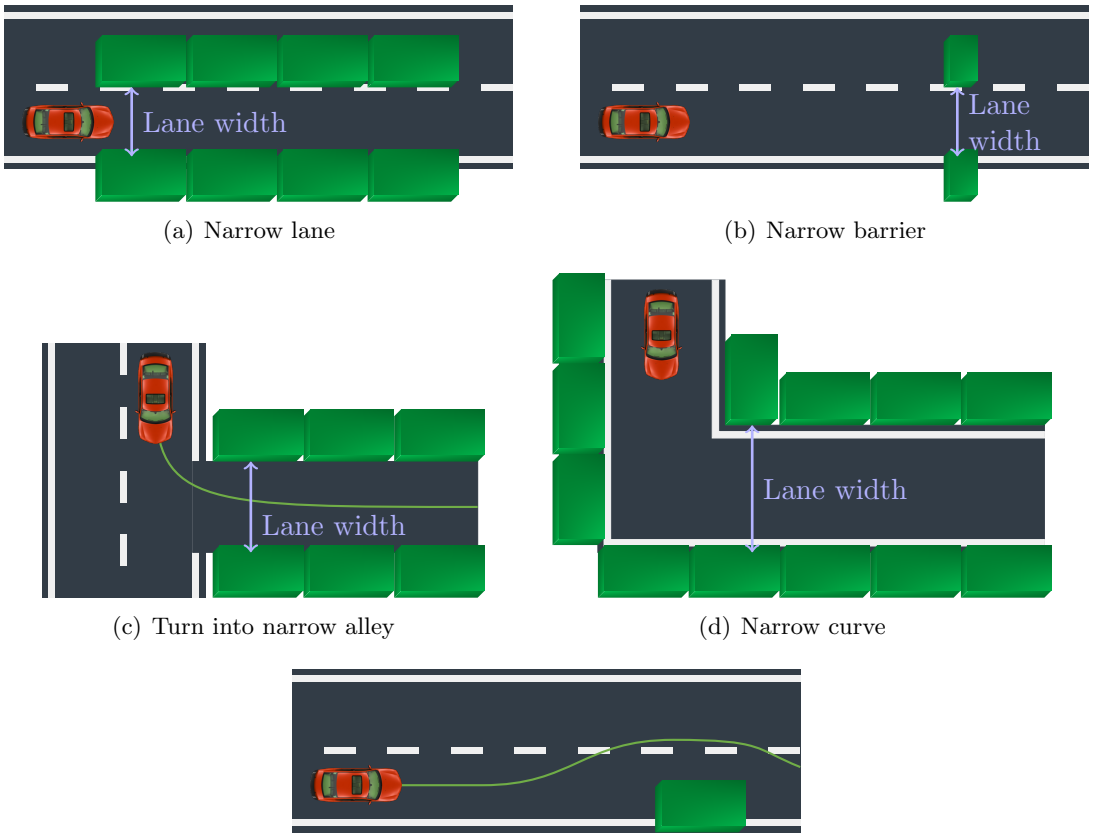

(a) Narrow lane

(b) Narrow barrier

(c) Turn into narrow alley

(d) Narrow curve

(e) Evading an obstacle

Figure 6.3: Static scenarios without direction change: Many static real world scenarios are similar to one of the depicted situations. Therefore, these scenarios are chosen as a test set for evaluating the competing algorithms.

In some scenarios, the narrow part is very short, for example at barriers or at a historic city gate. This situation is depicted in Figure 6.3(b) and is configured with a width identical to the path planner safety shape.

Finally, the lane might be narrow only at one side as depicted in Figure 6.3(e). The obstacle corresponds to a car parked at the side of the street or a construction site forcing the ego vehicle to evade with sufficient safety distance. For this scenario, the exact position of the obstacle makes a significant difference, as it only leads to an offset of the evasion path. It is configured such that the middle of the front of the vehicle would collide with one corner of the obstacle.

Parking scenarios mainly vary in the parking orientation, the available space and additional obstacles distributed in that space. Figure 6.4 shows four such scenarios. The width of the parking lots is set to equal the size of the path planner safety distance.

Although there is an infinite amount of static scenarios, many of them are similar to the scenarios listed above. For this reason, these scenarios are used as a test set for evaluating the performance of the *STARVEC* system.

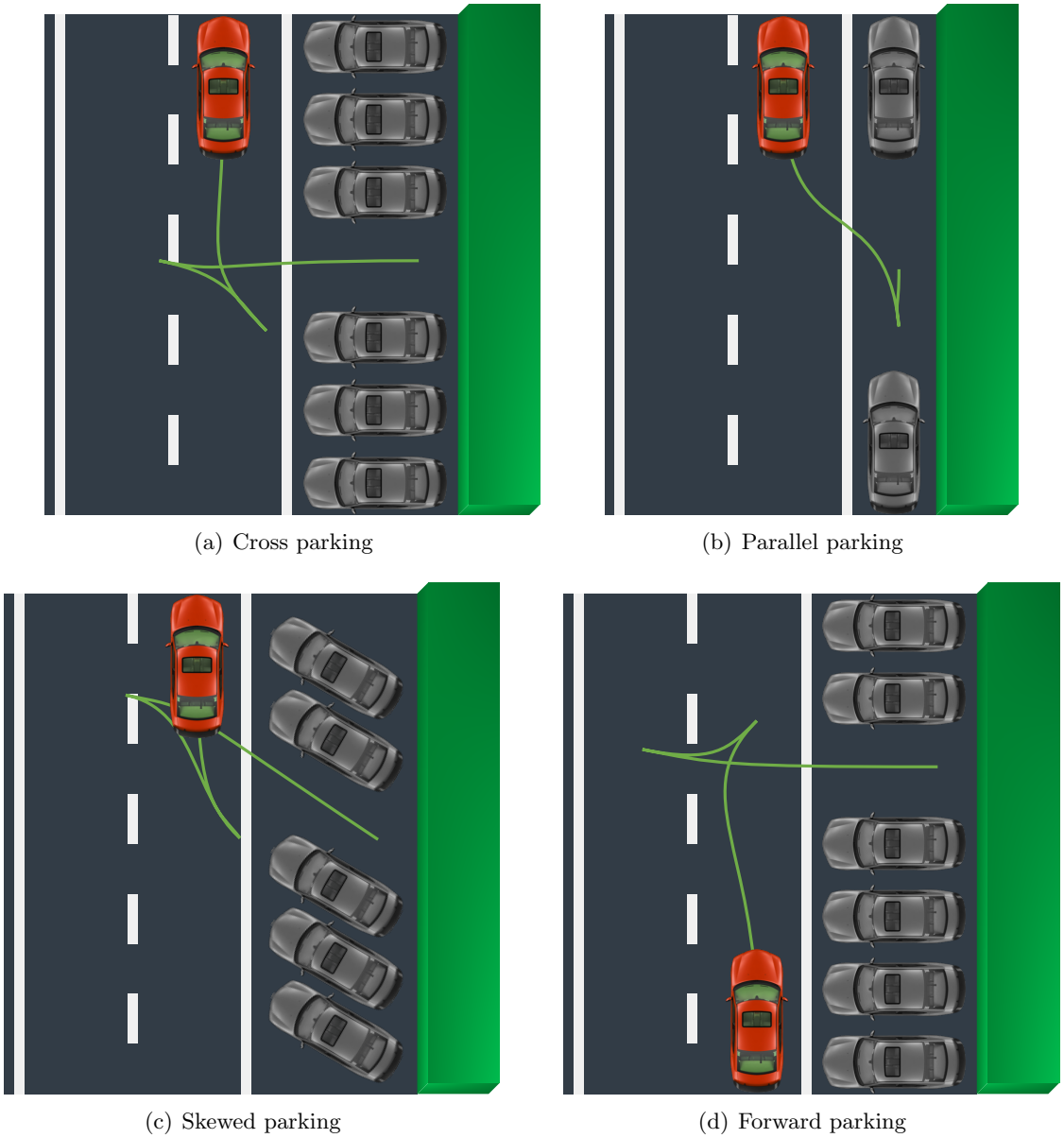

(a) Cross parking

(b) Parallel parking

(c) Skewed parking

(d) Forward parking

Figure 6.4: Parking scenarios with different orientations of the parking lot: The width of the parking lot is as narrow as the planning and control system accepts.

As described above, each of the scenarios can be configured by some parameters determining the available space. Additionally, the safety distances of the planning and control algorithm can be adjusted. It should be adjusted such that none of the following three descriptions applies:

- If the safety distances are high but there is little available space, the vehicle does not start to move at all.
- If the safety distances and the available space are both too large, there is never a collision.
- If they are both too small, there is almost always a collision.

The comparison between *STARVEC* and the competing methods is only conclusive if collisions occur seldom. For this case, the competing algorithms show different performance.

As described in Section 2.1, safety distances compensate deviations resulting of inaccuracies in combination with the planned path. The necessary safety distance depends on the scenario. For the development of autonomous driving systems, it needs to be set to the maximal necessary distance over all scenarios. For this evaluation, the safety distance (compare Section 6.1.1) is determined separately for each scenario. It is set to a just too small value that can lead to a collision. This way, each scenario is valuable for the comparison of the alternative test methods. In order to define the tested safety distance a set of preparing experiments is performed for each scenario. The set of experiments starts with the safety distances listed in Equation 6.2.

$$\begin{aligned} s_{\text{tp,lon}} &= 0.05\,\text{m} \\ s_{\text{tp,lat}} &= 0.00\,\text{m} \\ s_{\text{pp,lon}} &= s_{\text{tp,lon}} + 0.05\,\text{m} \\ s_{\text{pp,lat}} &= s_{\text{tp,lat}} + 0.05\,\text{m} \end{aligned} \tag{6.2}$$

In each step, the *STARVEC* framework is executed three times. If it needs more than $5,000$ simulated seconds on average to find a collision, the used set of safety distances is stored and the preparatory experiments sequence is finished. If it finds a collision in less than $5,000$ simulated seconds on average, the safety distances are increased and the next step of the experiment sequence is started. After each step, the safety distances are increased by $0.05\,\text{m}$ each. In some cases, one step results in a collision in less than $5,000$ simulation seconds while the following step leads to no collisions within $30,000$ simulation seconds. In these cases, a safety distance between these two steps is chosen by searching with smaller increments. For the parallel parking scenario these smaller increments also do not lead to a seldom collision. Instead, the offset between longitudinal and lateral safety distances is increased to $0.1\,\text{m}$. This way, instead of a little complex longitudinal collision a more complex lateral collision occurs.

For the barrier and the narrow target lane scenario, the lateral path-planning safety distance $s_{\text{pp,lat}}$ was set to $s_{\text{tp,lat}} + 0.2\,\text{m}$ in order to create a scenario with the target number of necessary simulation seconds. As result, the safety distances listed in Table 6.1 are used for the evaluations.

Table 6.1: Safety distances applied as a result of the preparatory experiments.

Scenario	$s_{\text{tp,lon}}$	$s_{\text{tp,lat}}$	$s_{\text{pp,lon}}$	$s_{\text{pp,lat}}$
Cross parking	0.37	0.32	0.42	0.37
Parallel parking	0.19	0.09	0.24	0.14
Skewed parking	0.25	0.2	0.3	0.25
Forward parking	0.24	0.19	0.29	0.24
Narrow lane	0.12	0.07	0.17	0.12
Barrier	0.09	0.04	0.14	0.24
Narrow target lane	0.161	0.111	0.211	0.311
Narrow curve	0.21	0.16	0.26	0.21
Obstacle	0.15	0.1	0.20	0.15
Ghost obstacle	0.35	0.3	0.40	0.35

Using these preparatory experiments, the resulting absolute number of simulated seconds required by *STARVEC* only demonstrates that the concept is applicable. The most valuable result of the evaluation experiments is the relative performance of the *STARVEC* framework and the alternative test methods.

In addition to the static scenarios, some scenarios with dynamic traffic participants are evaluated. These scenarios are described in Section 6.3.2.

6.2 Performance of the STARVEC Algorithm

Based on the scenarios described in Section 6.1.3, *STARVEC* is evaluated against the concepts described in Section 6.1.2. First, Section 6.2.1 describes the direct execution in the reference scenarios. Next, Section 6.2.2 discusses some detected examples of undesired behaviors. Section 6.2.3 compares the performance of the Monte Carlo and the *STARVEC* algorithm in a scenario with scalable complexity. In this scenario, it demonstrates the different orders of run time complexity of the two test principles. Finally, the *STARVEC* approach is compared to two versions of the RRT method in more detail.

The results show that *STARVEC* performs significantly better than the competing test methods. The difference increases with higher complexity of the detected inaccuracy patterns.

6.2.1 Comparison of Alternative Test Methods

Tables 6.2 and 6.3 show the performance of the involved test concepts. Each value in these tables is the average number of seconds in simulation time in 10 experiments until the listed test function finds a collision state in the listed scenario. For some scenarios, some test functions do not find a collision within one million simulated seconds. This is indicated by the term "> 1.0M".

Table 6.2: Average simulation time until the first collision state is detected for the scenarios listed in Section 6.1.3. > 1M indicates that no collision is found within 1 M (Million) seconds in simulation time.

Algorithm	*STARVEC*	Monte Carlo	Monte Carlo HF	Constant	Periodic
Cross parking	5,245	> 1.0M	> 1.0M	> 1.0M	> 1.0M
Parallel parking	9,088	769,203	> 1.0M	1,867	> 1.0M
Skewed parking	11,522	> 1.0M	> 1.0M	> 1.0M	> 1.0M
Forward parking	13,299	> 1.0M	> 1.0M	94,637	> 1.0M
Narrow lane	5,988	65,516	> 1.0M	> 1.0M	> 1.0M
Barrier	6,502	25,024	> 1.0M	> 1.0M	> 1.0M
Narrow target lane	34,162	> 1.0M	233,858	> 1.0M	> 1.0M
Narrow curve	2,059	8,067	> 1.0M	249,333	> 1.0M
Obstacle	10,384	> 1.0M	49,276	30,276	314,827
Ghost obstacle	16,369	> 1.0M	> 1.0M	> 1.0M	> 1.0M

Table 6.3: Average simulation time until the first collision state is detected for the scenarios listed in Section 6.1.3.

Algorithm	*STARVEC*	Optimized RRT	RRT
Cross parking	5,245	20,612	48,313
Parallel parking	9,088	6,485	21,669
Skewed parking	11,522	36,067	76,040
Forward parking	13,299	51,746	222,522
Narrow lane	5,988	> 0.9M	> 1.0M
Barrier	6,502	31,510	19,416
Narrow target lane	32,030	> 1.0M	> 0.6M
Narrow curve	2,059	109,733	111,316
Obstacle	10,384	17,186	38,004
Ghost obstacle	16,369	27,680	55,341

In this case, the corresponding one million states are executed only once. More precisely a set of experiments with a total of one million simulated seconds is executed. The Monte Carlo, the constant and the periodic algorithm consist of repeating the same test sequence many times. Thus, there is no difference between running several experiments with a low number of simulated seconds or a single experiment with a large number of simulated seconds. The two RRT versions continuously build up a search tree. Therefore, the number of required simulation states of two failing experiments cannot be added. It is possible that the RRT does not find a collision when executed a thousand times with a limit of a hundred simulation seconds. In the same scenario, the RRT might find a collision when executed a single time with a limit of $100,000$ simulation seconds. For this reason, the RRT experiments are only aborted after one million simulation seconds and repeated ten times. If none of the experiments leads to a detected collision, this is indicated by "$>$ 1.0M". If some of the experiments lead to a detected collision, the lower bound for the actual average is computed, for example "$>$ 0.6M".

Figures 6.5 and 6.6 illustrate the same values as tables 6.2 and 6.3. The visible part of the columns is limited to a maximum of $100,000$ states. The visual comparison allows making the observations described in the following paragraphs.

The *STARVEC* approach finds a collision in all tested scenarios. As explained in Section 6.1.3, the most interesting part about the experiments is the relative performance of *STARVEC* compared to the competing methods.

For most scenarios, the test function based on constant inaccuracies does not find a collision within 100,000 simulated seconds. However, there are three exceptions: evading an obstacle, forward parking and parallel parking. For the obstacle scenario, it is about as fast and for the parallel parking scenario, it is faster than *STARVEC*. Although the constant inaccuracy principle performs well for a few scenarios, the overall performance of it is bad. It can only cope with scenarios in which this specific class of inaccuracy pattern combinations can lead to a collision. For these scenarios, it can be relatively fast, as it is not distracted by alternative inaccuracy patterns to be tested.

The test system based on periodically changing inaccuracies needs more than $100,000$ simulation seconds to find a collision in each of the compared scenarios. On the one hand, the additional degree of freedom added by alternating patterns makes it slower in detecting the collisions caused by constant inaccuracies. For the obstacle scenario in which the constant inaccuracy approach is fast, the periodic inaccuracy method is significantly slower but does find a collision in less than one million states. On the other hand, it misses many possible collisions that are caused by non-alternating inaccuracy patterns.

In some scenarios, the Monte Carlo approach is better suited for detecting collision states because it does not constrain the class of possible inaccuracy pattern combinations. The result can be regarded in the scenario comparison. In three of the compared scenarios, the low frequency Monte Carlo algorithm is able to find a sequence of inaccuracies leading to a collision within

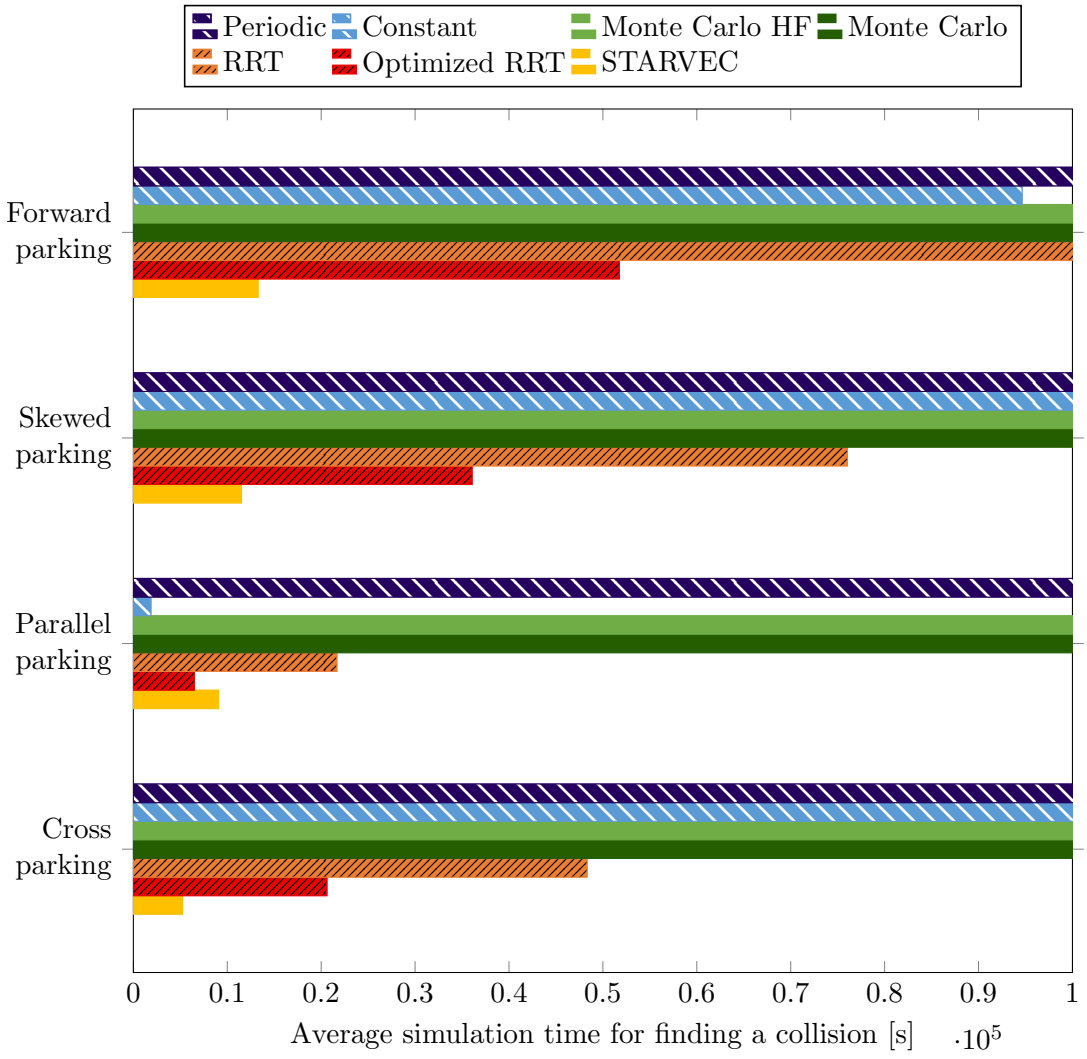

Figure 6.5: Comparison of the performance of different algorithms in a set of parking scenarios. Constant inaccuracies lead to an undesired behavior for parallel parking and forward parking. No other undesired behaviors are found for random, constant or periodic inaccuracies. The *STARVEC* approach performs better than both versions of RRT.

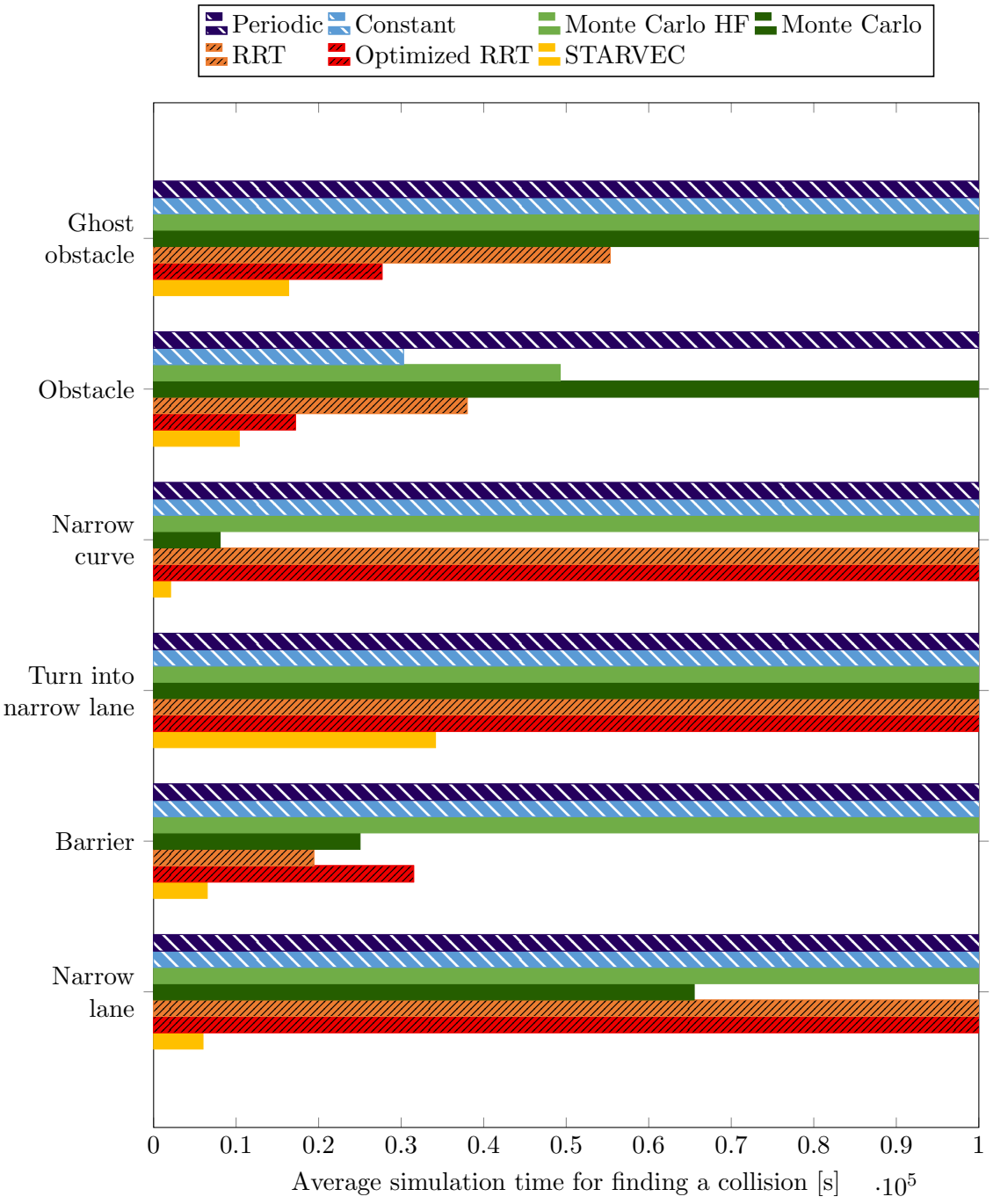

Figure 6.6: Comparison of the performance of different algorithms in a set of lane following scenarios. Constant inaccuracies lead to an undesired behavior for obstacle evasion but fail in the other scenarios. Periodic inaccuracies do not find a collision within less than 100,000 states in all six scenarios. Random inaccuracies and RRT are successful in some scenarios but slower than the *STARVEC* algorithm. *STARVEC* finds undesired behaviors in all examples.

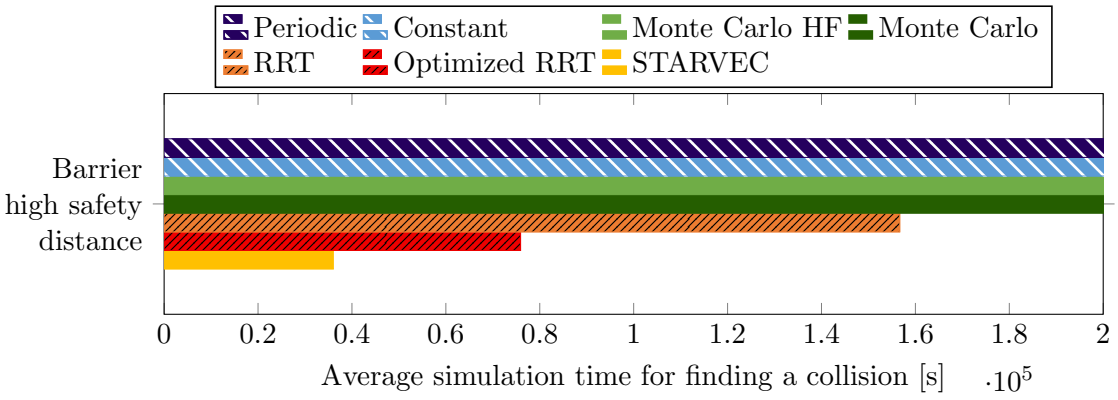

Figure 6.7: Repetition of the barrier scenario mentioned in Figure 6.5 with a higher safety distance: In contrast to the lower safety distance, the Monte Carlo method is significantly slower than the *STARVEC* algorithm.

100,000 seconds simulation time. However, in all cases the method is slower than the *STARVEC* system. The reason for this difference in efficiency is that the Monte Carlo algorithm suffers from the exponentially large number of possible inaccuracy combinations discussed in Section 4.1.2. The Monte Carlo algorithm performs best for the narrow curve scenario. In this scenario, the *STARVEC* concept is also very fast. This suggests that the necessary patterns of inaccuracy are less complex than for the other scenarios. For short patterns of inaccuracy, the relative performance of the Monte Carlo algorithm compared to *STARVEC* is better, as discussed in Section 6.2.3.

As explained in Section 6.1.3, the narrow curve scenario could not be adapted to require a high number of tested simulation seconds and still make a collision possible. The second scenario with a good performance of the Monte Carlo algorithm is the barrier scenario. In this scenario, it requires 25,024 simulation seconds for finding a collision. This is about four times more than the *STARVEC* approach takes. Figure 6.7 and Table 6.4 show the results of an analysis of the barrier scenario with slightly higher safety distances. The increased safety distances result in fewer combinations of inaccuracies leading to a collision. Therefore, the *STARVEC* component needs an average of 36,033 states (10 repetitions) for finding a collision, which is more than for the previous barrier scenario. The Monte Carlo algorithm does not find a collision within one million states. This demonstrates that the more complex the inaccuracy combinations searched for, the larger the performance difference between *STARVEC* and the competing random algorithms. A detailed analysis of the performance difference between *STARVEC* and the Monte Carlo approach is discussed in Section 6.2.3.

The high frequency Monte Carlo approach (Monte Carlo HF) finds a collision in only two of the compared scenarios. Due to the high frequency, it constrains the class of possible patterns of inaccuracy less than the low frequency version. However, the ten times higher frequency also increases the number of possible behaviors by an exponent of ten. This slows down the test principle.

Table 6.4: Parallel parking with high safety distances: Compare Figure 6.7.

Algorithm	*STARVEC*	Optimized RRT	RRT	
Barrier high safety distance	36,033	75,904	156,656	
Algorithm	**Monte Carlo**	**Monte Carlo HF**	**Constant**	**Periodic**
Barrier high safety distance	> 1.0M	> 1.0M	> 1.0M	> 1.0M

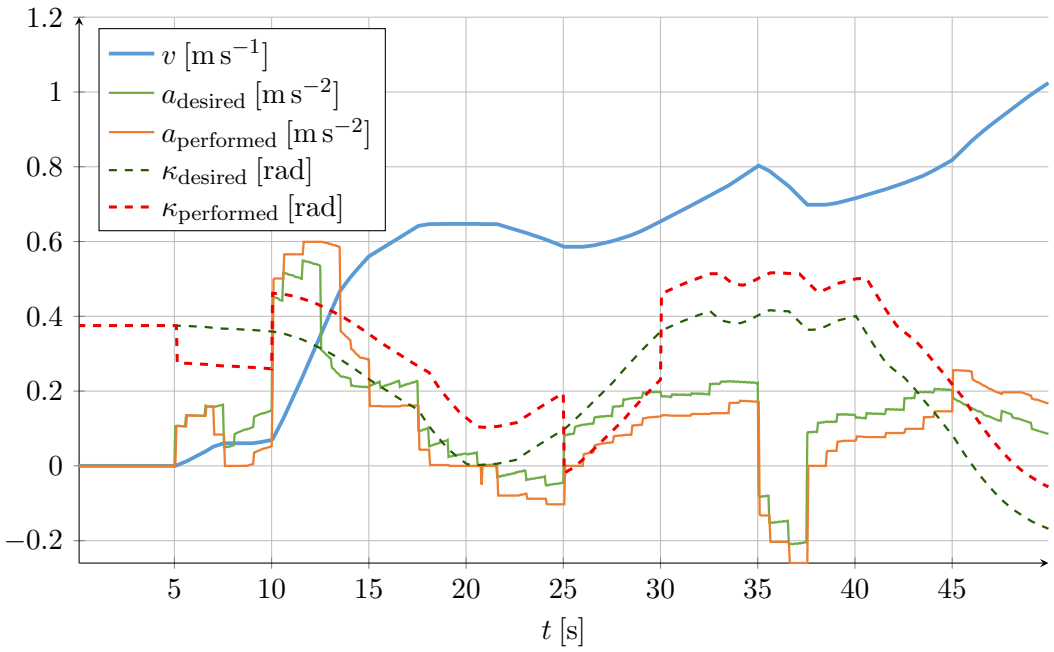

Figure 6.8: Plot of steering (dashed lines) and acceleration (solid lines) values desired by the controller (green) and performed by the car (red) leading to the detected collision: The inaccuracies include long constant sequences and changes at critical points in time that are unlikely to be detected by random search.

.

Finally, the two RRT based methods perform better than the other competing test concepts but not as well as *STARVEC*. The RRT based test functions share some of the concepts with the *STARVEC* framework and are discussed in more detail in Section 6.2.4.

6.2.2 Detected Combinations of Inaccuracies

As listed in Table 6.2, the *STARVEC* approach finds a collision for the forward parking scenario after an average of 13, 299 simulation seconds. Figure 6.8 shows the steering and acceleration errors leading to one such collision. The inaccuracies contain both long constant sequences and changes at critical points in time. For example, the steering inaccuracy is constant in the final 15 seconds, whereas the acceleration inaccuracy changes from negative to positive just before the collision occurs. The acceleration errors result in the velocity slightly exceeding the target value.

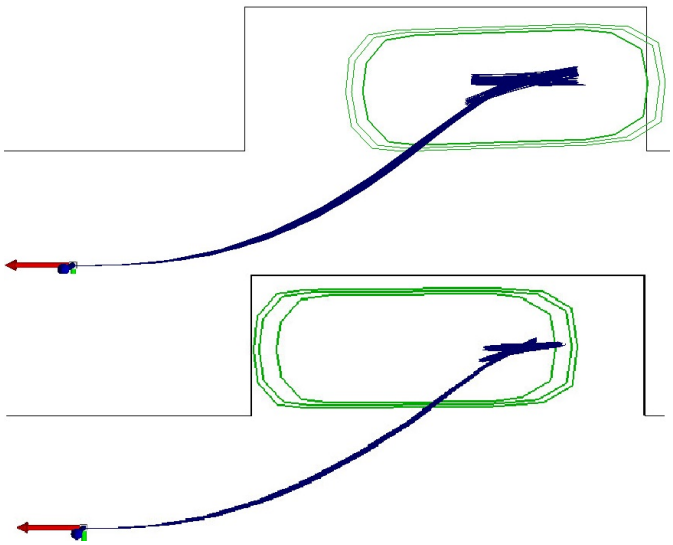

Figure 6.9: Results of *STARVEC* (top) and Monte Carlo (bottom) algorithm: The latter covers noticeably less area (blue path lines) and is less likely to find collisions.

This intensifies the effect of the steering inaccuracies leading to the collision. The illustrated pattern of inaccuracies also shows why the competing test principles perform worse in this scenario. Constant inaccuracies do not change at all and hence do not change at critical points in time. Periodic inaccuracies are unlikely to change at the critical point in time. For this reason, the method based on periodic inaccuracies does not find any collision. The method based on constant inaccuracies finds a different collision after a long simulation time.

The Monte Carlo algorithm also does not find a collision in this scenario. The reason for the performance difference to the *STARVEC* approach is illustrated in Figure 6.9. It compares the performance of the two test methods in the parallel parking scenario in the first $10,000$ simulation seconds. The blue lines represent driven trajectories of the vehicle during the simulation. They visualize that the *STARVEC* system covers significantly more area than the Monte Carlo algorithm. This correlates to the ability of both test principles to find undesired behaviors like collisions.

Figures B.1-B.10 in Appendix B show the motions and the controller states for one example of each of the remaining scenarios. In most cases, the combination of lateral and longitudinal controller errors at an effective point in time leads to the collision.

Apart from searching for collision states, the presented test functions can also search for temporal behavior patterns as described in Section 4.4. As depicted in Figure 6.10, applying the *STARVEC* and the Monte Carlo algorithm to the suggested double stop pattern reveals a similar performance difference. The higher the velocity of the second motion in the pattern searched for, the less often it occurs and the more complex are the necessary inaccuracy patterns. As the complexity of the inaccuracy pattern increases, so does the number of necessary simulation

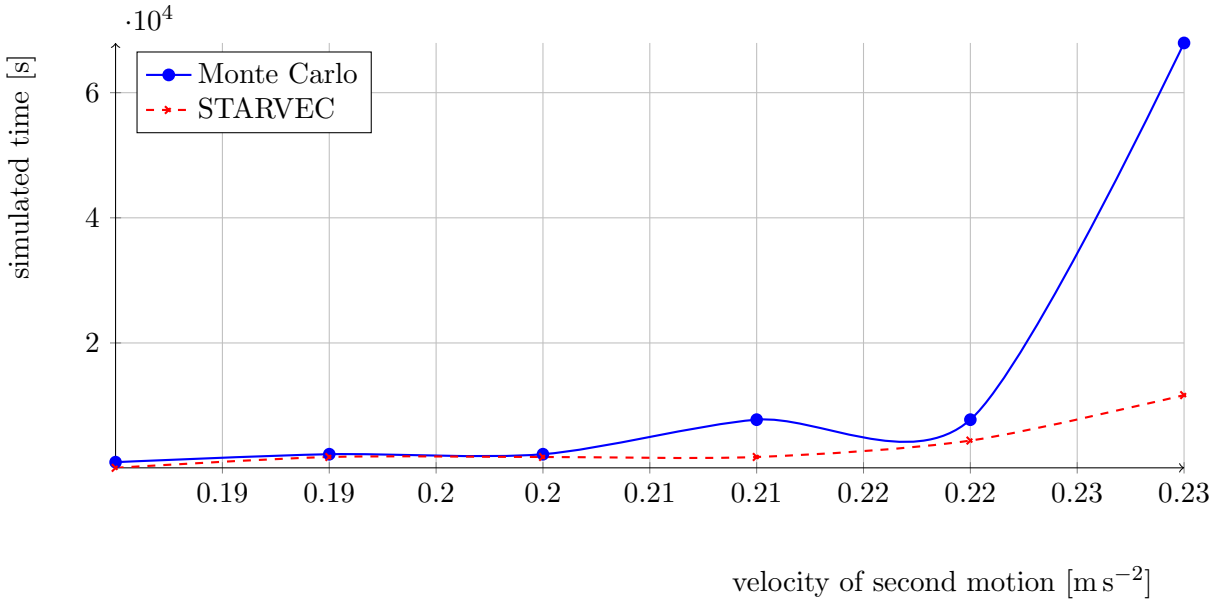

Figure 6.10: Simulated seconds of Monte Carlo vs. *STARVEC* algorithm until double stop pattern is found.

seconds for both algorithms to find them. However, for the Monte Carlo algorithm it increases significantly faster than for the *STARVEC* approach. The difference between both test functions is investigated in the next section.

6.2.3 Worst-Case Performance of the Monte Carlo Algorithm

As described in Section 4.1.2, there is an exponential number of possible behaviors that can be generated based on sensor and actuator inaccuracies. This makes the Monte Carlo algorithm often fail to find an undesired behavior within reasonable time. If the undesired behavior depends only on very few random choices, the Monte Carlo algorithm performs well. Scenarios can be adapted by changing some scenario parameters. However, for most scenarios, it is difficult to scale the number of random choices that influence whether the undesired behavior is performed. In these cases, the Monte Carlo algorithm either finds an undesired behavior quickly or does not find any undesired behavior depending on the chosen scenario parameters. Therefore, a scenario is needed that can be scaled. The scenario depicted in Figure 6.11 helps to demonstrate the difference between the *STARVEC* approach and the Monte Carlo algorithm. Its main component is a long corridor consisting of a variable number of barriers and a following obstacle that is not detected by the ego vehicle. The ego vehicle only collides with the not detected obstacle at the end of the corridor if it does not get stuck on the path. As the corridor is very narrow, it is likely to get stuck at each barrier. The more repetitions of the barrier, the smaller the share of behaviors that result in hitting the obstacle.

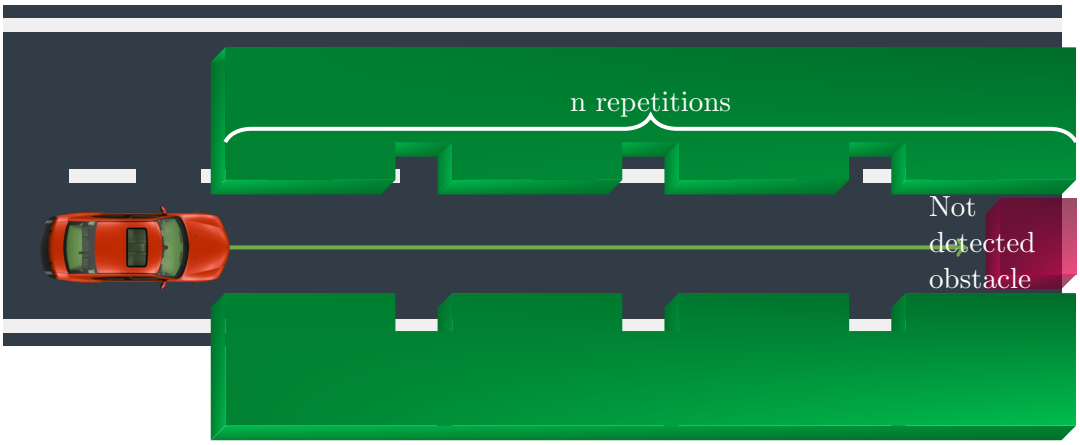

Figure 6.11: n repetitions of a barrier situation: The ego vehicle only collides with the not detected obstacle at the end of the corridor if it does not get stuck on the path.

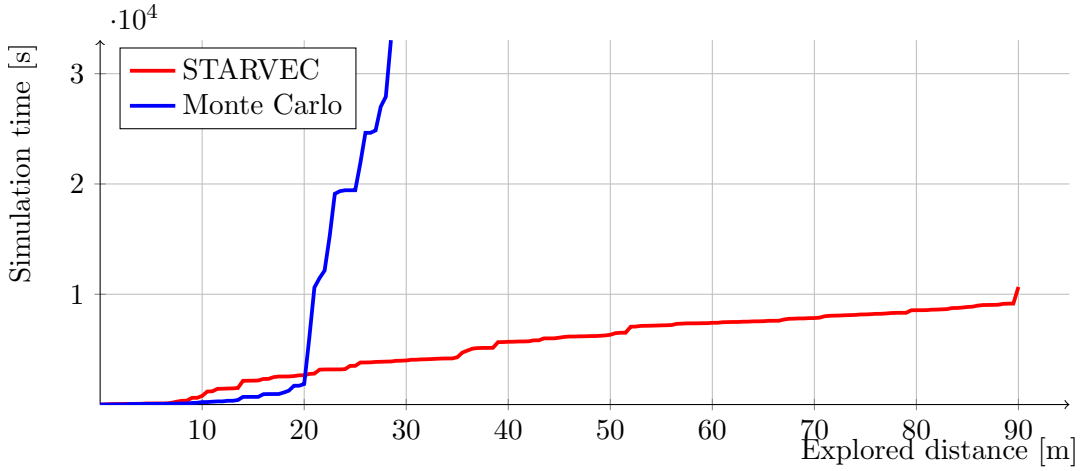

Figure 6.12: Comparison of the *STARVEC* and the Monte Carlo algorithm in the scenario depicted in Figure 6.11: After 20 meters, the Monte Carlo algorithm is slower than *STARVEC* and quickly exceeds 100.000 simulated seconds.

Figure 6.12 shows the relation between length of the corridor and the necessary simulation time of the *STARVEC* and the Monte Carlo algorithm. It plots the number of simulated seconds necessary to reach a distance in the narrow barrier corridor on average of ten repetitions. In the first 20 meters, the Monte Carlo algorithm is faster than the *STARVEC* system. Afterward, it grows quickly and exceeds 100.000 simulated seconds for covering less than 30 m. In contrast, the number of necessary simulated seconds for the *STARVEC* method grows almost linearly.

These results confirm the time complexity of the involved test functions computed in Section 4.1.2. The Monte Carlo algorithm randomly picks any of the exponentially many behaviors. Thus, the necessary simulation time grows with the number of possible behaviors and hence with the distance to cover. In contrast, the *STARVEC* approach uniformly covers the available space, which grows only linearly with the distance to cover.

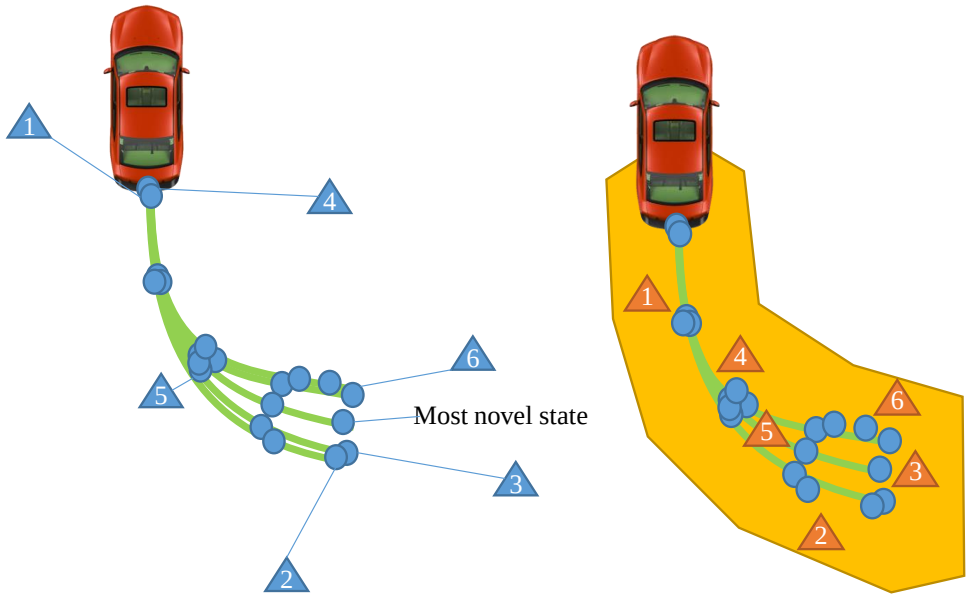

(a) RRT vs. *STARVEC* (b) Optimized RRT

Figure 6.13: Comparison of RRT, *STARVEC* and a modified version of RRT: RRT focuses on states at the border of the set of explored states, whereas *STARVEC* explores the "most novel state". The modified version of RRT explores more states in the center of the set of explored states.

6.2.4 Comparison between STARVEC and RRT

Two of the compared test methods are based on the RRT concept. Similarly to the *STARVEC* approach, the RRT principle aims to cover the state space quickly by evenly distributing the nodes that are expanded. The even distribution is reached by randomly picking states in the configuration space and expanding the nearest explored node. However, for testing against inaccuracies this does not lead to an even distribution as illustrated in Figure 6.13(a). The inaccuracies do not fully control the motion of the vehicle, but only influence it. Different inaccuracies lead to different trajectories driven by the vehicle. Some of these trajectories are illustrated by the green lines. The blue circles represent states along these trajectories that have been stored as described in Section 4.1. The RRT algorithm tries to cover the remaining area by randomly picking states in the configuration space. These states are depicted by the triangles 1-6. As the inaccuracies do not fully control the vehicle, the resulting trajectories still move along the planned trajectory instead of towards the sampled random states. The lines from the triangles to the explored states (blue circles) indicate which state is chosen to be expanded next according to the RRT concept. Almost all chosen states are at the border of the explored space of reachable states, because sampling a random node in the middle of the reachable state space occurs seldom. States at the start and the end of the trajectory are sampled particularly often.

In contrast, *STARVEC* picks the state that is farthest away from all already expanded states. In Figure 6.13 this is labeled as the "most novel state". The result is that the RRT algorithm

performs significantly worse than the *STARVEC* system in the evaluated scenarios (compare Figures 6.5 and 6.6). Most undesired behaviors occur at the border of the reachable state space. However, some states at the border of the set of reachable states can only be reached by traversing intermediate states that are not at the border of this state space. These intermediate states are disregarded by the RRT concept.

The RRT concept is faster than the *STARVEC* approach in finding the final seconds before an undesired behavior occurs because it is biased to extreme states. The *STARVEC* test supervisor does not expand the extreme states if a very similar state has already been expanded. This makes the test method slower in this part of the search.

Therefore, an optimized version of the RRT is created for comparison. The sampling strategy of the optimized RRT concept is limited to an area around already explored states as depicted in Figure 6.13(b). The new test method only samples states with a distance of less than a threshold to already explored states. If a state with a higher distance is sampled, a new random sample is created. The allowed area is depicted as a yellow shape surrounding the explored trajectories. The modification makes it more likely to sample states in the middle of the reachable state space. The strategy corresponds to increasing the sampling density in narrow passages as used by many RRT based planning techniques like [164]. The resulting test function performs significantly better than the basic RRT method as shown in Figures 6.5 and 6.6. The test function is labeled as "Optimized RRT". It is faster than the original RRT approach in most scenarios. In one case, it performs better than the *STARVEC* principle while the *STARVEC* system dominates the other scenarios. Section 7.3 discusses potential benefits of creating a combined version of *STARVEC* and RRT.

6.3 Scenarios with additional Patterns of Inaccuracy

In addition to the scenarios with actuator inaccuracies evaluated in Section 6.2.1, further inaccuracy models have been developed and evaluated. Section 6.3.1 discusses experiments with a large set of sensor inaccuracies in addition to the actuator inaccuracies. Section 6.3.2 evaluates the nondeterministic models of traffic participants introduced in Section 4.5.

6.3.1 Scenarios with Errors of the Environment Sensors

In the scenarios evaluated in this section, three kinds of inaccuracy models are added. They affect the odometry-based localization, the global localization and the environment mapping sensors. The corresponding inaccuracy models are described in Sections 3.3.3 and 3.3.4. For the odometry-based localization and environment map errors, an implementation created in [131] is applied. The odometry localization errors in that work have been developed based on a global localization error implementation created in the present thesis.

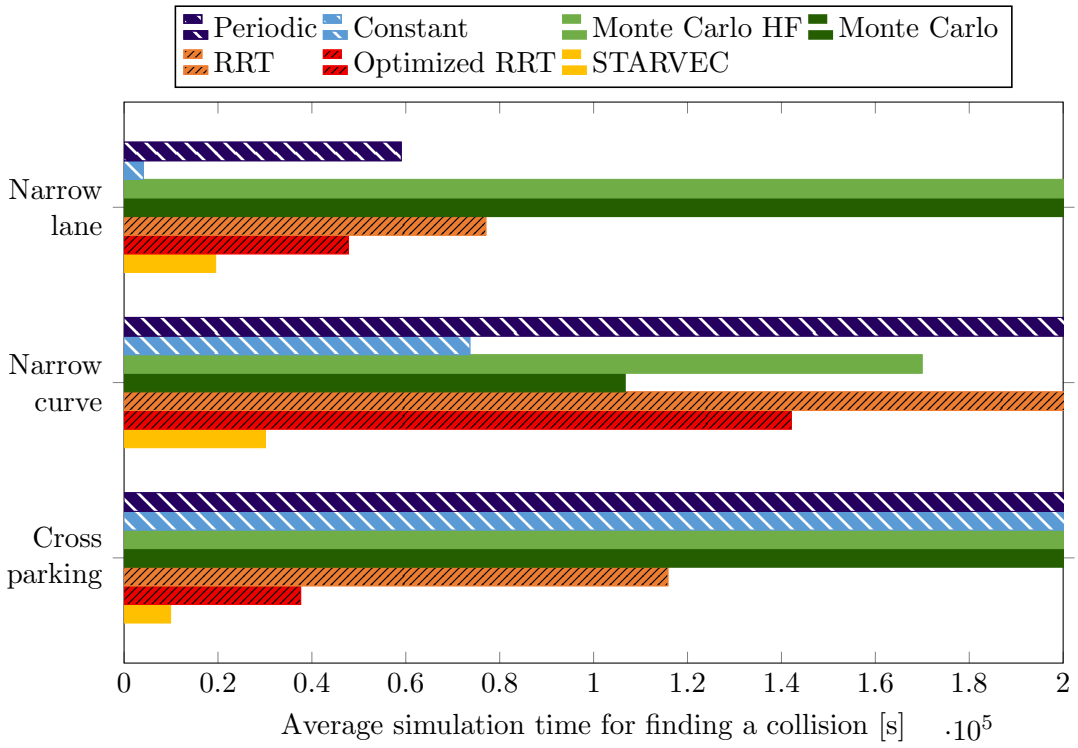

Figure 6.14: Comparison of the test competing principles with a large set of sensor and actuator inaccuracies in a parking and two lane following scenarios. *STARVEC* outperforms the competing test methods.

Figure 6.14 shows the results of the application of the competing algorithms to three scenarios with these inaccuracy patterns. The scenarios correspond to those used in Section 6.2.1. The only difference is that the safety distances of the planning component have been adjusted to the additional inaccuracy models as described in Section 6.1.3. The maximum of the bars in Figure 6.14 is $200,000$ instead of $100,000$ in order to account for the higher number of possible inaccuracy patterns in each step.

The experiments show that *STARVEC* performs significantly better than the Monte Carlo methods in all three examples. In two cases the constant inaccuracy patterns perform similar to *STARVEC* while they do not find the collision in the cross parking scenario. This corresponds to the results in Section 6.2.1 where the constant inaccuracy algorithm performs well in some cases but does not find the collision in the other scenarios. As in Section 6.2.1, the periodic inaccuracy approach eventually finds a collision in the scenario in which the constant inaccuracy method is very fast. It does not find an undesired behavior in the other two scenarios. Finally, the RRT based systems perform better than Monte Carlo, but worse than *STARVEC*.

All in all, the experiments in this Section show that the *STARVEC* approach can cope with a high number of simultaneously active inaccuracy patterns. For such scenarios, the *STARVEC* system requires more simulation seconds for reliably testing a planning and control system. Existing test methods are less efficient in finding undesired behaviors for these cases.

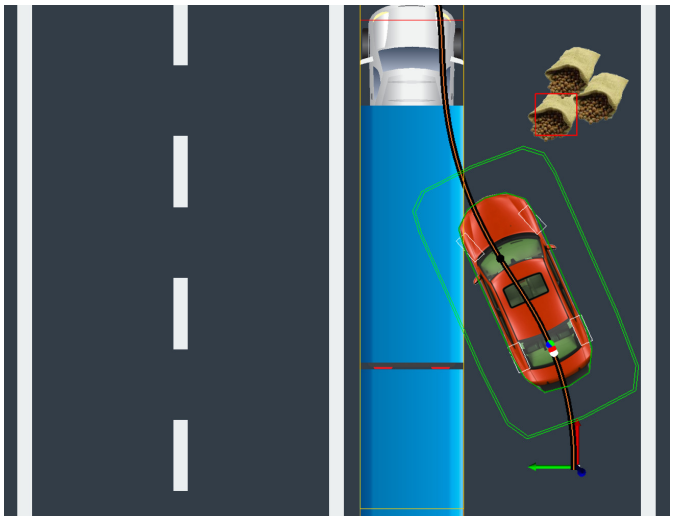

Figure 6.15: Collision of the ego vehicle with a long truck during the attempt to merge into the line of traffic of the truck.

6.3.2 Scenarios with Traffic Participants

In addition to the static scenarios, the presented concept has been tested in two scenarios involving the interaction with traffic participants:

1. a scenario involving merging into another lane with traffic coming from behind and
2. an intersection scenario with traffic coming from the side.

In both scenarios, the opposing traffic participant has the right of way. The first scenario is depicted in Figure 6.15 and is similar to the situation that lead to the accident caused by a Google autonomous driving prototype [165]. At the beginning, the autonomous vehicle is commanded to merge into the left part of the lane because the right part is obstructed by some obstacle. In this case, the obstacles are a pile of sand bags. A truck is approaching from behind and the ego vehicle has to decide whether it can complete the merge before the truck arrives. In the second scenario (Figure 4.18), the ego vehicle wants to cross a street on which the arriving truck has the right of way. The truck is modeled as described in Section 4.5.1 and the ego vehicle collision-avoidance system includes the weaknesses described in Section 6.1.1.

STARVEC and the Monte Carlo algorithm are applied to these scenarios trying to find collisions that are the fault of the ego vehicle. Figure 6.16 compares the performance of the two test functions. The smaller the assumed safety distance described in Section 6.1.1, the more difficult it is to find the collision. This assumed safety distance decreases towards the right part of Figure 6.16. The comparison shows that the required simulation time grows faster for the Monte Carlo algorithm than for the *STARVEC* approach. Moreover, the *STARVEC* method is also more efficient regarding the absolute numbers.

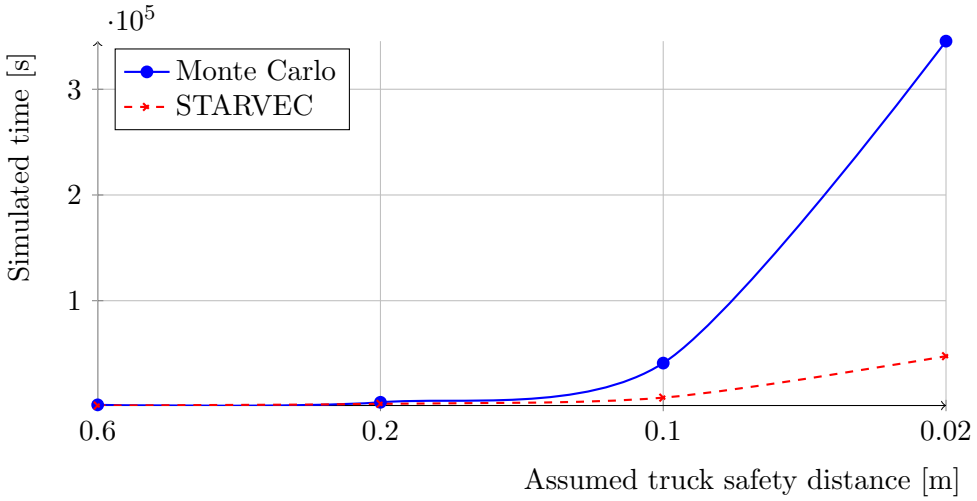

Figure 6.16: Simulated seconds of Monte Carlo vs. *STARVEC* algorithm until a clearly assignable collision is found. Smaller assumed safety distances make both concepts take longer to find the collision. *STARVEC* outperforms the Monte Carlo method.

The sequences leading to a collision can be relatively complex as shown in Figure 6.17. It depicts one behavior detected by the *STARVEC* system. First, the truck decelerates and is predicted to stop soon. Therefore, the ego vehicle starts driving towards the lane (Figure 6.17(a)). Next, the truck accelerates again and the ego vehicle brakes in order to prevent a collision (Figure 6.17(b)). When the truck repeats braking, the ego vehicle reacts by accelerating (Figure 6.17(c)) but does not reach the initially intended speed. Thus, it has to halt when it realizes that the truck does not stop (Figure 6.17(d)). However, it reaches standstill only just soon enough, but falsely assumes that the truck will not be able to pass anymore. It concludes that the truck will stop, too. Consequently, it starts driving. This leads to the collision depicted in Figure 6.15.

All in all, the experiments demonstrate that the *STARVEC* approach can be efficiently applied to scenarios containing the interaction with traffic participants. As for the scenarios in the previous sections, *STARVEC* analyzed these scenarios significantly more efficiently than the Monte Carlo approach.

6.4 Summary of the Evaluation

In summary, the evaluation shows that the *STARVEC* system outperforms existing methods for finding undesired behaviors caused by nondeterministic events. The performance difference has been demonstrated in scenarios with and without direction changes. Moreover, the demonstration contains scenarios with few and with many nondeterministic events including scenarios with traffic participants. In some scenarios the exponential worst-case complexity of the Monte Carlo approach can be observed while *STARVEC* solves these scenarios in linear time.

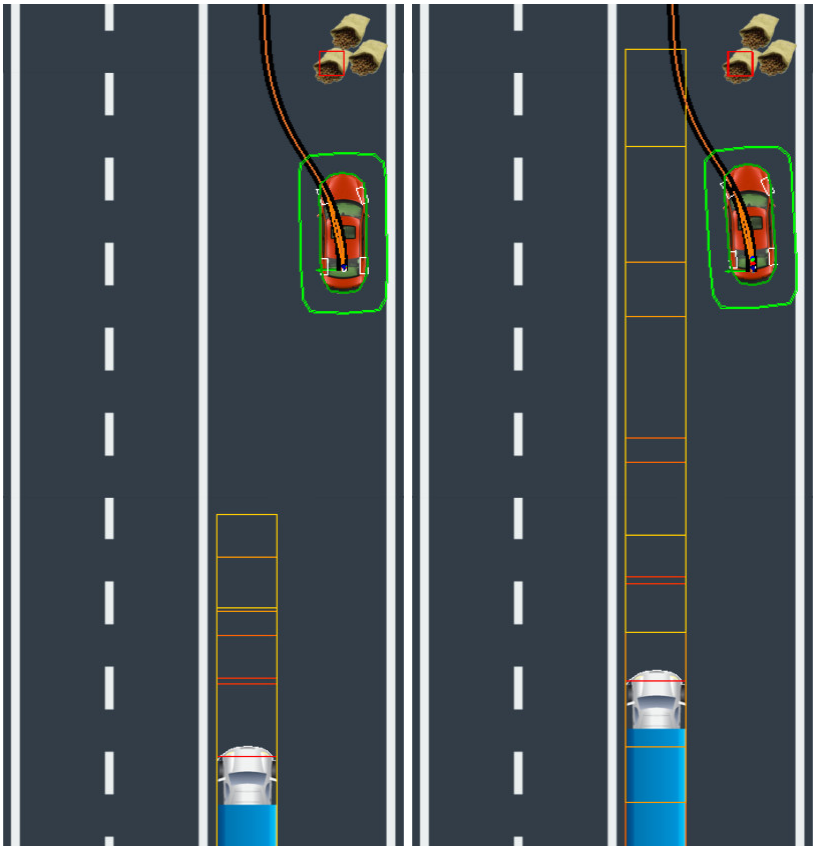

(a) Truck decelerates (b) Truck accelerates

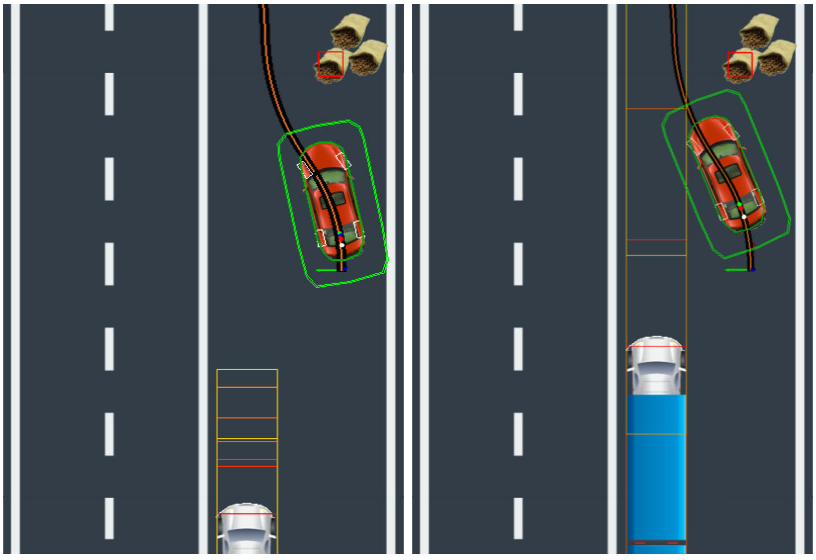

(c) Truck decelerates (d) Truck accelerates

Figure 6.17: The red vehicle tries to merge back (black curve) into the main lane avoiding a collision of its safety distance (green perimeter) with the predicted positions of the truck (orange lines). The truck switches between deceleration and acceleration ultimately leading to the collision in Figure 6.15.

Chapter 7

Future Work

The work in this thesis presents a method for testing autonomous driving systems more efficiently than previous approaches. In order to exploit the potential of this new concept fully, further research is necessary. This chapter outlines several research projects that would extend the benefit on the *STARVEC* framework. First, Section 7.1 suggests extending the application to mature autonomous driving systems in order to get a bigger amount of experimental results. Next, Section 7.2 describes how an online learning system can be designed and tested using the *STARVEC* method. Section 7.3 advocates combining the *STARVEC* and the RRT approach in order to increase testing efficiency further. Another research project is to apply the *STARVEC* approach to high-speed scenarios outlined in Section 7.4. Finally, the interaction with a large number of traffic participants is one of the major challenges for both development and testing of autonomous driving systems as addressed in Section 7.5.

7.1 Extending the Application of the STARVEC Algorithm

The *STARVEC* concept has been implemented and evaluated against the combination of several scenarios, a planning and control system and a set of models of sensor and actuator inaccuracies. All three aspects should be extended in future research.

The tested scenarios include the set of scenarios listed in Section 6.1.3. While this is a reasonable set for evaluating the performance of the test function, requirement specifications list many more special cases in which a planning and control system has to function. A comprehensive analysis includes all of the scenarios specified in the requirement documents. Furthermore, it includes some scenarios as described in Section 4.3. Such an analysis can demonstrate both: the applicability of *STARVEC* and the performance of the tested planning and control system.

Sections 3.3 and 3.4 provide sensor and actuator error models that cover major kinds of inaccuracies. Additionally, a method is described for finding the necessary parameters that

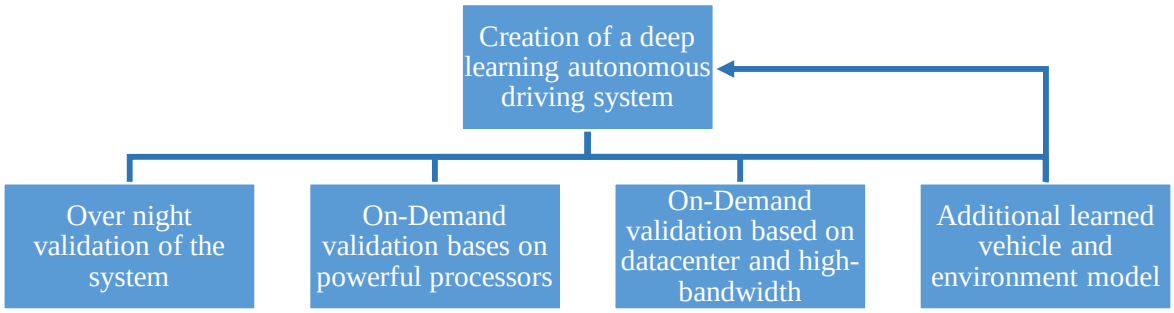

Figure 7.1: The first step of the proposed research effort is the development of a self-learning autonomous driving system. Using this system, four paths of research can be followed.

make the models useful. Vehicles involved in research projects accompanying this thesis, often displayed quite large offsets and delays between requested and performed actions. Partially this is due to the development of the actuator software not being finished. Some of the deficiencies will remain after optimization of the actuator software. For example, actuators can be inaccurate when starting the vehicle or rapidly changing the requests. Therefore, a valuable research project would be to use a vehicle with optimized actuators and create inaccuracy models including all vehicle specific deficiencies.

7.2 Application to Online Validation of Learned Planning and Control Systems

Section 5.4 describes how the *STARVEC* approach can be used for validating a planning and control system that is adapted by machine learning mechanisms. A research project can implement a system that continuously improves its planning performance using deep learning. As this planning and control component changes its behavior with each additional piece of information, the prior executed tests are not sufficient for attesting the safety of the system. The *STARVEC* concept can improve the safety by evaluating either a specific scenario or a set of scenarios before applying changes over night.

Figure 7.1 shows a possible setup of a research project. The research project starts with the creation of a continuously learning autonomous driving system. Such a system can be based on existing works of [155], [156]. However, these demonstrations do not consider reliability issues, yet. The general idea of these methods is to learn the behavior of human drivers without explicitly punishing collisions. With enough data, the system will not create collisions, because humans avoid collisions, too. The *STARVEC* algorithm would detect the rare cases of collisions and reject most versions of the learned system.

Therefore, the learning system needs to be extended by an additional collision-avoidance mechanism. This can be a simulation environment that is used as supplementary data source

rewarding collision preventing systems. In a further step, this simulation can be based on the *STARVEC* algorithm as described in [140]. This would lead to detecting more possible collisions and hence a stronger reward for collision preventing systems.

Based on this learning system, Figure 7.1 depicts four lines of research that are worth investigating:

1. Validation of the autonomous driving system in the vehicle over night,
2. on-demand validation based on powerful computation resources,
3. on-demand validation based on a data center and a high communication bandwidth and
4. validation of the autonomous driving system with learned environment and vehicle models.

The first research path is to validate the autonomous driving system over night. During the day, the system collects data but does not use it for changing its behavior, yet. As soon as the vehicle is parked, the changes are applied to a virtual duplicate of the vehicle. The *STARVEC* algorithm tests this duplicate in various test scenarios trying to find situations and environment events in which the system would create a collision. The changes are only applied if *STARVEC* does not find any safety issues. If the car is started before the tests are completed, the changes are not applied.

In this path of development, several research questions need to be answered:

- How many scenarios need to be tested in order reach sufficient confidence in the reliability of the system?
- Can the learning system recognize if it encounters a situation that is not similar to one of the tested scenarios?
- How should the system cope with failing tests? If the tests fail once, they may be likely to fail again in the next night.

The second path of research is the on-demand validation based on powerful computation resources. For example, the learning system is queried to park into a very narrow parking lot. Before starting the parking motion, the scenario is tested in simulation using the *STARVEC* algorithm. This requires a very large number of processor cores–probably more than 1000–available in the vehicle. The research project may assume the availability of such resources in the future. This leaves some research questions still to be answered:

- How can the execution of the *STARVEC* algorithm be parallelized on a large number of processor cores?
- How should the vehicle behave if the system is not considered safe for this motion?

For massively parallelizing the *STARVEC* algorithm there needs to be an analysis master that manages the queue of simulation states. Instead of choosing a single state to be executed next,

it picks one or more states for each processing core. The processing cores execute the simulation starting with the input state. This leads to a new state, which they report to the analysis master who adds the state to the search queue.

The availability of more than 1000 processor cores becomes more realistic in a data center, which is the third research path. Additionally to the research questions for a local execution of the *STARVEC* algorithm, this requires reasoning about the communication:

- Can all necessary data of the current scenario be transmitted to the datacenter sufficiently fast?
- Does the data center need a remote copy of the currently active autonomous driving software of each vehicle?

Finally, a fourth path of research investigates learning vehicle and environment models, too. The models have to interact with the *STARVEC* framework in order to reach maximal efficiency.

All in all, the described efforts would generate an insight into how self-learning autonomous driving systems can be continuously tested in order to increase their reliability.

7.3 Combining RRT and Novelty Based Exploration

The evaluation in Chapter 6 shows that the *STARVEC* system performs better than the implemented approaches based on an RRT algorithm. However, as explained in Section 6.2.4, the RRT based approach has advantages in finding the final seconds leading to an undesired behavior. The implemented modification of the RRT principle does not close the gap between the RRT based approach and the *STARVEC* method. Instead, a combination of both ideas might lead to a better performance in particular when applied to very complex scenarios like those proposed in Section 7.5. A simple combination of both algorithms would alternate between the RRT approach and the *STARVEC* approach for choosing the next node to be expanded. Alternatively, the priority of each state in the priority queue introduced in Section 4.2 could be adapted. The priority could be based on a combination of the distances to the nearest expanded node and to a random node. On the one hand, this would still lead to novel nodes being expanded. On the other hand, nodes at the border of the reachable state space would be expanded sooner.

7.4 Testing High Speed Scenarios

A promising application for the *STARVEC* approach are high-speed scenarios like highway driving or platooning. The goal of platooning is to reduce fuel consumption and improve traffic flow by reducing the distance between succeeding vehicles. Figure 7.2 sketches a platooning scenario. The vehicles try to keep a safety distance as between the red vehicle and the second

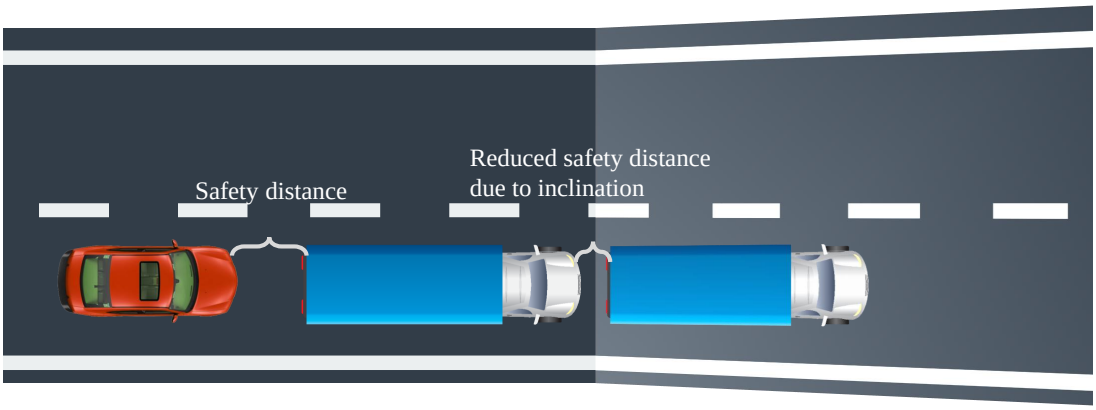

Figure 7.2: Sketch of a platooning scenario. The vehicles try to keep a safety distance as between the red vehicle and the second truck. The first truck slows down because of the inclination leading to a temporarily reduced safety distance between the two trucks.

truck. The first truck slows down because of the inclination. This leads to a temporarily reduced safety distance between the two trucks. At this moment, the first truck might be forced to perform an emergency brake action due to an unexpected event happening in front of him. The second truck has to be able to brake despite of the reduced safety distance and possibly other negative current conditions. In addition, the red vehicle also needs to brake fast enough.

On the one hand, this has to be ensured by applying a well-constructed control mechanism. On the other hand, the actual implementation and an accurate vehicle model may lead to states not predicted by the simplified models used for the concept design. Instead, the *STARVEC* concept can be applied to determine whether the safety distances and braking concepts applied in different situations are sufficient for ensuring the platoon's safety.

Figure 7.3 sketches a project consisting of five research tasks to be addressed. The first task is to implement a platooning system based on existing work for example of [166] or [167]. This has to include the controller for the good cases, i.e. cases in which no seldom disturbances occur. Additionally, there need to be functions dealing with emergencies. If the vehicle leading the platoon has to perform an emergency brake action, there needs to be a strategy minimizing or preventing damage to the following vehicles. The capability of handling such situations determines how close the vehicle can approach during normal operation. The closer the vehicles can approach, the more fuel they are saving. The *STARVEC* framework can then be applied to the implemented platooning control system in order to find weaknesses in its emergency handling.

The implementation of the platooning controller is sufficient for first experiments about the applicability of the *STARVEC* concept to the platooning problem. For more comprehensive experiments with the platooning technology, it is necessary to implement further platooning or high-speed scenario specific environment events. One such event is the change of the road inclination described in the first paragraph of this section. Another important event is a late

Platooning System	Environment events	Adjustments to the STARVEC algorithm	Standard ACC	High speed merge maneuvers
• Good case controller • Emergency maneuvers	• Change of road inclination • Late detected static obstacle • Changed road friction • Wind • Instable communication	• Relative positions and velocities • Analyze efficiency	• Sudden lane change of vehicle in front	• Nondeterministic behavior of involved vehicles • Limited length of own lane

Figure 7.3: Five parallel research tasks for analyzing high-speed scenarios.

detected static obstacle in front of the leading vehicle. This obstacle might trigger the emergency brake maneuver mentioned in the first paragraph of this section. Furthermore, the road friction might change at an unfavorable point in time. This affects the emergency brake maneuver. If the road friction is low during the whole scenario, the platooning control system might adapt by increasing the safety distances. A low road friction occurring shortly before the emergency braking starts can have more severe effects. The fourth event listed in Figure 7.3 is wind influencing the controller behavior. It can lead to some deviations from the planned vehicle trajectory that can accumulate with other effects in an emergency brake maneuver. Finally, communication problems are a major factor for platooning systems. These problems include communication delays, or temporarily or permanently lost connections to platooning participants. The platooning system has to cope with the deficiencies and continue safe operation. As for the other tested events, communication problems occurring in a favorable moment can be handled differently to those affecting emergency maneuvers.

The third research task to be investigated are adjustments to the *STARVEC* algorithm. The *STARVEC* concept is designed to support different kinds of autonomous driving systems. However, the experiments in this thesis focus on low speed scenarios. For gaining efficiency in high-speed scenarios, some properties of them can be exploited. One such property is low relative velocities. The velocity of the rear vehicles typically only deviates by less than one meter per second from the velocity of the leading vehicle. Instead of using the absolute position and velocity of the involved vehicles for the state abstraction introduced in Section 4.1, these relative values can be used. This can reduce the size of the explored state space.

The results of the first three development lanes cover efficient tests of a platooning system. The insights gained in these efforts can be extended to other high-speed scenarios. One such scenario involves a standard ACC (Adaptive Cruise Control) system. Such systems can be tested against a vehicle cutting into the ego vehicle's lane at a close distance. This behavior can occur in unfavorable moments like when the car is currently accelerating.

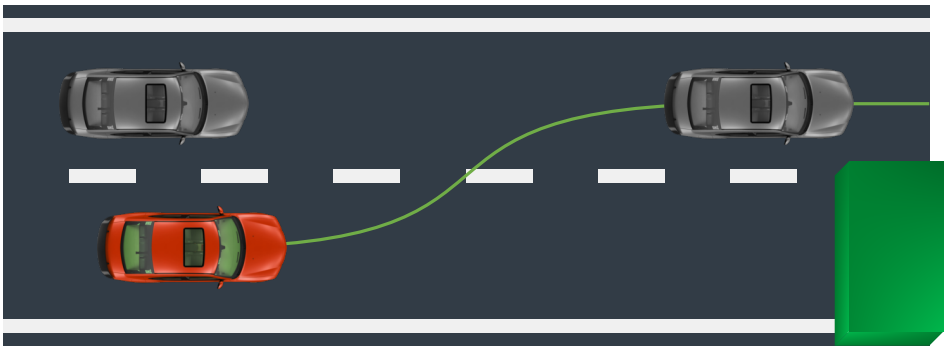

Figure 7.4: The ego vehicle (red) wants to merge into the left lane between the two other cars. The lane of the ego vehicle ends after a limited distance.

Finally, the insights can be applied to high-speed merge maneuvers as listed in Figure 7.3 and illustrated in Figure 7.4. As regarded in Section 4.5, the traffic participants can behave nondeterministically. The merging controller has to ensure safe operation as long as the behavior of the other vehicles is acceptable. The maneuver can become more difficult due to the events listed in the previous paragraphs. Additionally, the system has to cope with situations in which the own lane ends.

In summary, the research efforts described in this section improve testing of autonomous systems in high-speed scenarios by applying the *STARVEC* concept to them.

7.5 Testing the Interaction with Many Traffic Participants

Another direction of future research are scenarios with many traffic participants. The basis for this has been presented in Section 4.5. It demonstrates tests of the planning and control system in the presence of a traffic participant behaving nondeterministically. Figure 7.5 shows a more complex traffic situation. It depicts a large number of traffic participants simultaneously using a roundabout. Each traffic participant has many options for his future trajectory. The vehicles can change lanes, turn into the roundabout exit, accelerate, decelerate and do many more things. The ego vehicle has to find a plan that does not cause a collision for any behavior of the traffic participants.

Three main challenges have to be addressed for testing such a scenario with the *STARVEC* framework:

1. efficiently modeling other traffic participants
2. exploring adaptations to the *STARVEC* algorithm core, and
3. identifying who is responsible for which collision.

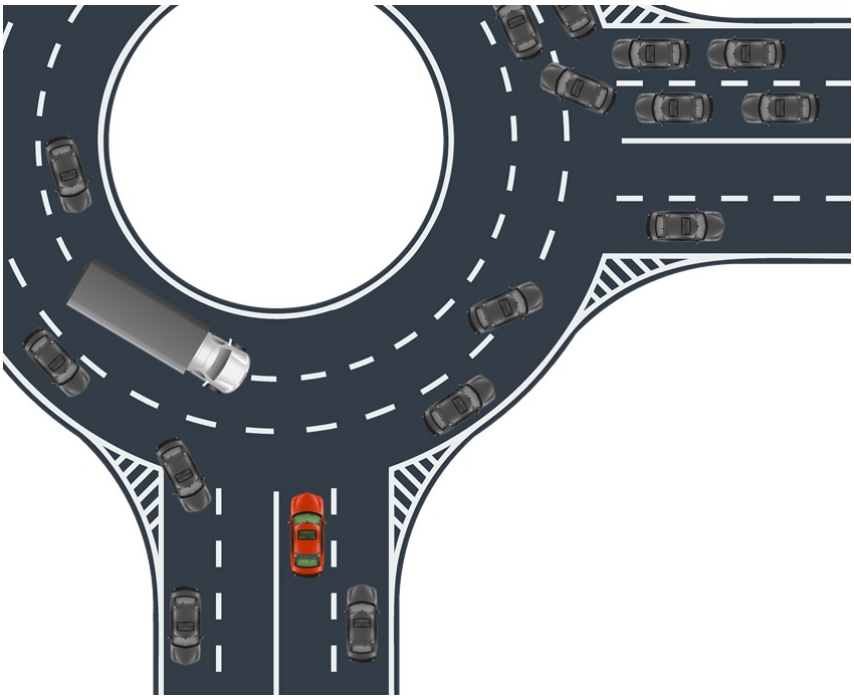

Figure 7.5: A complex roundabout with many traffic participants. Each traffic participant has many options for his future trajectory. The ego vehicle must not cause an accident for any behavior of other traffic participants.

The large number of traffic participants has to be modeled such that the possible behaviors are well covered and the analysis remains efficient. First, this requires implementing a small set of atomic actions that cover the behaviors of the vehicle similar to the set in Section 4.5. Additionally to the challenges solved in this thesis, the total number of different actions possible by the large number of traffic participants is significantly higher. In order to keep the simulation efficient several abstractions of the vehicle actions are reasonable. Three possible abstractions are:

1. Adapting the set of possible actions based on the distance of a car to the ego vehicle,
2. limiting nondeterminism to vehicles relevant in the near future and
3. modeling the behavior of car convoys instead of single cars.

The first abstraction means that cars with a high distance to the ego vehicle are modeled with less possible actions. For example, the actions can be limited to only acceleration and lane changes without lateral deviations within a lane. Instead of modeling acceleration, the vehicles can also be limited to a small set of possible target velocities. The second abstraction implies that some cars in the scene behave deterministically, because they only slightly influence the ego vehicle. For example, the vehicles at the top right corner will not get close to the ego vehicle soon. Their presence is important as they might affect the chosen future path, but small deviations of their behavior does not influence the current plan. Finally, convoys of cars can be modeled

together instead of modeling the behavior of every single car. This limits the range of possible resulting behavior patterns only slightly but increases the efficiency of the analysis. The convoy can perform the same actions as a single vehicle plus it can dissolve or merge with another convoy or vehicle. All three abstractions limit the set of possible behavior patterns of the full system. It has to be researched whether these limitations significantly influence the analysis results. Furthermore, additional abstractions can be developed and compared.

The second research challenge are adaptations to the *STARVEC* algorithm. Two reasonable adaptations are a comparison of different search techniques and changing the abstraction of traffic states. One possible search technique to investigate is the combination of *STARVEC* and RRT suggested in Section 7.3. The abstraction of traffic states can exploit the different consequences of deviations of the ego position and deviations of the traffic participants' positions. The position of traffic participants can be mapped to a coarser grid. Additionally, it can be defined as a position on a lane and the distance to this position.

Finally, the third research challenge copes with identifying those collisions that are actually caused by the ego vehicle. As described in Section 4.5, temporal behavior patterns can support this filtering. However, the situations possible in the sketched roundabout are more complex and require research for defining the temporal logic behavior patterns.

All in all, interaction with many traffic participants is one of the major challenges of autonomous driving. A system for efficiently testing these interactions can speed up the development and evaluation of new concepts addressing this challenge.

Chapter 8

Conclusion

In this thesis, a new method for testing autonomous driving planning and control software against nondeterminism resulting from sensor and actuator inaccuracies or behavior of traffic participants is presented. It searches for behaviors that can be specified either based on a single state like collisions or based on a time sequence like repeated stops during a parking maneuver. The approach exploits the geometric nature of these behaviors in order to reduce the complexity of their detection. A comparison shows that it is significantly more efficient than a classical Monte Carlo algorithm. Based on the approach, scenarios from physical test-drives can be analyzed finding almost-accidents that could have been accidents but have not been. If a fault actually occurs in a test-drive, parts of the method can be reused for robust reproduction of the fault in a simulation environment. The concept has been implemented as a prototype and tested with an autonomous driving system created for an industrial partner.

It can be applied to autonomous driving projects by implementing load and store operations for the involved software components. In future projects the system can be optimized for execution on high performance computers. This makes it applicable to testing a large set of scenarios simultaneously. Furthermore, additional research is necessary for creating the most valid and efficient sensor and actuator inaccuracy models. It also seems promising to apply it to high-speed scenarios like platooning or highway driving. Finally, scenarios with many traffic participants can be tested by the concept.

Appendices

Appendix A

NuSMV base model

Listing A.1: NuSMV transition table for one state

```
MODULE main
DEFINE
 <NuSMV-tables> -- Has to be replaced by the tables generated from
                -- the STARVEC search graph

 ---------------------------------------------------------------------
 ---------------------- Special States -------------------------------
 ---------------------------------------------------------------------
 INVALID := FALSE;
 NO_STATE := MAX_STATE_ID + 1; -- The successor state of not
                -- expanded states
 TERMINAL_STATE := MAX_STATE_ID + 2; -- The successor state of all
                   -- terminal states
 -- Replaces not expanded successor states if, similar states are
 -- not included in the behavior pattern searched for
 SIMILAR_STATE := MAX_STATE_ID + 3;
                    --
                   --
                   --

VAR
 state_id : 0 .. SIMILAR_STATE; -- The STARVEC node id. Each state
                 -- corresponds to one simulated
                 -- second
 sub_step : 0 .. 99; -- The base simulation steps. Each base step
           -- corresponds to 0.01 simulated seconds
 error_number : 0..3; -- The currently active error pattern number.
            -- It can only change when the STARVEC
            -- state_id changes

IVAR
 next_error_number : 0..3;

ASSIGN

next(state_id) := NEXT_STATE_ID; -- NEXT_STATE_ID is a table
```

```
37                  -- generated from the STARVEC
38                  -- search graph
39
40
41 next(sub_step) :=
42  case
43   sub_step = 99 : 0;
44   TRUE : sub_step + 1;
45  esac;
46
47 -- The active error number can only change when the STARVEC
48 -- state_id changes
49 next(error_number) :=
50  case
51   sub_step = 99 : next_error_number;
52   TRUE : error_number;
53  esac;
54
55 -- The initial error_number is a free variable
56 INIT state_id = 0 & sub_step = 0;
57
58 -- Model plausibility check: Special state NO_STATE is not
59 -- reachable
60 INVARSPEC state_id != NO_STATE;
61
62 DEFINE
63
64 -- Example pattern to be checked: Double forward pattern. G0-G3
65 -- are property tables generated from the STARVEC search graph:
66 -- G0: velocity>0.3
67 -- G1: velocity=0
68 -- G2: velocity>-0.05
69 -- G3: velocity>0.3
70 SPEC !EF(G0 & E[G2 U G1 & E[G2 U G3 & state_id < NO_STATE]]);
71
72 -- The NuSMV output can be very long. The following regex can be
73 -- used for search+replace by "" in order to get only STARVEC
74 -- state changes
75 --(    sub_step = \d+|  -> (Input|State): \d+\.\d+ <-
76 --|    NEXT_STATE_ID = \d+)\r\n
```

Appendix B

Plots of Collisions in the Analyzed Scenarios

Figures B.1-B.10 show examples of detected collisions for each of the scenarios compared in Section 6.2.1. For each displayed pair, the left Figure shows the path leading to the detected collision. The right Figure shows controller states in the final about 10 seconds before the collision occurs. In these plots, σ_{tra} is the steering angle planned by the trajectory planner, σ_{des} is the steering angle desired by the controller and σ_{act} is the actually performed steering angle. e_n is the lateral position error of the controller and e_ψ is the orientation error of the controller.

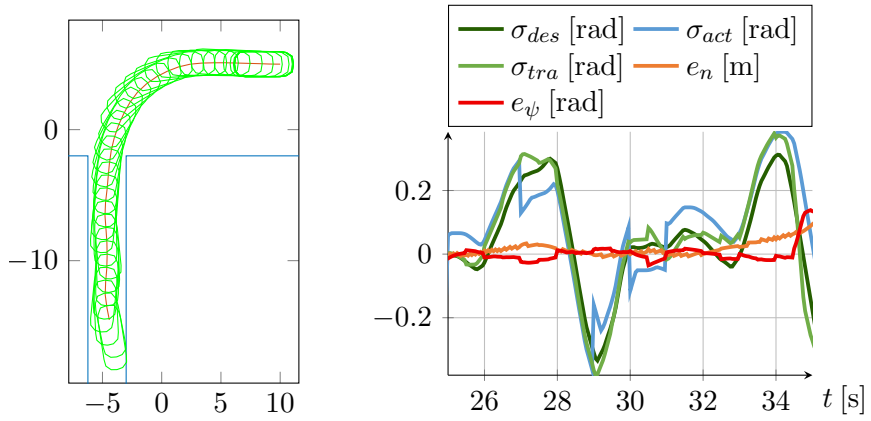

(a) Driven path

(b) Controller states in the final seconds

Figure B.1: Collision detected in the "turn into narrow lane" scenario: The controller fails to follow the final curve to the right: The planned curvature σ_{tra} and the performed curvature σ_{act} deviate in the final second. This leads to a growing orientation error e_ψ that adds up with an already present high position error e_n.

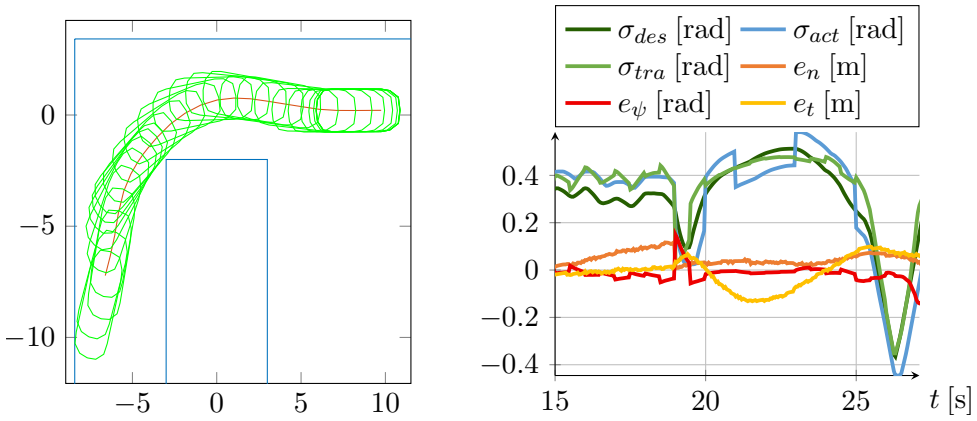

(a) Driven path

(b) Controller states in the final seconds

Figure B.2: Collision detected in the "narrow curve" scenario: The trajectory planner plans to change the steering angle σ_{tra} too fast for the controller to compensate current errors. This leads to an orientation error e_ψ that makes the vehicle touch the obstacle and is not compensated by the small position error.

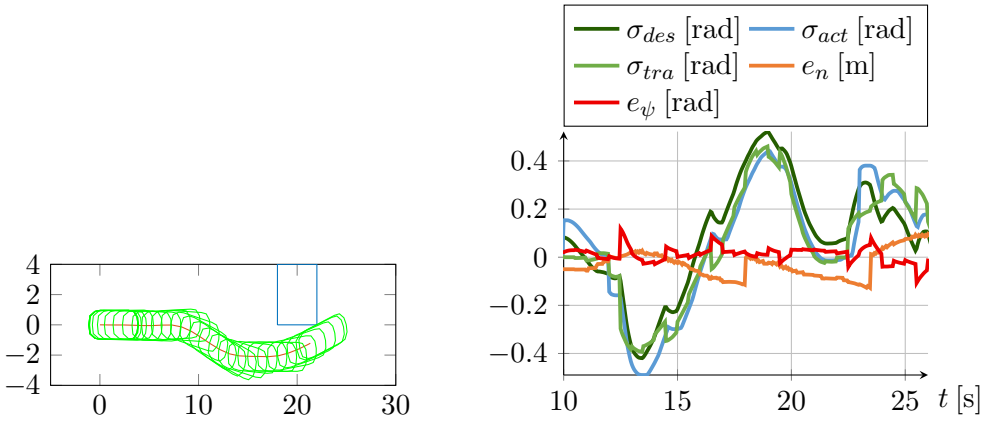

(a) Driven path

(b) Controller states in the final seconds

Figure B.3: Collision detected in the "obstacle" scenario: The controller perceives changes of the trajectory plan as non-continuous σ_{tra} values due to inaccurate predictions of the planner. This adds up with the inaccurate steering to a high position error e_n exactly when the vehicle passes the obstacle.

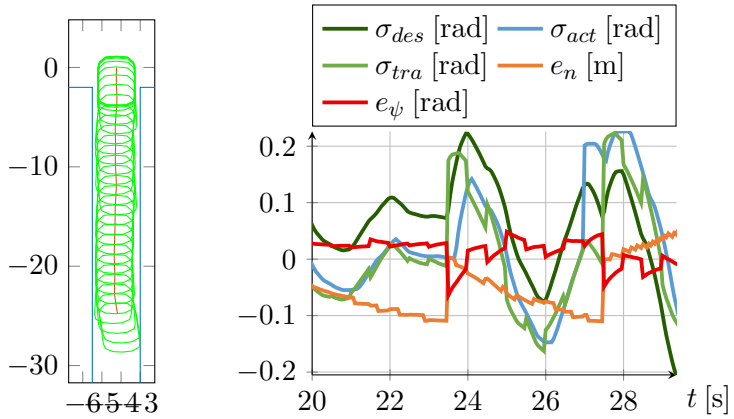

(a) Driven path (b) Controller states in the final seconds

Figure B.4: Collision detected in the "narrow lane" scenario: The trajectory planner defines slight S-shaped curves for compensating controller errors. One of these curves leads to the trajectory planning safety distance touching an obstacle. Additionally the controller fails to follow the curves exactly leading to a collision.

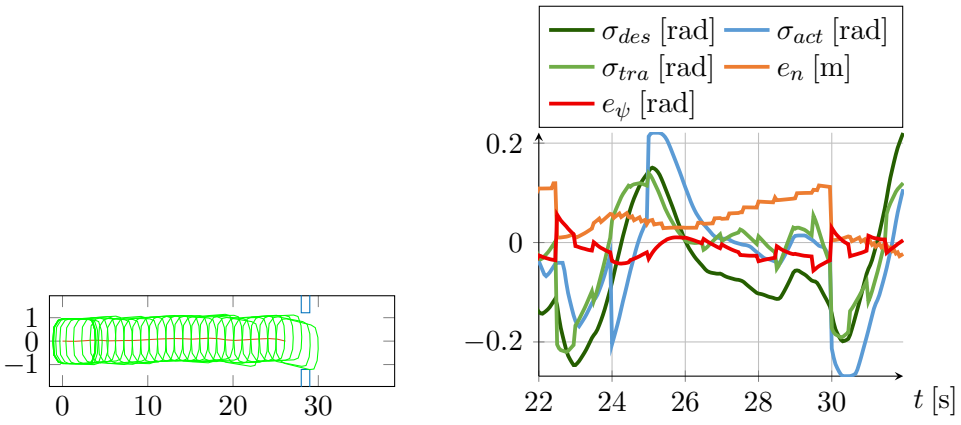

(a) Driven path (b) Controller states in the final seconds

Figure B.5: Collision detected in the "narrow barrier" scenario: In this scenario, the safety distances are set to very small values. Some seconds before the collision the controller error are small enough for the trajectory planner to compensate and big enough for the safety distance to touch the obstacle. Therefore, the vehicle tries to pass the barrier despite of the controller errors. At the barrier, inaccurate steering leads to a position error that is as large as the safety distance.

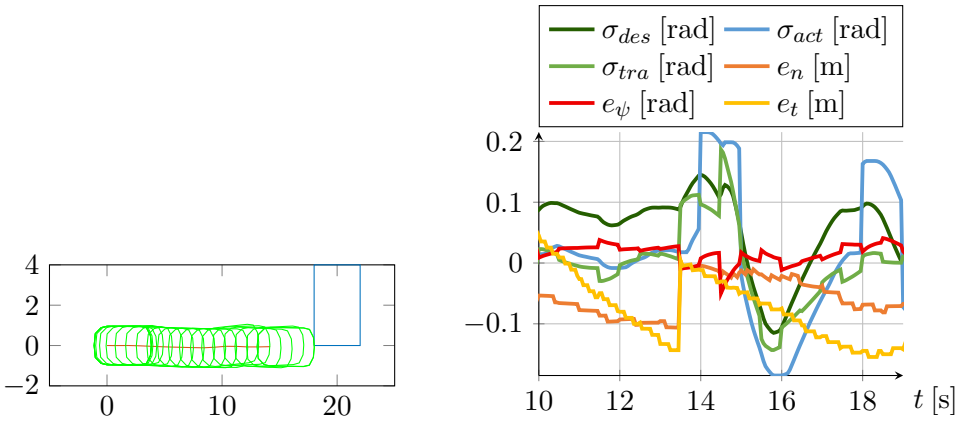

(a) Driven path (b) Controller states in the final seconds

Figure B.6: Collision detected in the "ghost obstacle" scenario: Inaccurate actuators lead to a longitudinal controller error e_t that adds up with an orientation error and leads to a collision.

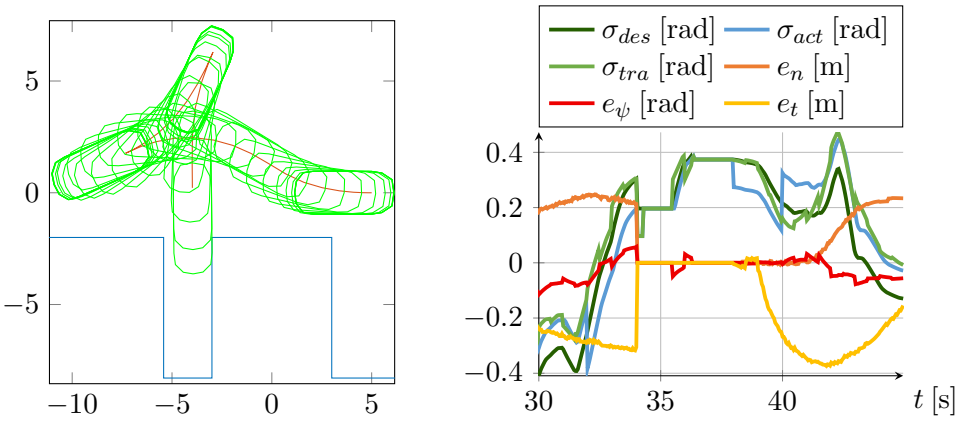

(a) Driven path (b) Controller states in the final seconds

Figure B.7: Collision detected in the "forward parking" scenario: Inaccurate acceleration in the 40th second leads to a high longitudinal error e_t during a sharp curve. This leads to a lateral error e_n that the controller does not compensate fast enough. Additionally, the trajectory planning safety distance already touches the obstacle due to a previous lateral error in the 34th second.

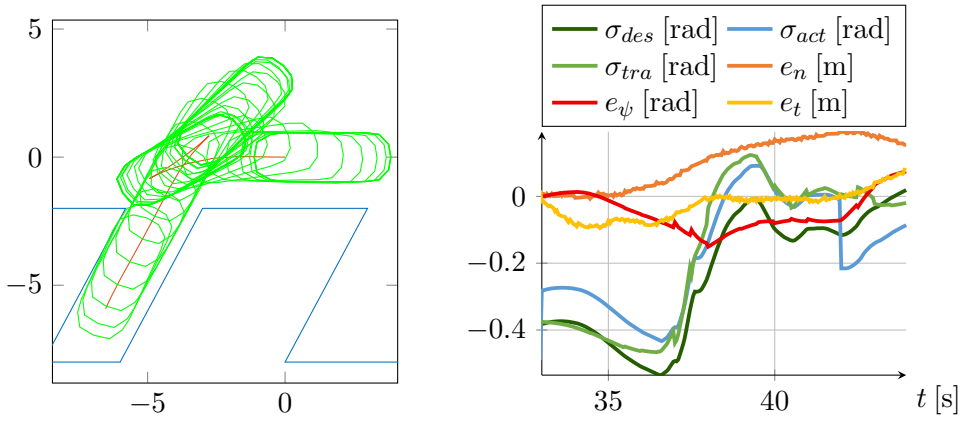

(a) Driven path (b) Controller states in the final seconds

Figure B.8: Collision detected in the "skewed parking" scenario: Inaccurate steering leads to an orientation error e_ψ in the 42nd second. It adds up with an already present lateral error e_n leading to a collision.

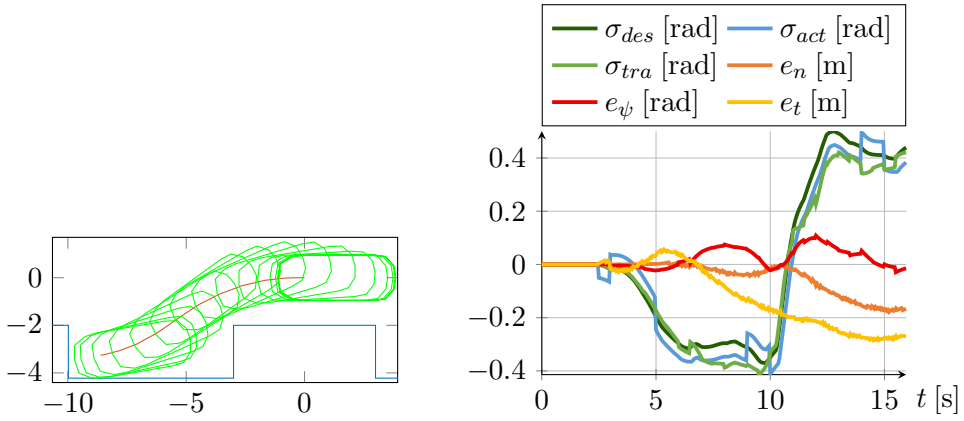

(a) Driven path (b) Controller states in the final seconds

Figure B.9: Collision detected in the "parallel parking" scenario: High longitudinal errors e_t lead to lateral errors e_n due to a sharp curve. This leads to a collision with the side wall.

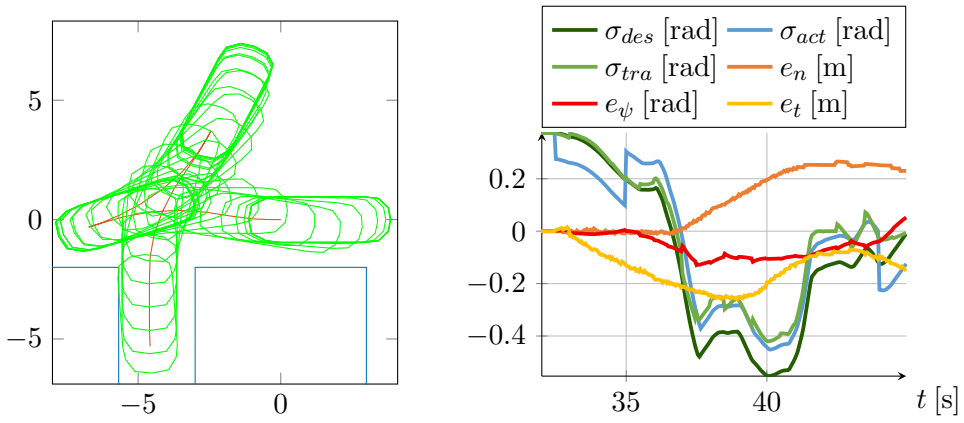

(a) Driven path

(b) Controller states in the final seconds

Figure B.10: Collision detected in the "cross parking" scenario: High longitudinal errors e_t lead to lateral errors e_n due to a sharp curve. In the 44th second, steering inaccuracy leads to an orientation error e_ψ that adds up with the lateral error e_n leading to a collision.

List of Figures

Abbreviations

ACC Adaptive Cruise Control 117

ADAS Advanced Driver Assistance System 15

ADTF Automotive Data and Time triggered Framework 52, 83

BFS Breadth First Search 62–64

CTL Computation Tree Logic 40, 58, 61–64, 134

DFS Depth First Search 62

ECU Engine Control Unit 27

FLANN Fast Library for Approximate Nearest Neighbors 50

GDP Gross Domestic Product 1

GIDAS German In-Depth Accident Study 15

GUI Graphical User Interface 72, 79

HIL Hardware In the Loop 2, 9, 11

JSON JavaScript Object Notation 46

LTE Long Term Evolution 86

LTL Linear Temporal Logic 61

M Million 96–98, 102, 141

Monte Carlo HF Monte Carlo with High Frequency 91, 92, 97, 101, 102

NuSMV New Symbolic Model Verifier 58, 61–64, 134

PVS Prototype Verification System 8

RRT Rapidly-exploring Random Tree 50, 91, 92, 96, 98–100, 102, 106–108, 112, 115, 120, 136

SE Simulation Environment 18

SIL Software In the Loop 2

STARVEC Systematic Testing of Autonomous Road Vehicles against Error Combinations 5, 23, 36, 39, 41, 44, 48, 49, 52, 54, 56, 57, 59, 61–66, 68, 70–74, 76, 78, 83–87, 89, 91–93, 95–110, 112–118, 120, 133–136

SUT System Under Test 12, 132

USA United States of America 1

WHO World Health Organization 1

XML Extensible Markup Language 46

List of Tables

Bibliography

[1] T. Toroyan, M. M. Peden, and K. Iaych, "Global status on road report 2015," Management of Noncommunicable Diseases, Disability, Violence and Injury Prevention (NVI), Geneva, Switzerland, Tech. Rep., 2015, p. 150.

[2] M. Peden, T. Toroyan, E. Krug, *et al.*, "The Status of Global Road Safety: The Agenda for Sustainable Development encourages urgent action," *Journal of the Australasian College of Road Safety*, vol. 27, no. 2, pp. 37–39, 2016.

[3] M. D. W. Bertoncello, "Automotive Software Engineering: Grundlagen, Prozesse, Methoden und Werkzeuge effizient einsetzen," *McKinsey Quarterly*, 2015.

[4] S. Elfström, *Volvo Car Group initiates world unique Swedish pilot project with self-driving cars on public roads*, Gothenburg, Sweden, 2013.

[5] Y. Freemark, "Will autonomous cars change the role and value of public transportation?" *The Transport Politic*, pp. 1–9, 2015.

[6] G. R. Campos, P. Falcone, and J. Sjöberg, "Traffic safety at intersections: a priority based approach for cooperative collision avoidance," in *3rd International Symposium on Future Active Safety Technology Towards zero traffic accidents (FAST-zero)*, Göteborg, Sweden, 2015.

[7] ERTRAC Task Force Connectivity and Automated Driving, "Automated Driving Roadmap," ERTRAC, Brussels, Belgium, Tech. Rep., 2015.

[8] K. Bengler, K. Dietmayer, B. Farber, *et al.*, "Three Decades of Driver Assistance Systems: Review and Future Perspectives," *IEEE Intelligent Transportation Systems Magazine*, vol. 6, no. 4, pp. 6–22, Jan. 2014.

[9] J. E. Stellet, M. R. Zofka, J. Schumacher, *et al.*, "Testing of advanced driver assistance towards automated driving: A survey and taxonomy on existing approaches and open questions," in *18th IEEE International Conference on Intelligent Transportation Systems (ITSC)*, 2015.

[10] M. Fausten, M. Helmle, and F. von Zeppelin, "Absicherung von FAS und AD Systemen," in *Fahrerassistenz und Aktive Sicherheit*, Essen: Klaffke, Werner, 2015, pp. 219–229.

[11] A. J. Ramirez, A. C. Jensen, and B. H. C. Cheng, "A taxonomy of uncertainty for dynamically adaptive systems," in *7th ICSE Workshop on Software Engineering for Adaptive and Self-Managing Systems (SEAMS)*, Zürich, Switzerland, Jun. 2012, pp. 99–108.

[12] A. G. Millard, J. Timmis, and A. F. Winfield, "Run-time detection of faults in autonomous mobile robots based on the comparison of simulated and real robot behaviour," in *IEEE/RSJ International Conference on Intelligent Robots and Systems (IROS)*, Chicago, USA: IEEE, Sep. 2014, pp. 3720–3725.

[13] A. Cacilo, S. Schmidt, P. Wittlinger, *et al.*, "Hochautomatisiertes Fahren Auf Autobahnen – Industriepolitische Schlussfolgerungen," Fraunhofer-Institut für Arbeitswirtschaft und Organisation IAO, Tech. Rep., 2015.

[14] C. Urmson, *Google Self-Driving Car Project - SXSW Interactive*, 2016.

[15] J. Schäuffele and T. Zurawka, *Automotive Software Engineering*, 5th ed. Wiesbaden: Springer Fachmedien, 2013, p. 346. arXiv: `arXiv:1011.1669v3`.

[16] K. Stapel, E. Knauss, and C. Allmann, "Lightweight Process Documentation: Just Enough Structure in Automotive Pre-development," *Software Process Improvement*, vol. 16, pp. 142–151, 2008.

[17] C. Allmann, "Requirements Engineering in der automotive Entwicklung – Von der Idee bis zum Produkt," *Softwaretechnik-Trends*, p. 2, 2009.

[18] J. Schröder, "Adaptive Verhaltensentscheidung und Bahnplanung für kognitive Automobile," PhD thesis, Universität Karlsruhe (TH), 2009. arXiv: `arXiv:1011.1669v3`.

[19] T. Fraichard and A. Scheuer, "From Reeds and Shepp's to Continuous-Curvature Paths," *IEEE Transactions on Robotics*, vol. 20, no. 6, pp. 1025–1035, Dec. 2004.

[20] U. Schwesinger, M. Rufli, P. Furgale, *et al.*, "A sampling-based partial motion planning framework for system-compliant navigation along a reference path," in *IEEE Intelligent Vehicles Symposium (IV)*, Gold Coast, Australia: IEEE, 2013, pp. 391–396.

[21] J. Ziegler, P. Bender, T. Dang, *et al.*, "Trajectory planning for Bertha — A local, continuous method," in *IEEE Intelligent Vehicles Symposium (IV)*, Dearborn, USA: IEEE, 2014, pp. 450–457.

[22] X. Li, Z. Sun, D. Cao, *et al.*, "Real-time trajectory planning for autonomous urban driving: Framework, algorithms, and verifications," *IEEE/ASME Transactions on Mechatronics*, vol. 21, no. 2, pp. 740–753, 2016.

[23] U. Schwesinger, M. Bürki, J. Timpner, *et al.*, "Automated Valet Parking and Charging for e-Mobility—Results of the V-Charge Project," in *IEEE Intelligent Vehicles Symposium (IV)*, Gothenburg, Sweden: IEEE, 2016.

[24] B. Paden, M. Cap, S. Z. Yong, *et al.*, "A Survey of Motion Planning and Control Techniques for Self-driving Urban Vehicles," *arXiv preprint*, pp. 1–27, 2016. arXiv: `1604.07446`.

[25] M. Werling, "Ein neues Konzept für die Trajektoriengenerierung und -stabilisierung in zeitkritischen Verkehrsszenarien," PhD thesis, Karlsruher Institut für Technologie, 2010.

[26] A. R. Willms and S. X. Yang, "Real-time robot path planning via a distance-propagating dynamic system with obstacle clearance," *IEEE Transactions on Systems, Man, and Cybernetics, Part B: Cybernetics*, vol. 38, no. 3, pp. 884–893, 2008.

[27] O. Khatib, "Real-time obstacle avoidance for manipulators and mobile robots," *International Journal of Robotics Research*, pp. 500–505, 1985.

[28] S. Ge and Y. Cui, "Dynamic motion planning for mobile robots using potential field method," *Autonomous Robots*, vol. 13, no. 3, pp. 207–222, 2002.

[29] R. Tilove, "Local obstacle avoidance for mobile robots based on the method ofartificial potentials," in *IEEE International Conference on Robotics and Automation (ICRA)*, Cincinnati, USA: IEEE, 1990.

[30] Y. Koren, S. Member, J. Borenstein, *et al.*, "Potential Field Methods and Their Inherent Limitations for Mobile Robot Navigation," in *IEEE International Conference on Robotics and Automation (ICRA)*, Sacramento, USA: IEEE, 1991, pp. 1398–1404.

[31] D. Dolgov, S. Thrun, M. Montemerlo, *et al.*, "Practical Search Techniques in Path Planning for Autonomous Driving," in *First International Symposium on Search Techniques in Artificial Intelligence and Robotics (STAIR-08)*, Chicago, USA, 2008.

[32] T. Fraichard, H. Asama, I. Collision, *et al.*, "Inevitable Collision States . A Step Towards Safer Robots?" In *IEEE-RSJ International Conference on Intelligent Robots and Systems (IROS)*, Las Vegas, USA, 2003.

[33] S. Petti and T. Fraichard, "Safe Motion Planning in Dynamic Environments," in *IEEE/RSJ International Conference on Intelligent Robots and Systems (IROS)*, Edmonton, Canada, 2005.

[34] S. Patil, Y. Duan, J. Schulman, *et al.*, "Gaussian belief space planning with discontinuities in sensing domains," in *IEEE International Conference on Robotics and Automation (ICRA)*, Hong Kong, China: IEEE, 2014, pp. 6483–6490.

[35] S. Patil, G. Kahn, M. Laskey, *et al.*, "Scaling up Gaussian belief space planning through covariance-free trajectory optimization and automatic differentiation," *Springer Tracts in Advanced Robotics*, vol. 107, pp. 515–533, 2015.

[36] D. Lenz, M. Rickert, and A. Knoll, "Heuristic search in belief space for motion planning under uncertainties," in *IEEE/RSJ International Conference on Intelligent Robots and Systems (IROS)*, Hamburg, Germany, 2015.

[37] E. Galceran, A. G. Cunningham, R. M. Eustice, *et al.*, "Multipolicy Decision-Making for Autonomous Driving via Changepoint-based Behavior Prediction," *Robotics: Science and Systems*, 2015.

[38] C. Munoz and V. Carreno, "Aircraft Trajectory Modeling and Alerting Algorithm Verification," in *The 13th International Conference on Theorem Proving in Higher Order Logics*, ser. Lecture Notes in Computer Science, Portland, USA: Springer Berlin Heidelberg, Jan. 2000, pp. 90–105.

[39] S. Owre, J. M. Rushby, and N. Shankar, "PVS: a prototype verification system," in *11th International Conference on Automated Deduction*, Saratoga Springs, USA, 1992, pp. 748–752.

[40] M. Althoff, "Reachability Analysis and its Application to the Safety Assessment of Autonomous Cars," PhD thesis, Technische Universität München, Munich, Feb. 2010, p. 221.

[41] M. Althoff and J. M. Dolan, "Online verification of automated road vehicles using reachability analysis," *IEEE Transactions on Robotics*, vol. 30, no. 4, pp. 903–918, 2014.

[42] M. Althoff, "An Introduction to CORA 2015 (Tool Presentation)," in *Proc. of the Workshop on Applied Verification for Continuous and Hybrid Systems*, vol. 2015, Seattle, 2015, pp. 1–28. arXiv: 052186571997805218657 15.

[43] N. Jakobi, P. Husbands, and I. Harvey, "Noise and the Reality Gab: The Use of Simulation in Evolutionary Robotics," *Lecture Notes in Computer Science*, vol. 929, pp. 704–720, 1995.

[44] S. Thrun, "Learning Occupancy Grid Maps With Forward Sensor Models," *Autonomous Robots*, no. 1998, pp. 1–28, 2003.

[45] P. Lohmann, A. Koch, and M. Schaeffer, "Approaches to the filtering of laser scanner data," *International Archives of Photogrammetry and Remote Sensing*, vol. 33, no. B3/1; PART 3, pp. 540–547, 2000.

[46] E. Roth, T. Dirndorfer, and K. von Neumann-Cosel, "Analyse und Validierung vorausschauender Sensormodelle in einer integrierten Fahrzeug-und Umfeldsimulation," *VDI-Berichte*, 2010.

[47] E. Roth, T. J. Dirndorfer, A. Knoll, *et al.*, "Analysis and Validation of Perception Sensor Models in an Integrated Vehicle and Environment Simulation," in *22nd International Technical Conference on the Enhanced Safety of Vehicles (ESV)*, Washington, DC, USA, 2011.

[48] F. Netter, F. Gauterin, and B. Butterer, "Real-data validation of simulation models in a function-based modular framework," in *Sixth IEEE International Conference on Software Testing, Verification and Validation (ICST)*, Luxembourg, 2013, pp. 41–47.

[49] D. Gruyer, M. Grapinet, and P. De Souza, "Modeling and validation of a new generic virtual optical sensor for ADAS prototyping," in *IEEE Intelligent Vehicles Symposium (IV)*, Alcalá de Henares, Spain: IEEE, 2012, pp. 969–974.

[50] N. Viandier, D. Nahimana, J. Marais, *et al.*, "Gnss performance enhancement in urban environment based on pseudo-range error model," in *IEEE/ION Position, Location and Navigation Symposium (PLANS)*, Monterey, USA, 2008, pp. 377–382.

[51] L. Wang, P. D. Groves, and M. K. Ziebart, "GNSS shadow matching: Improving urban positioning accuracy using a 3D city model with optimized visibility scoring scheme," *Navigation, Journal of the Institute of Navigation*, vol. 60, no. 3, pp. 195–207, 2013.

[52] J. Ziegler, H. Lategahn, M. Schreiber, *et al.*, "Video based localization for BERTHA," in *IEEE Intelligent Vehicles Symposium (IV)*, Dearborn, USA: IEEE, 2014, pp. 1231–1238.

[53] S. Houben, M. Neuhausen, M. Michael, *et al.*, "Park marking-based vehicle self-localization with a fisheye topview system," *Journal of Real-Time Image Processing*, pp. 1–16, Sep. 2015.

[54] M. Baer, M. E. Bouzouraa, C. Demiral, *et al.*, "Egomaster: A central ego motion estimation for driver assist systems," in *IEEE International Conference on Control and Automation (ICCA)*, Christchurch, New Zealand, 2009, pp. 1708–1715.

[55] T. Seibert and G. Rill, "Fahrkomfortberechnungen unter einbeziehung der motorschwingungen," *VDI-Berichte*, 1998.

[56] G. Rill, "Vehicle Dynamics," *Lecture Notes - Fachhochschule Regensburg*, no. October, 2006.

[57] J. C. Bongard, "Accelerating self-modeling in cooperative robot teams," *IEEE Transactions on Evolutionary Computation*, vol. 13, no. 2, pp. 321–332, 2009.

[58] P. O'Dowd, A. F. Winfield, and M. Studley, "The distributed co-evolution of an embodied simulator and controller for swarm robot behaviours," in *IEEE/RSJ International Conference on Intelligent Robots and Systems (IROS)*, San Francisco, USA, Sep. 2011.

[59] D. Krajzewicz and G. Hertkorn, "SUMO (Simulation of Urban MObility) An open-source traffic simulation," in *4th Middle East Symposium on Simulation and Modelling (MESM20002)*, Sharjah, UAE, 2002, pp. 63–68.

[60] S. H. A. Niaki and I. Sander, "An automated parallel simulation flow for heterogeneous embedded systems," in *Conference on Design, Automation and Test in Europe (DATE)*, ser. DATE '13, Grenoble, France: EDA Consortium, 2013, pp. 27–30.

[61] F. Netter, "Komplexitätsadaption integrierter Gesamtfahrzeugsimulationen," PhD thesis, Karlsruher Institut für Technologie (KIT), 2015.

[62] K. von Neumann-Cosel, "Virtual Test Drive," PhD thesis, Technische Universität München, 2014.

[63] O. Gietelink, K. Labibes, D. Verburg, *et al.*, "Pre-crash system validation with PRESCAN and VEHIL," in *IEEE Intelligent Vehicles Symposium (IV)*, Parma, Italy: IEEE, 2004, pp. 913–918.

[64] M. R. Zofka, S. Klemm, F. Kuhnt, *et al.*, "Testing and Validating High Level Components for Automated Driving : Simulation Framework for Traffic Scenarios," in *IEEE Intelligent Vehicles Symposium (IV)*, Gothenburg, Sweden: IEEE, 2016.

[65] M. Nentwig and M. Stamminger, "Hardware-in-the-loop testing of computer vision based driver assistance systems," in *IEEE Intelligent Vehicles Symposium (IV)*, Baden-Baden, Germany: IEEE, 2011, pp. 339–344.

[66] L. Verhoeff, D. Verburg, H. Lupker, *et al.*, "VEHIL: a full-scale test methodology for intelligent transport systems, vehicles and subsystems," in *IEEE Intelligent Vehicles Symposium (IV)*, Dearborn, USA: IEEE, 2000, pp. 369–375.

[67] D. J. Verburg, A. C. van der Knaap, and J. Ploeg, "VEHIL - Developing and Testing Intelligent Vehicles," in *IEEE Intelligent Vehicles Symposium (IV)*, Versailles, France: IEEE, 2002.

[68] O. Gietelink, J. Ploeg, B. De Schutter, *et al.*, "Development of advanced driver assistance systems with vehicle hardware-in-the-loop simulations," *International Journal of Vehicle System Dynamics*, vol. 44, no. 7, pp. 569–590, 2006.

[69] V. Schill, T. Schulz, A. Kemeny, *et al.*, "Renewal of the Renault Ultimate Simulator," in *Driving simulation conference*, Paris, France, 2012.

[70] K. Stahl and K.-D. Leimbach, "Vehicle dynamics simulation by using hardware in the loop techniques," in *17th International IEEE Conference on Intelligent Transportation Systems (ITSC)*, IEEE, Oct. 2014, pp. 520–524.

[71] E. Zeeb, "Daimlers new full-scale, high-dynamic driving simulator - a technical overview," in *Driving Simulation Conference*, Paris, France, 2010, pp. 157–165.

[72] H. Lin, X. Wang, Z. Wu, *et al.*, "Tongji University Advanced Driving Behavior and Traffic Safety Research Simulator (TUDS simulator)," in *Driving Simulation Conference*, Paris, France, 2012.

[73] J. Jansson, J. Sandin, B. Augusto, *et al.*, "Design and performance of the VTI Sim IV," in *Driving simulation conference*, Paris, France, 2014.

[74] Y. Yasuno, E. Kitahara, T. Takeuchi, *et al.*, "Nissan's New High Performance Driving Simulator for Vehicle Dynamics Performance & Man-Machine Interface Studies," in *Driving simulation conference*, Paris, France, 2014, pp. 30–33.

[75] M. Kleer, O. Hermanns, K. Dreßler, *et al.*, "Driving simulations for commercial vehicles-A technical overview of a robot based approach," in *Driving simulation conference*, Paris, France, 2012, pp. 1–8.

[76] H. Winner, S. Hakuli, and G. Wolf, "Handbuch Fahrerassistenzsysteme," *Vieweg+ Teubner Verlag,*, p. 719, 2009.

[77] I. Karl, G. Berg, F. Ruger, *et al.*, "Driving Behavior and Simulator Sickness While Driving the Vehicle in the Loop: Validation of Longitudinal Driving Behavior," *IEEE Intelligent Transportation Systems Magazine*, vol. 5, no. 1, pp. 42–57, 2013.

[78] G. Berg, "Das Vehicle in the Loop - Ein Werkzeug für die Entwicklung und Evaluation von sicherheitskritischen Fahrerassistenzsystemen," PhD thesis, Universität der Bundeswehr München, 2014.

[79] G. Schildbach and F. Borrelli, "A Dynamic Programming Approach for Nonholonomic Vehicle Maneuvering in Tight Environments," in *IEEE Intelligent Vehicles Symposium (IV)*, Gothenburg, Sweden: IEEE, 2016, pp. 1–6.

[80] C. Cadar, D. Dunbar, and D. R. Engler, "KLEE: Unassisted and Automatic Generation of High-Coverage Tests for Complex Systems Programs," in *8th USENIX conference on Operating systems design and implementation*, San Diego, USA, 2008, pp. 209–224.

[81] M. Stephen, "Automatic Exploit Generation (AEG)," *Communications of the ACM*, vol. 47.2, 2014.

[82] B. Y. C. Cadar and K. Sen, "Symbolic Execution for Software Testing: Three Decades Later," *Communications of the ACM*, vol. 56, no. 2, pp. 1–8, 2013.

[83] A. Groce and R. Joshi, "Extending model checking with dynamic analysis," in *Lecture Notes in Computer Science*, vol. 4905 LNCS, Springer Berlin Heidelberg, Jan. 2008, pp. 142–156.

[84] G. Fraser, F. Wotawa, and P. E. Ammann, "Testing with model checkers: a survey," *Software Testing, Verification and Reliability*, vol. 19, no. 3, pp. 215–261, Sep. 2009.

[85] O. Sokolsky, "Specification-based testing with linear temporal logic," in *IEEE International Conference on Information Reuse and Integration (IRI)*, Las Vegas, USA: IEEE, 2004, pp. 493–498.

[86] AEV, "Exact 3.0," Audi Electronic Venture, Tech. Rep., 2012.

[87] E. Bringmann, "Besonderheiten beim Test automobiler Steuerungs- und Regelungssysteme," *Softwaretechnik-Trends*, 2008.

[88] Elektrobit, "Open robinos specification," Elektrobit Automotive GmbH, Tech. Rep., 2016, pp. 1–42.

[89] T. Dirndorfer and M. Botsch, "Model-Based Analysis of Sensor-Noise in Predictive Passive Safety Algorithms," in *22nd International Technical Conference on the Enhanced Safety of Vehicles (ESV)*, Washington, DC, USA, 2011.

[90] D. Gruyer, S. Pechberti, and S. Glaser, "Development of Full Speed Range ACC with SiVIC, a virtual platform for ADAS Prototyping, test and evaluation," in *IEEE Intelligent Vehicles Symposium (IV)*, Gold Coast, Australia: IEEE, 2013, pp. 100–105.

[91] O. Gietelink, B. De Schutter, and M. Verhaegen, "A Probabilistic Approach for Validation of Advanced Driver Assistance Systems," *Transportation Research Record: Journal of the Transportation Research Board*, vol. 1910, pp. 20–28, Jan. 2005.

[92] O. Gietelink, "Design and validation of advanced driver assistance systems," PhD thesis, Technische Universiteit Delft, 2007.

[93] A. J. Ramirez, A. C. Jensen, B. H. C. Cheng, *et al.*, "Automatically exploring how uncertainty impacts behavior of dynamically adaptive systems," in *26th IEEE/ACM International Conference on Automated Software Engineering (ASE)*, ser. ASE '11, Washington, DC, USA: IEEE Computer Society, 2011, pp. 568–571.

[94] J. Lehman and K. Stanley, "Exploiting Open-Endedness to Solve Problems Through the Search for Novelty.," *Artificial Life*, vol. XI, 2008.

[95] D. Hes, M. Althoff, and T. Sattel, "Comparison of trajectory tracking controllers for emergency situations," in *IEEE Intelligent Vehicles Symposium (IV)*, Gold Coast, Australia: IEEE, 2013, pp. 163–170.

[96] J. Jacobson, P. Janevik, and P. Wallin, "Challenges in creating AstaZero , the active safety test area," *Transport Research Arena*, vol. 46, no. 0, 2014.

[97] A. Dobrindt, "Innovationscharta "Digitales Testfeld Autobahn" auf der Bundesautobahn A9," Bundesministerium für Verkehr und digitale Infrastruktur, Berlin, Germany, Tech. Rep., 2015.

[98] DARPA, "Urban Challenge," Defense Advanced Research Projects Agency, Tech. Rep., 2007.

[99] A. Bacha, C. Bauman, R. Faruque, *et al.*, "Odin: Team VictorTango's entry in the DARPA Urban Challenge," *Journal of Field Robotics*, vol. 25, no. 8, pp. 467–492, 2008.

[100] B. J. Patz, Y. Papelis, R. Pillat, *et al.*, "A practical approach to robotic design for the DARPA Urban Challenge," *Journal of Field Robotics*, vol. 25, no. 8, pp. 528–566, 2008.

[101] Y.-L. Chen, V. Sundareswaran, C. Anderson, *et al.*, "TerraMax$^{\text{TM}}$: Team Oshkosh urban robot," *Journal of Field Robotics*, vol. 25, no. 10, pp. 841–860, Oct. 2008.

[102] J. R. McBride, J. C. Ivan, D. S. Rhode, *et al.*, "A perspective on emerging automotive safety applications, derived from lessons learned through participation in the DARPA Grand Challenges," *Journal of Field Robotics*, vol. 25, no. 10, pp. 808–840, Oct. 2008.

[103] F. W. Rauskolb, K. Berger, C. Lipski, *et al.*, "Caroline: An autonomously driving vehicle for urban environments," *Journal of Field Robotics*, vol. 25, no. 9, pp. 674–724, Sep. 2008.

[104] J. Bohren, T. Foote, J. Keller, *et al.*, "Little Ben: The Ben Franklin Racing Team's entry in the 2007 DARPA Urban Challenge," *Journal of Field Robotics*, vol. 25, no. 9, pp. 598–614, Sep. 2008.

[105] J. Leonard, J. How, and S. Teller, "A perception-driven autonomous urban vehicle," *Journal of Field Robotics*, vol. 25, no. 9, 2008.

[106] I. Miller, M. Campbell, D. Huttenlocher, *et al.*, "Team Cornell's Skynet: Robust perception and planning in an urban environment," *Journal of Field Robotics*, vol. 25, no. 8, pp. 493–527, 2008.

[107] C. Urmson, J. Anhalt, D. Bagnell, *et al.*, "Autonomous driving in urban environments: Boss and the Urban Challenge," *Journal of Field Robotics*, vol. 25, no. 8, pp. 425–466, 2008.

[108] M. Montemerlo, J. Becker, and S. Bhat, "Junior: the stanford entry in the urban challenge," *Journal of Field Robotics*, vol. 25, no. 9, 2008.

[109] S. Kammel, J. Ziegler, B. Pitzer, *et al.*, "Team AnnieWAY's autonomous system for the 2007 DARPA Urban Challenge," *Journal of Field Robotics*, vol. 25, no. 9, pp. 615–639, 2008.

[110] J. Clause and A. Orso, "A Technique for Enabling and Supporting Debugging of Field Failures," in *29th International Conference on Software Engineering (ICSE'07)*, Minneapolis, USA: IEEE, May 2007, pp. 261–270.

[111] C. Zamfir, G. Altekar, and I. Stoica, "Automating the debugging of datacenter applications with ADDA," in *43rd Annual IEEE/IFIP International Conference on Dependable Systems and Networks (DSN)*, Budapest, Hungary: IEEE, Jun. 2013, pp. 1–12.

[112] S. Artzi, S. Kim, and M. D. Ernst, "ReCrash:Making Software Failures Reproducible by Preserving Object States Shay," in *European Conference on Object-Oriented Programming*, ser. Lecture Notes in Computer Science, Berlin, Heidelberg: Springer, 2008.

[113] D. Yuan, H. Mai, W. Xiong, *et al.*, "SherLog: Error Diagnosis by Connecting Clues from Run-time Logs," *ACM SIGPLAN Notices*, vol. 45, no. 3, p. 143, Mar. 2010.

[114] D. Yuan, J. Zheng, S. Park, *et al.*, "Improving Software Diagnosability via Log Enhancement," *ACM Transactions on Computer Systems*, vol. 30, no. 1, pp. 1–28, Feb. 2012.

[115] J. Rößler, "From software failure to explanation," PhD thesis, Universität des Saarlandes, Aug. 2013.

[116] J. Bach, S. Otten, and E. Sax, "Model based scenario specification for development and test of automated driving functions," in *IEEE Intelligent Vehicles Symposium (IV)*, Gothenburg, Sweden: IEEE, 2016, pp. 1149–1155.

[117] O. Buhler and J. Wegener, "Automatic testing of an autonomous parking system using evolutionary computation," *Society of Automotive Engineers Inc.*, pp. 115–122, 2004.

[118] J. Wegener and O. Buhler, "Evaluation of different fitness functions for the evolutionary testing of an autonomous parking system," in *Genetic and Evolutionary Computation Gecco 2004*, vol. 3103, 2004, pp. 1400–1412.

[119] D. Otte, C. Krettek, H. Brunner, *et al.*, "Scientific approach and methodology of a new in-depth investigation study in germany called gidas," in *18th Technical Conference on the Enhanced Safety of Vehicles*, Nagoya, Japan, 2003.

[120] D. Ockel, J. Bakker, and R. Schoeneburg, "An initiative towards a simplified international in-depth accident database," *Berichte der Bundesanstalt fuer Strassenwesen*, 2013.

[121] C. Erbsmehl and L. Hannawald, "Simulation realer Unfalleinlaufszenarien der German In-Depth Accident Study (GIDAS)," *VDI-Berichte*, 2008.

[122] D. P. Wood and S. O'Riordain, "Monte Carlo Simulation Methods Applied to Accident Reconstruction and Avoidance Analysis," SAE Technical Paper, Tech. Rep., Mar. 1994.

[123] C. Erbsmehl, "Simulation of real crashes as a method for estimating the potential benefits of advanced safety technologies," in *21st Conference on the Enhanced Safety of Vehicles*, Stuttgart, Germany, 2009.

[124] W. Wachenfeld and H. Winner, "Virtual Assessment of Automation in Field Operation A New Runtime Validation Method," in *10. Workshop Fahrerassistenzsysteme*, Walting, Germany, 2015, pp. 161–170.

[125] U. Lages, M. Spencer, and R. Katz, "Automatic scenario generation based on laserscanner reference data and advanced offline processing," in *IEEE Intelligent Vehicles Symposium Workshops (IV Workshops)*, Gold Coast, Australia: IEEE, Jun. 2013, pp. 146–148.

[126] A. Geiger, P. Lenz, and R. Urtasun, "Are we ready for autonomous driving? The KITTI vision benchmark suite," in *IEEE Conference on Computer Vision and Pattern Recognition (CVPR)*, Providence, USA: IEEE, Jun. 2012, pp. 3354–3361.

[127] V. Alexiadis, J. Colyar, J. Halkias, *et al.*, "The next generation simulation program," *ITE Journal (Institute of Transportation Engineers)*, vol. 74, no. 8, pp. 22–26, 2004.

[128] P. Riekert and T. E. Schunck, "Zur Fahrmechanik des gummibereiften Kraftfahrzeugs," *Ingenieur-Archiv*, vol. 12, no. 1, p. 70, 1941.

[129] S. Russell, P. Norvig, J. Canny, *et al.*, *Artificial intelligence: a modern approach*. Upper Saddle River: Pearson Education, Inc., 2003.

[130] C.-H. Cheng, M. Rickert, C. Buckl, *et al.*, "Toward the Design of Robotic Software with Verifiable Safety," in *33rd Annual IEEE International Computer Software and Applications Conference*, vol. 1, Seattle, USA, 2009, pp. 622–623.

[131] Y. Yu, "Development and Evaluation of Realistic Fault Models Based on Data of Real Vehicles," Technical University of Munich, 2016.

[132] TU Dresden, "Ultraschall Laufzeitverfahren zur Distanzmessung," Dresden, Tech. Rep., 2013.

[133] T. Kubertschak, M. Maehlisch, and H.-J. Wuensche, "Towards a unified architecture for mapping static environments," in *17th International Conference on Information Fusion (FUSION)*, Salamanca, Spain, 2014, pp. 1–8.

[134] T. Kubertschak and M. Maehlisch, "Fusion Routine Independent Implementation of Advanced Driver Assistance Systems with Polygonal Environment Models," in *19th International Conference on Information Fusion (FUSION)*, Heidelberg, Germany, 2016.

[135] K. Deb, "Multi-objective optimization using evolutionary algorithms: an introduction," *Multi-objective evolutionary optimisation for product design and manufacturing*, pp. 1–24, 2011.

[136] S. Thielman, *Fatal crash prompts federal investigation of Tesla self-driving cars*, New York, USA, Jul. 2016.

[137] P. Minnerup and A. Knoll, "Testing autonomous driving systems against sensor and actuator error combinations," in *IEEE Intelligent Vehicles Symposium (IV)*, Dearborn, USA: IEEE, 2014.

[138] A. Sumaray and S. K. Makki, "A comparison of data serialization formats for optimal efficiency on a mobile platform," in *Proceedings of the 6th International Conference on Ubiquitous Information Management and Communication - ICUIMC '12*, New York, New York, USA: ACM Press, Feb. 2012, p. 1.

[139] P. Deutsch and J.-L. Gailly, "ZLIB Compressed Data Format Speci cation version 3.3," Aladdin Enterprises, Tech. Rep., 1996, pp. 1–10.

[140] P. Minnerup and A. Knoll, "Testing Automated Vehicles against Actuator Inaccuracies in a Large State Space," in *9th IFAC Symposium on Intelligent Autonomous Vehicles*, Leipzig, Germany, 2016.

[141] M. Muja and D. G. Lowe, "Fast approximate nearest neighbors with automatic algorithm configuration," in *International Conference on Computer Vision Theory and Applications (VISAPP)*, Lisboa, Portugal, 2009, pp. 331–340.

[142] S. M. Lavalle, "Rapidly-Exploring Random Trees: A New Tool for Path Planning," Computer Science Dept., Iowa State University, Tech. Rep., 1998.

[143] Elektrobit, "EB Assist ADTF 2.13.3 User Manual," Elektrobit Group Plc., Erlangen, Tech. Rep., 2016. arXiv: `arXiv:1011.1669v3`.

[144] P. Minnerup, T. Kessler, and A. Knoll, "Collecting Simulation Scenarios by Analyzing Physical Test Drives," in *18th International IEEE Conference on Intelligent Transportation Systems (ITSC)*, Las Palmas de Gran Canaria, 2015, pp. 2915–2920.

[145] B. Bartels, C. Erbsmehl, and L. Hannawald, "Reconstruction of accidents based on 3D-geodata," *Berichte der Bundesanstalt fuer Strassenwesen*, 2013.

[146] H. Kraft, "Mercedes-Benz Disengagment Report," California Department of Motor Vehicles, Sacramento, USA, Tech. Rep., 2015.

[147] C. L. Winterman, "Volkswagen Group of America, Inc.'s Disengagement Reports," California Department of Motor Vehicles, Sacramento, USA, Tech. Rep., 2015.

[148] J. Becker, "Annual Report of Autonomous Mode Disengagements," California Department of Motor Vehicles, Sacramento, USA, Tech. Rep., 2015.

[149] Google, "Google Self-Driving Car Testing Report on Disengagements of Autonomous Mode," California Department of Motor Vehicles, Sacramento, USA, Tech. Rep., 2015.

[150] P. Minnerup and A. Knoll, "Temporal Logic for finding Undesired Behaviors of Autonomous Vehicles in a State Space Explored by Dynamic Analysis," in *IEEE Intelligent Vehicles Symposium (IV)*, Gothenburg, Sweden: IEEE, 2016.

[151] B. Bérard, M. Bidoit, A. Finkel, *et al.*, *Systems and software verification: model-checking techniques and tools*. Springer-Verlag Berlin Heidelberg, 2003, pp. 39–40.

[152] A. Cimatti, E. Clarke, E. Giunchiglia, *et al.*, "NuSMV 2: An OpenSource Tool for Symbolic Model Checking," in *Computer Aided Verification*, ser. Lecture Notes in Computer Science, Springer Berlin Heidelberg, Jan. 2002, pp. 359–364.

[153] P. Minnerup, D. Lenz, T. Kessler, *et al.*, "Debugging Autonomous Driving Systems Using Serialized Software Components," in *9th IFAC Symposium on Intelligent Autonomous Vehicles*, Leipzig, Germany, 2016.

[154] A. F. Winfield, "Robots with internal models: A route to self-aware and hence safer robots," *The Computer After Me: Awareness And Self-Awareness In Autonomic Systems*, pp. 237–252, 2014.

[155] A. Vance, *The First Person to Hack the iPhone Built a Self-Driving Car. In His Garage*, 2015.

[156] M. Felsberg, A. Robinson, and K. Ofj, "Visual Autonomous Road Following by Symbiotic Online Learning," in *IEEE Intelligent Vehicles Symposium (IV)*, Gothenburg, Sweden: IEEE, 2016.

[157] E. Santana and G. Hotz, "Learning a Driving Simulator," pp. 1–8, 2016. arXiv: 1608.01230.

[158] R. El Hattachi and J. Erfanian, "5G White Paper," Next Generation Mobile Networks Alliance, Tech. Rep., 2015, pp. 1–125.

[159] T. Kessler, P. Minnerup, and A. Knoll, "Systematically Comparing Control Approaches in the Presence of Actuator Errors," in *IEEE Intelligent Vehicles Symposium (IV)*, Redondo Beach, USA, 2017.

[160] D. Lenz, P. Minnerup, C. Chen, *et al.*, "Mehrstufiges Planungskonzept fuer pilotierte Parkhausfunktionen," in *30. VDI/VW-Gemeinschaftstagung "Fahrerassistenz und Integrierte Sicherheit 2014"*, Wolfsburg, Germany, 2014.

[161] C.-b. Moon and W. Chung, "Kinodynamic Planner Dual-Tree RRT (DT-RRT) for Two-Wheeled Mobile Robots Using the Rapidly Exploring Random Tree," *IEEE Transactions on Industrial Electronics*, vol. 62, no. 2, pp. 1080–1090, 2015.

[162] J. Nieto, E. Slawinski, V. Mut, *et al.*, "Online path planning based on rapidly-exploring random trees," *Proceedings of the IEEE International Conference on Industrial Technology*, vol. 1109, pp. 1451–1456, 2010.

[163] K. Solovey, O. Salzman, and D. Halperin, "Finding a needle in an exponential haystack: Discrete RRT for exploration of implicit roadmaps in multi-robot motion planning," in *Springer Tracts in Advanced Robotics*, 255827, vol. 107, 2015, pp. 591–607. arXiv: 1305.2889.

[164] L. Zhang and D. Manocha, "An efficient retraction-based RRT planner," in *IEEE International Conference on Robotics and Automation (ICRA)*, Pasadena, USA: IEEE, 2008, pp. 3743–3750.

[165] Google, "Google Self-Driving Car Project Monthly Report," Google Self-Driving Car Project, Tech. Rep. February, 2016.

[166] M. Fusco, E. Semsar-Kazerooni, J. Ploeg, *et al.*, "Vehicular platooning: Multi-Layer Consensus Seeking," in *IEEE Intelligent Vehicles Symposium (IV)*, Gothenburg, Sweden: IEEE, 2016, pp. 382–387.

[167] M. Di Bernardo, A. Salvi, and S. Santini, "Distributed consensus strategy for platooning of vehicles in the presence of time-varying heterogeneous communication delays," *IEEE Transactions on Intelligent Transportation Systems*, vol. 16, no. 1, pp. 102–112, 2015.